Helga Rún Hlöðversdóttir

Geotechnical Characteristics of Fluvial Material at Øysand, Norway

Based on in-situ testing with CPTu, DMT and sampling

June 2019

NTNU
Norwegian University of
Science and Technology
Faculty of Engineering
and Environmental Engineering
Department of Civil

Helga Rún Hlöðversdóttir

Master's thesis

2019

Master's thesis

NTNU
Norwegian University of
Science and Technology

NTNU
Norwegian University of
Science and Technology

NTNU
Norwegian University of
Science and Technology

Geotechnical Characteristics of Fluvial Material at Øysand, Norway

Based on in-situ testing with CPTu, DMT and sampling

Helga Rún Hlöðversdóttir

Geotechnics and Geohazards
Submission date: June 2019
Supervisor: Jean-Sebastien L'Heureux

Norwegian University of Science and Technology
Department of Civil and Environmental Engineering

Preface

This thesis is the final project of my master's degree in Geotechnics and Geohazard at the Norwegian University of Science and Technology and was pursued during the spring semester of 2019. The sand site, Øysand, used for this project is a part of a much larger project called the Norwegian Geo-Tests Sites (NGTS) and is one of five test sites located in Norway. The main objective is to look at the geotechnical characteristics in gravelly soils. Large amount of field investigations have been perused at the site by the Norwegian Geotechnical Institute (NGI) and the Norwegian University of Science and Technology (NTNU), making this project possible.

Trondheim, 2019-06-06

Helga Rún Hlöðversdóttir

Acknowledgment

I am very thankful for my supervisor, Jean-Sebastien L'Heureux, for his time and patience to answer endless questions and discussions that surfaced during this work. I also want to thank Santiago Quinteros from the Norwegian Geotechnical Institute (NGI) for his help in the field and Kate, a.k.a. Katherine Emily, for her assistance in the laboratory. I also want to thank my boss from work, Guðjón Örn Björnsson, my dear friend, Unnur Þorsteinssdóttir and last but not least, my father, Hlöðver Þorsteinsson, for reading over the project and providing me with feedback. As well as all others who gave their time on the behalf of this project. Without them this project wouldn't be what it is today.

At last, I want to thank my colleagues at NTNU for a blast of a time during the last two years. Also all the others who had my back during these years, through the good times and not as good times, both family and friends. You know who you are!

H.R.H.

Abstract

Obtaining high quality, representative samples of granular soil (gravel, sand and silt) is a challenge in geotechnical practice. Instead, field investigation tests have become more effective to gain useful geotechnical information about the sub-soil. The most popular penetration test nowadays is the Cone Penetration Test with pore pressure measurements (CPTu). One of the most valuable information obtained from the CPTu is the determination of the sub-surface stratigraphy and identification of the present materials. Over the years, various empirical charts which correlate the CPTu parameters to soil classification have been developed, as well as a soil behaviour index which numerically classifies the soil. The aim of this project is to test these charts for the soil at Øysand and find the most efficient and reliable way for classification of the soil using results of CPTu. Also, to present engineering parameters describing the soil. Øysand is a natural sand site used in this project, located in Melhus municipality central Norway. The site is a part of a much larger project called the Norwegian Geo-Tests Sites (NGTS) and is one of five test sites located in Norway. To back up the results of the CPTu, they are compared to samples taken at Øysand and also results from seismic Dilatometer tests. The disadvantage of these penetration tests is that they do not work well in coarse soils, as the penetration can damage the equipment. The results divide the fluvial material in the top ten meters of the stratigraphy in three groups. The first layer (I) of clean sands from 1.8-3.5 m depth, the second layer (II) which lies on the boarder of gravelly sands and clean sands from 3.5-5 m depth and the third layer (III) of clean sands to sand mixtures, silty sand to sandy silt, from 5 - 10m depth. However, it seems that the fine content within the soil has big impact on the soil behaviour under penetration. Meaning that the coarse layers seen in samples are not recognized using the popular soil behaviour charts presented by Robertson (1990) and Robertson (2016). Therefore it is recommended, for the Øysans sand site, to use a classification chart based on shear wave velocity measurements, as it fully recognize the coarseness of the soil. However, if shear wave velocity data is not available it is recommended to use the soil behaviour index for soil classification. For the Øysand site it is recommended to shift the boundary between the gravelly sand and clean sand (zones (7) and (6) according to the Robertson 1990 chart) from 1.31 to 1.61 to account for the gravelly material.

Contents

List of Figures

List of Tables

Acronyms and symbols

CPT Cone Penetration Test

CPTu Cone Penetration Test with pore pressure measurements

DMT Dilatometer Test

SDMT Dilatometer Test with seismic module

USCS Unified Soil Classification System

$\mathbf{C}_c$ Coefficient of curvature

$\mathbf{C}_u$ Coefficient of uniformity

SBT Soil behaviour type

SBTn chart Soil behaviour chart/Classification chart presented by Robertson (1990)

GSDC Grain size distribution curve

$\mathbf{q}_c$ Cone resistance [MPa or kPa]

$\mathbf{f}_s$ Resistance at the friction sleeve [kPa]

u Pore pressure [kPa]

$\mathbf{u}_2$ Pore pressure measured behind the piezocone [kPa]

$\mathbf{q}_t$ Corrected cone resistance for un-equal end area effects [MPa or kPa]

z Depth [m]

$\mathbf{z}_c$ Corrected depth for inclination [m]

$\mathbf{Q}_t$ Normalized cone resistance

$\mathbf{F}_r$ Normalized Friction ratio

$\mathbf{B}_q$ Pore pressure ratio

σ_v Overburden stress [kPa]

σ'_v Effective overburden stress [kPa]

γ Unit weight [kN/m^3]

$\mathbf{u}_0$ *In-situ* pore pressure [kPa]

$\Delta\mathbf{u}$ Excess pore pressure [kPa]

Q_{tn} Normalized cone resistance based on the stress exponent, n

$Q_{tn,cs}$ Clean sand equivalent normalized cone resistance

n Stress exponent

I_c Soil behaviour index

K^*_G Normalized rigidity index

U_2 Normalized excess pore pressure

V_s Shear wave velocity [m/s]

G_0 Small strain shear modulus [kPa]

I_G Rigidity index

I_D The material index

K_D The horizontal stress index

E_D The dilatometer modulus

D_r Relative density

Ψ State parameter

ϕ' Peak friction angle [°]

E' Young's Modulus

k Hydraulic conductivity [m/s]

Chapter 1

Introduction

"*The objectives of any subsurface investigation are to determine the following: Nature and sequence of the subsurface strata (geologic regime), groundwater conditions (hydrologic regime), and physical and mechanical properties of the subsurface strata*" (Clayton et al. (1995)). Geotechnical engineering analyses and designs call for precise identification and characterization of sub-soil layering and also a good representative information of soil stratigraphy at the site being investigated (Sadrekarimi (2016)). Obtaining high quality, representative samples of granular soil (gravel, sand and silt) is a challenge in geotechnical practice. Do to lack of cohesion in these soils the soils normally get disturbed under sampling and some material, both fine and coarse, is missed (Clayton et al. (1995)). Therefore it is difficult to collect samples that fully represent the *in-situ* state of the soil (Huang and Huang (2007)). Instead, field investigation tests have become more effective to gain useful geotechnical information about the sub-soil. The most popular penetration test in geotechnical practise nowadays is the Cone Penetration Test with pore pressure measurements (CPTu) (Schneider et al. (2008)). The test, as we recognize it today, has been in use since the mid 1970's. It is described by a cone attached on a series of rods which are penetrated into the ground at a constant rate of 2 cm/s. While penetrating measurements are made of the cone resistance (q_c), resistance at the friction sleeve (f_s) and pore pressure measurements (u_2) (Lunne et al. (1997)). The popularity of the CPTu measurements above other well-known methods of field investigation (e.g. Standard penetration test, Total sounding and Dilatometer) is related to the investigation being simple and fast, repeatable, accurate, economical, provides near continuous record of data and has a strong theoretical background (Robertson (2009a), Sadrekarimi (2016)). The test is highly suitable in soft and loose soil, however, in conditions in coarse sands and gravel the CPTu is not as applicable. The cone system does not have the capacity to penetrate through the coarse material and therefore can the penetration damage the equipment. In those cases pre-drilling is necessary (Lunne et al. (1997)). The CPTu does not measure any geotechnical properties directly, however, many empirical correlations have been developed between the engineering properties and the CPTu data (i.e. unit weight, relative density, state parameter, friction angle and stiffness modulus) (Sadrekarimi (2016)). One of the most valuable information obtained from the CPTu is the determination of the sub-surface stratigraphy and identification of the present materials. Over the years, various charts which correlate different CPT/CPTu parameters to soil classification have been developed. The most popular classification

chart used in geotechnical practice nowadays is a pair of charts presented by Robertson (1990) which depends on all three parameters measured. More charts have been presented based on this one chart to provide more useful information (Robertson and Cabal (2014), Robertson (2009a), Robertson (2016), Schneider et al. (2008)). Another useful parameter for interpretation of soil type is the soil behaviour index which is a numerical value for the soil classification (Robertson (2009a)). These charts are global in use and the data can fall within the wrong zone, therefore do these charts need to be tested. To make sure that the classification based on the CPTu is correct the addition of a seismic module, to obtain information about he shear wave velocity, can be a good factor to properly classify the soil, along with visualization of the soil, dissipation tests and proper engineering judgment (Lunne et al. (1997)).

Located at Øysand in central Norway is a testing site consisting of natural sand, or fluvial and deltaic sediments which are a product of glacially eroded bedrock and fluvially eroded marine- and glacial deposits (Quinteros et al. (2019)). As a part of a larger project, large number of both *in-situ* and laboratory investigations have been performed at the site to gain deeper understanding of behaviour of sands (Gundersen et al. (2018), Quinteros et al. (2019)). Preliminary results have shown that the site consists of coarse, sandy and gravelly, fluvial material in the top ten meters, underlain by finer, more silty, deltaic material. Within the top ten meters is a layer of coarse/gravelly sand which will be the main focus in this project.

1.1 Problem statement

As CPTu measurements are more difficult in coarse grained/gravelly soils, there is a partial lack of reliability to those parts in the classification charts, due to general lack of data. The behaviour of sands under penetration is highly dependent on the grain size distribution as well as the proportion of fines. The interpretation of soil properties of sand is done by estimating fully drained conditions (excess pore pressure generated by the penetration is dissipated as fast as it is generated). A problem known from previous studies has shown that the SBTn charts do not fully recognize the gravelly behaviour of the soil as the behaviour of the fines in the soil is dominating. With the extensive research at the Øysand test site, more information about physical and mechanical behaviour of sands is to be gained. Since the sampling process is not fully reliable the importance of quality results from *in-site* investigations increases. The main significance of this study is to test the empirical classification charts and find the best and most reliable method to classify the soil at Øysand. As well as to see how the parameters calculated with data from *in-situ* tests correlates with empirical values expected in granular soils.

1.2 Research Objectives

The main objective of this project is to identify the coarse layers at Øysand using data from samples and *in-situ* testing. To test the available classification charts in literature based on CPTu data and compare the results with the samples from the site which will be classified according to the Unified Soil Classification System (USCS). Also will results from Dilatometer testing (DMT) be used for support and comparison. Since the classification charts

are empirical and based on experience it can be expected that they do not classify the coarse/gravelly soil found at Øysand perfectly. In that case, it is necessary to localize the charts. The goal of this project is to provide suggestions on possible modifications on the available classification methods to improve the classification on the Øysand soil. The same will be done for results of calculated geotechnical parameters obtained by CPTu and DMT data. Those values will be compared to theoretical values and design values representing the top ten meters of the Øysand site presented. The project is based on the results of the top ten meters of 17 CPTu's, 2 DMT's and samples from two different boreholes at Øysand.

1.3 Structure of thesis

The thesis is comprised of 7 chapters. The first chapter includes the introduction and the objectives of the research. The second chapter outlines important literature review and explanations of theory behind the work done in this project. The third chapter investigates the Øysand site, the geology and previous investigations on site. The fourth chapter discusses, in more detail, the research and strategies used in the project, as well as methodology. Chapter 5 and 6 present the results of the project and necessary discussions around the results. At last, chapter 7 summarizes the project and gives ideas for future work.

Chapter 2

Literature review

This chapter will provide a review of important literature used in this study. That is factors affecting CPTu measurements and corrections, methods to classify soil using CPTu data as well as Dilatometer test (DMT) and the Unified Soil Classification System.

2.1 Soil Investigation

Obtaining high quality samples of granular soil is difficult and attaining undisturbed samples of granular material is considered a big challenge in geotechnical practice. The coarseness of the soil implies a high hydraulic conductivity and large average pore size, so water or air can rapidly penetrate the soil and dissipate the negative pore pressures. Thus, the total and effective stresses are reduced to zero and the granular soil has little strength and no cohesion, making the sampling process difficult. Due to the low strength and lack of cohesion the samples become easily disturbed when the sampler is pulled out of the ground and the chance of loosing grains, both fine and coarse, increases. The fines in the granular soil can be washed away in the drilling process and the coarse grained particles tend to accumulate and stay at the bottom of the hole (Clayton et al. (1995)). Therefore are samples of granular soils generally not perfectly representable of the *in-situ* ground conditions (Huang and Huang (2007)). Because of this, the necessity to use other field methods to gain accurate desired information about granular soils is high. The sampling is typically replaced by the use of geophysical testing or geotechnical penetration testing (Clayton et al. (1995)).

2.1.1 CPTu

The most popular penetration test used in geotechnical practice nowadays is the Cone Penetration Test with pore pressure measurements (CPTu) (Schneider et al. (2008)). Its popularity is related to the investigation being simple and fast, repeatable, accurate, economical and has a strong theoretical background (Robertson (2009a)), as well as it provides a near continuous profile of data with depth. The test is carried out by penetrating a 60° cone with a

face area of 10 cm^2 ($r = 35.7mm$), attached to a 150 cm^2 rod system, into the ground at a constant rate of 2 cm/sec. Simultaneously values of the cone resistance (q_c), the force needed to penetrate the cone, is measured as well as the side friction on the sleeve (f_s) and the pore pressure behind the tip of the cone (u_2) (Lunne et al. (1997)), see figure 2.1. The test is used in soils consisting of clay, silt and sand. In coarser soil (such as coarse sands, gravels and/or rock) the soil resistance can be too large and exceeds the thrusting capacity of the drill rig and can lead to damage in the equipment (Lunne et al. (1997)). Because of this, pre-drilling through coarse layers can be necessary to prevent the equipment from damage. A thrust machine is used to provide continuous penetration as well as to maintain a thrust direction as close to vertical. The deviation should not exceed 2° from the original direction of penetration (Lunne et al. (1997)).

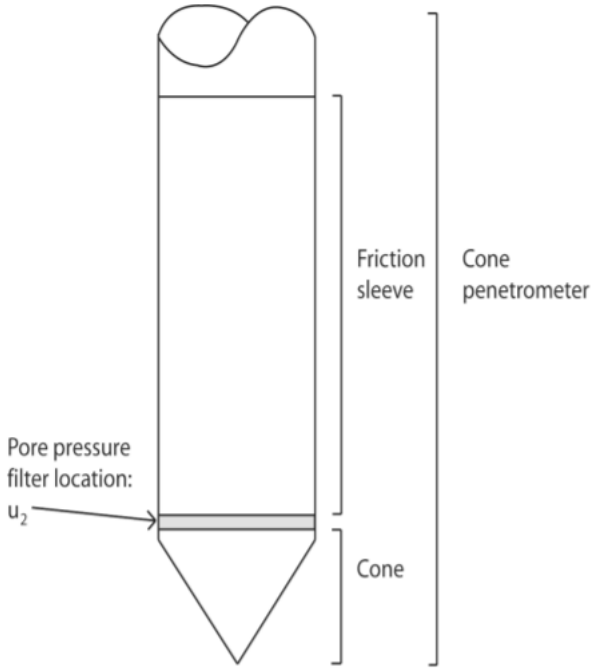

Figure 2.1: Basic terminology of the Cone Penetration test (Robertson and Cabal (2014)).

Penetration in sandy soils is generally drained, meaning that the generated excess pore pressure made by the penetration dissipates instantly. The opposite is be expected for penetration in clayey soil. The drained penetration results in a differential pore pressure of zero which is an important identification for sandy soils. Penetration in sands can also be identified with high bearing capacity (q_c >5 MPa (NGF (2010)) and sleeve friction (Campanella et al. (1982)). The sleeve friction is used for evaluation of the pile capacity and driving resistance. However, it is more sensitive to errors and shortcomings in the measurements than the other two parameters (Lunne et al. (1997)). The largest advantage of the CPTu is how much information about the soil can be interpreted from the measured parameters. Such as information about soil layering, soil type, the in-situ conditions and the soils mechanical properties, strength parameters, deformation- and consolidation properties (Vegdirektoratet (1997a), NGF (2010)).

It has been observed that the measured CPTu parameters increase with depth and overburden stress (σ'_v) (Cam-

panella et al. (1986). Therefore it is necessary to normalize the CPT parameters for the effective overburden stress in deep penetrations (Lunne et al. (1997), Robertson (1990), Schneider et al. (2008), Robertson (2009a)). The normalized parameters are presented as follows:

1. Normalized cone resistance

$$Q_t = \frac{q_t - \sigma_{v0}}{\sigma'_{v0}} \tag{2.1}$$

2. Normalized friction ratio

$$F_r = \frac{f_s}{q_t - \sigma'_{v0}} \tag{2.2}$$

3. Pore pressure ratio

$$B_q = \frac{\Delta u}{q_t - \sigma_{v0}} \tag{2.3}$$

Where q_t is the corrected cone resistance corrected for effects of un-equal end area ($q_t = q_c + (1+a) \cdot u_2$, a is the cone area ratio ($\frac{A_N}{A_q}$) which usually takes value between 0,6 and 0,9 depending on the design of the probe (Campanella et al. (1982), Lunne et al. (1997))), σ'_{v0} is the effective vertical overburden stress, Δu is the excess penetration pore pressure (u_2-u_0) and u_0 is the *in-situ* equilibrium pore pressure. The disadvantage of using the normalized parameters is the need of assuming the unit weight (γ) and the equilibrium pore pressure used in the calculation of the vertical stress (σ_{v0}) and the vertical effective stress (σ'_{v0}). However, even with those predictions, the results are still more precise than the ones without normalization (Robertson (1990)). The corrected cone resistance (q_t) is mostly important in soft clays and silty soil where high pore pressure and low cone resistance are measured. In soil where the penetration is usually drained and resistance against the cone is large the corrected resistance does generally not differ from the uncorrected resistance and therefore are the corrections negligible (Robertson (1990)). Even though, it is a good rule of thumb to apply the correction to any CPTu data for further work using the parameters (Lunne et al. (1997)).

2.1.2 DMT

Another commonly used penetration test used in geotechnical practice is the Flat dilatometer test. A test which is carried out by penetrating a stainless steel blade with an expandable steel membrane into the ground at a constant rate of 2 cm/sec. Every 20 cm the penetration is stopped and a reading is done. The reading is done by inflating the membrane, and consequently the pressure needed to begin movement of membrane off the sensing disc (*reading A*) and cause a 1 mm expansion at the centre of the membrane (*reading B*) are recorded (Marchetti (1980), Robertson (1986)), see figure 2.2. Readings A and B are corrected for the membrane stiffness and offset in the measuring gauge in order to determine pressures, $P_0 = A + \Delta A$ and $P_1 = B - \Delta B$, which are applied to the soil at the start and at

the end of expansion (where ΔA is the external pressure which must be applied to the membrane in free air to keep it in contact with its seating and ΔB is the internal pressure which, in free air, lifts the membrane center 1 mm from its seating) (Marchetti (1980)). The difference between P_0 and P_1, symbolized as ΔP, can be used along with P_1 and P_2 to derive the intermediate parameters of the DMT (Marchetti (1980)):

- The material index (Soil behaviour type)

$$I_D = \frac{\Delta P}{P_0 - u_0} \tag{2.4}$$

- The horizontal stress index

$$K_D = \frac{P_0 - u_0}{\sigma'_v} \tag{2.5}$$

- The dilatometer modulus (Stiffness)

$$E_D = 38.2 \cdot \Delta P \tag{2.6}$$

The DMT is applicable in material where the grains are small compared to the membrane diameter (60 mm), the test is not suitable in gravels. However, the blade should be able to penetrate through 0.5 m thick gravel layers according to Marchetti et al. (2001). The method has not reached the same popularity as the CPTu test as it is slower, takes fewer measurements (~2 cm vs ~20 cm) and does not provide as much information (Robertson (2009b)).

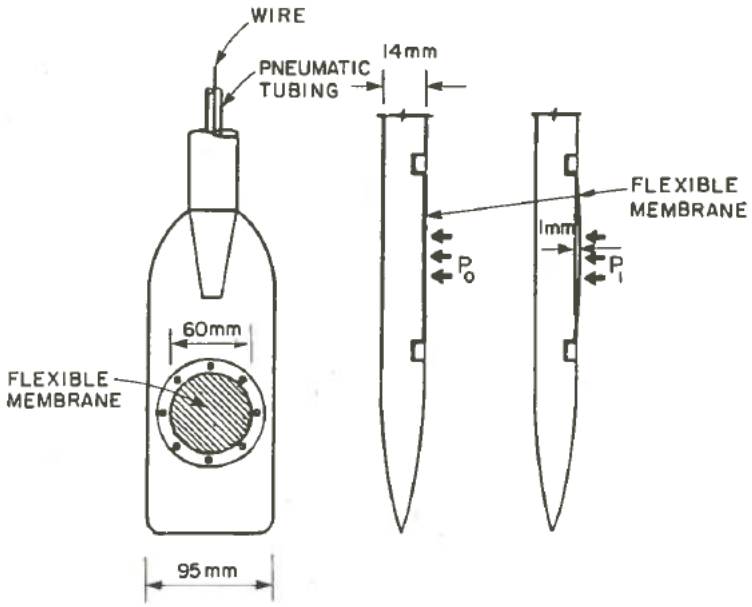

Figure 2.2: Technical drawing of the Marchetti's dilatometer (Marchetti (1980)).

2.1.2.1 SDMT

A Seismic module is commonly used with the normal DMT. Then two receivers above the blade, spaced 0.5 m apart, are added to the penetration system. The shear wave is made at the surface by hitting a 10 kg pendulum hammer

horizontally to a steel rectangular base which is pressed vertically against the soil by the weight of a truck, see figure 2.3. The shear wave velocity (V_s) is then obtained as the ratio between the difference in distance between the source and the two receivers (S_2 - S_1) and the difference in arrival time of the impulse from the first to the second receiver (Δt) (Marchetti et al. (2008)).

$$V_s = \frac{S_2 - S_1}{\Delta t} \tag{2.7}$$

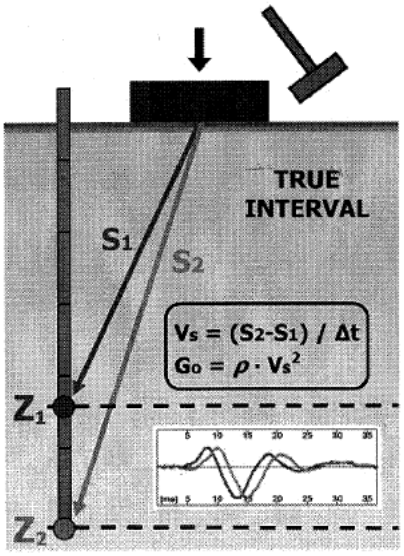

Figure 2.3: Schematic layout of the seismic dilatometer test (Marchetti et al. (2008)).

S-waves move like a snake in the ground, they shear the ground sideways at right angles to the direction of travel. As it forces only shear deformation in the material its velocity (V_s) can be considered as an effective stress parameter which directly relates to the rigidity or stiffness of the material (I_G) (Kokusho and Yoshide (1997)). V_s in sands is generally controlled by the number and area of grain-to-grain contact. Therefore is the speed controlled by the relative density, the effective stress state and rearrangement of particles in the soil with age and cementation (Schneider et al. (2004)). The speed decreases with increasing fines content and decreasing compaction in the soil. According to Kokusho and Yoshide (1997) the V_s of sandy soils range from 150-375 m/s depending on the initial void radio, for gravelly soils the velocity can go as fast as 450 m/s.

2.2 Soil identification with CPTu

One of the three main applications in the CPT/CPTu site investigation process is the determination of the subsurface stratigraphy and identification of the present materials on site. The continuous measurement of pore pressures along with cone resistance and side friction has enhanced the CPTu to be the premier tool for stratification logging of soil deposits (Campanella et al. (1982)). "*In the most common sense, the purpose of soil classification*

is two-fold: (a) as a part of overall program of site exploration, to develop a reliable and comprehensive picture of in-situ conditions; and (b) to allow development of a set of expectations about how the site or soils will respond to the environmental changes brought about by a particular project" (Douglas and Olsen (1981)). The soil behaviour is dominantly controlled by arrangement of grains and void space, strength and stiffness of a material, as well as its elasticity or in-elasticity. Other important factors are geological features, environmental factors, physical- and chemical processes and internal structure (Robertson (2016)). The internal structure of the soil can be of macro-scale (deposits, e.g. layering and fissures) and micro-scale (particles, e.g. cementation). The micro-structure is developed by aging, secondary compression, cementation and cold welding and results in increased strength and stiffness in the soil. The "ideal"-soil has no or little micro-structure, whereas structured-soils that have developed significant micro-structure.

Studies have shown that the tip senses an interface 1-20 times the cone diameters ahead and behind the tip, the distance increasing with increasing difference in the strength and stiffness between the soils at the boundary (Robertson and Campanella (1983), Robertson and Ahmadi (205)). Hence, the cone starts to sense the new material before it penetrates it, and it will continue to sense it after penetrating it. This does skew the recorded cone resistance and the soil layer must be relatively thick to ensure a fully corresponding value. It is easier to spot thin soft layers (clayey) and a layer thickness down to 10 cm can be detected in soft soils. However, detection of more resistant (sandy) layers is harder and the layer needs to be of 35-75 cm thickness to get a representative value of the cone resistance (Robertson and Campanella (1983), Lunne et al. (1997)). Because of this an increasing error in the properties of sand can be expected and care should be taken when interpreting the cone resistance in thin dense sand layers (Robertson and Ahmadi (205), Lunne et al. (1997)).

Many charts and theoretical approaches have been proposed for realistic soil classification using the measured CPTu data. The first charts were based on the measured cone resistance (q_c) and the friction ratio (f_s) (Begemann (1965), Sanglerat (1972), Sanglerat et al. (1974), Schmertmann (1978), Douglas and Olsen (1981), Robertson and Campanella (1983)). With the development of the piezocone, classification charts based upon pore pressure measurements were presented (Baligh and Levadouz (1980), Jones and Rust (1982), Senneset et al. (1982), Campanella et al. (1986)). The first set of classification charts based upon all three parameters measured with CPTu (q_c, f_s and u_2) was presented by Robertson (1986). These charts identify 12 soil types, from sensitive fine grained soils to over-consolidated or cemented sand to clayey sand (see table 2.1). Since these charts do not depend on the normalized parameters, they are precise only down to about 30 m depth (Campanella et al. (1986)).

Robertson (1990) proposed two classification charts based on the normalized CPTu parameters for the total overburden stress (see figure 2.4 and corresponding explanations in table 2.1) which, currently, are one of the most used charts in geotechnical practice (Schneider et al. (2008)). This set of classification charts also provides information about (1) overconsolidation ratio (OCR), age and sensitivity (S_t) for fine grained soils, and (2) OCR, age, cementation and friction angle (ϕ') in cohesionless soils (zones 6 & 7).

Out of the two charts shown in figure 2.4, Robertson (1990) recommended that the Q_t-F_r chart was generally more reliable as it provides the best overall success rates for classification of soil compared with samples. It is

usually referred to this chart as the Robertson SBTn chart. The piezocone has difficulties in maintaining saturation when passing through partially saturated material or in stiff and dilatant deposits, as well as it lacks readings above the water table. Because of this the Q_t-B_q chart is more applicable in offshore practice whereas the Q_t-F_r chart is generally used in onshore geotechnical practice (Schneider et al. (2008)).

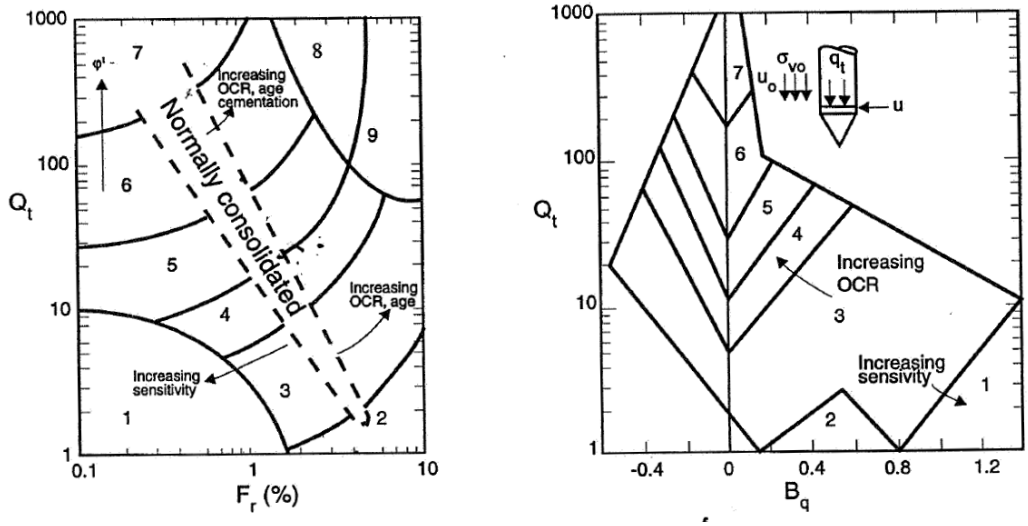

Figure 2.4: The Robertson SBTn chart based on normalized CPT/CPtu data (Robertson (1990)).

Table 2.1: Description of soil classifications based on a) Campanella et al. (1986) b) Robertson (1990) with corresponding values of the soil behaviour index (I_c) and the soils hydraulic conductivity (k) (Robertson (2009a)).

Robertson *et. al.* (1986)	**Robertson (1990)**	**Descrption of classification**	**I_c**	**k [m/s]**
1	1	Sensitive fine grained	N/A	$3{\cdot}10^{-9}$ - $3{\cdot}10^{-9}$
2	2	Organic soils - peat	3.600	$1{\cdot}10^{-8}$ - $1{\cdot}10^{-6}$
3	3	Clays - clay to silty clay	2.95-3.6	$1{\cdot}10^{-10}$ - $1{\cdot}10^{-9}$
4&5	4	Silt mixtures - clayey silt to silty clay	2.6-2.95	$3{\cdot}10^{-9}$ - $1{\cdot}10^{-7}$
6&7	5	Sand mixtures - silty sand to sand silty	2.05-2.6	$1{\cdot}10^{-7}$ - $1{\cdot}10^{-5}$
8	6	Clean sands - sand to silty sand	1.31-2.05	$1{\cdot}10^{-5}$ - $1{\cdot}10^{-3}$
9&10	7	Gravelly sand to sand	< 1.31	$1{\cdot}10^{-3}$ - 1
11	8	Very stiff sand to clayey sand*	N/A	$1{\cdot}10^{-8}$ - $1{\cdot}10^{-6}$
12	9	Very stiff fine grained*	N/A	$1{\cdot}10^{-9}$ - $1{\cdot}10^{-7}$

*Overconsolidated or cemented

In 1995 Robertson presented another classification chart based on shear wave velocity measurements (Lunne et al. (1997)). These measurements can be from any shear wave measurement technique, i.e. seismic CPT, seismic Dilatometer and/or geophones. This chart, see figure 2.5, is based on the normalized cone resistance (Q_t) and the ratio of the small-strain shear modulus (G_0) and the corrected cone resistance (q_t), given as the small-strain rigidity

index ($I_G = G_0/q_t$). It is the small-strain shear modulus which describes the shear wave velocity as:

$$G_0 = \rho \cdot V_s^2 \tag{2.8}$$

where ρ is mass density (γ/g) and V_s is the shear wave velocity.

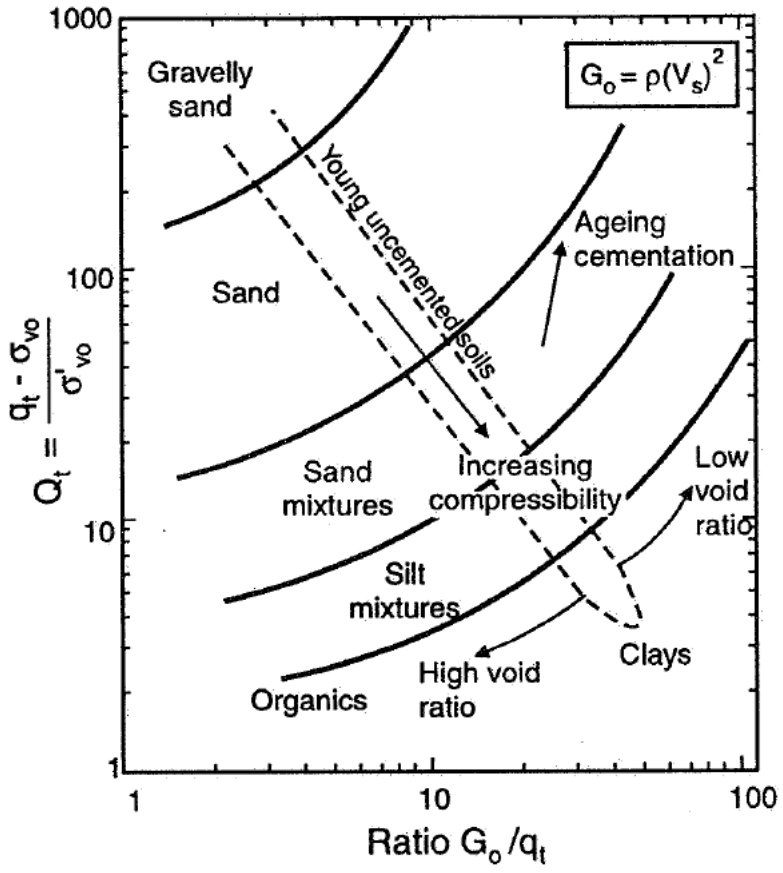

Figure 2.5: Soil classification chart based on normalized cone resistance and small strain shear modulus.

The benefit of adding this classification chart to the previously presented charts is that it allows identification of "unusual" soils such as highly compressible sands, cemented and aged soils and clays with either a high or low void ratio (Lunne et al. (1997)).

Jefferies and Davies (1993) introduced the Soil Behaviour Index (I_c), based on Q_t and F_r which represents the approximate radius of the concentric circles that define the boundaries of soil type in the chart and can be used to classify the soil numerically. Robertson and Wride (1998) then updated the SBT Index to apply to the Robertson SBTn chart as follows:

$$I_c = \sqrt{(3.47 - \log Q_t)^2 + (1.22 + \log F_r)^2} \tag{2.9}$$

The value of I_c can be used to approximate the boundaries between different soil types numerically as the index

increases with increasing apparent fines content and soil plasticity (Robertson and Wride (1998)). As already mentioned, the soil before and after the penetrating cone does influence the measured cone resistance at an interface. Therefore some points will be *in transition* as the cone penetrates through an interface between two soil types. By using the SBTn index it is easy to identify the transition as it moves from low values in sand to high values in clay (and vise-versa). The boundary between gravelly sands and clean sands lies at a value of 1.31 and from clean sands to sand mixtures the value lies at 2.05. The boundary between sand-like and clay-like behaviour is approximately at I_c = 2.6 (Robertson and Wride (1998), Robertson (2009a)). The value of I_c does not apply for zones 1, 8 and 9 as seen in table 2.1.

Robertson and Wride (1998) also updated the normalized cone resistance (Q_t), with a normalized cone resistance with an additional stress exponent (n), which varies with soil type, presented as the SBTn index.

$$Q_{tn} = \left(\frac{q_t - \sigma_{v0}}{p_a}\right) \cdot \left(\frac{p_a}{\sigma'_{v0}}\right)^n \tag{2.10}$$

Where p_a is the atmospheric reference pressure of 100 kPa. The original Robertson (1990) method uses n = 1, which is recommended for clay-type soils ($I_c > 2.6$) where $Q_t \sim Q_{tn}$. However, in coarse-grained soils ($I_c < 2.6$) Q_t is significantly larger than Q_{tn} which makes this process more complicated. Generally, n = 0.5 is used in sandy soil. The recommended procedure to calculate Q_{tn} would be to start with n = 1.0 and calculate Q_t and the SBT index. If $I_c > 2.6$ the data is plotted directly on to the Robertson 1990 chart. However, if $I_c < 2.6$ a calculated stress exponent (equation 2.11) should be used for the calculation of Q_{tn} (Robertson and Wride (1998), Robertson (2009a)).

$$n = 0.381 \cdot I_c + 0.05 \cdot \frac{\sigma'_{v0}}{pa} - 0.15 \tag{2.11}$$

By using the above stress exponent a more precise *in-situ* state for the soil at high stress level is reached and a new SBTn index can also be calculated. Robertson (2009a) updated the original Robertson SBTn chart for the SBTn index, see figure 2.6.

The classification of soils using CPTu data can be affected by the change in stress history, sensitivity, stiffness and void ratio in the soil. The data can also fall within different zones of each chart and in those cases engineering judgment is important. Over 25 years of experience working with the Robertson charts has shown that they compare well with soils classified as "ideal" but are less precise in structured soils. Therefore it is of increasing importance to identify the structure of the soil. It has been proven that if the soils have a significant micro-structure it influences their *in-situ* behaviour (Robertson (2016)). For that, information about shear-wave velocity (V_s) can be very helpful as the small-strain stiffness (G_0) increases with aging and bonding in the soil. The small-strain rigidity index (I_G) in relation to Q_{tn} gives a good indication about the present micro-structure, see fig 2.7.

The chart also references to the normalized rigidity index (K^*_G, see equation 2.12) which is useful for giving a numerical indication of the micro-structure: if $K^*_G < 330$ the soils are likely young and uncemented with little or no micro-structure and would classify as “ideal”. However, soils with $K^*_G > 330$ tend to have a significant micro-structure and classify as "structured"-soils.

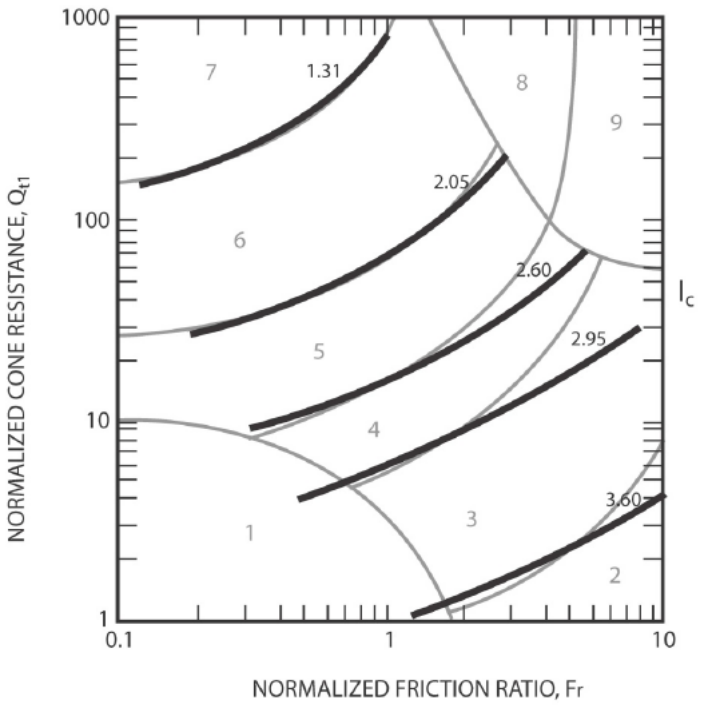

Figure 2.6: Contours of soil Behaviour Type Index, I_c, on normalized Q_t-F_r classification chart (Robertson (2009a)).

$$K_G^* = I_G \cdot Q_{tn}^{0.75} \tag{2.12}$$

In 2016 Robertson (2016) presented a new classification chart, based Q_{tn}-F_r, where boundaries separate ideal soils by their soil type as well as their contractive or dilative behaviour at large shear-strains. Those boundaries are plotted on top of the original SBTn chart, see figure 2.7. Subsequently, Robertson (2016) presented a modified SBT index (I_B) to go with the chart where the value of I_B = 32 represents the approximate boundary from sand-like to clay-like behaviour. Values higher represent coarser soil (sand/gravelly) and values lower than 32 represent finer soil (clayey).

The information about the behavior of soils in shear prior to failure (contractive or dilative) can be of high importance for the soil behaviour. Saturated soils that contract at large strains have a higher strength in drained loading then the strength in undrained loading, whereas saturates soils that dilate at large strains generally have the same shear strength in drained- and undrained loading (Robertson (2016)).

To get the optimized soil classification it is recommended to use charts shown in figure 2.7 together, if the soil classifies as ideal. If the soil classifies as structured, caution is to be taken when using the empirical correlations (Robertson (2016)).

The correlations with engineering design parameters can be relatively reliable for penetrations in sands and clays, which occur under fully drained and undrained conditions, respectively. The uncertainty increases in "transitional" soils (i.e. clayey sands and silts, silty clays, silts and residual soil). These soils are characterized by partial

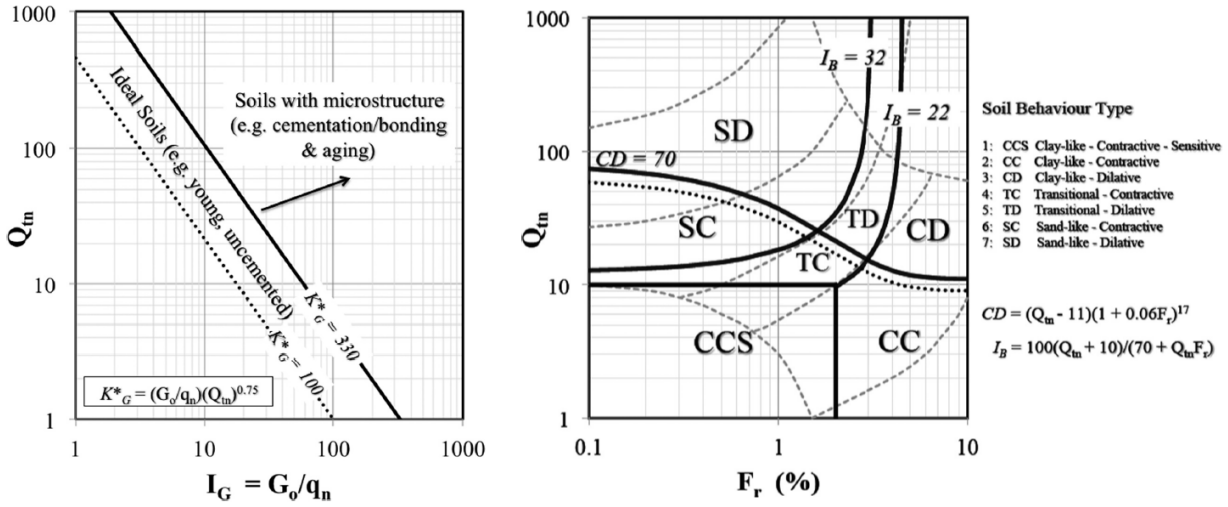

Figure 2.7: Classification charts presented by Robertson (2016). Chart do identify soils with micro-structure (left) and (right) the updated soil classification chart based on Q_{tn} and F_r. Solid lines show behaviour type boundaries and dashed lines show boundaries suggested by Robertson (1990).

consolidation where some (not full) dissipation of excess pore-water pressure occurs locally around the penetrating cone. Schneider et al. (2008) proposed three classification charts based on normalized cone tip resistance (Q_t), the pore pressure ratio (B_q) and normalized excess pore pressures ($U_2 = u_2/\sigma'_{v0}$). The charts emphasize on whether the penetration is drained, undrained or partially drained, see figure 2.8. The three classification charts show exactly the same "zones" though the parameters are plotted differently;

1. *Log-log Q_t-U_2 space*, most representative for clays, clayey silts, silts, sandy silts and sand with no negative penetration pore pressures.

2. *Semilog Q_t-U_2 space* which represents sands and transitional soils with small negative excess penetration pore pressures.

3. *Semilog Q_t-B_q space* for clay soils with large negative excess penetration pore pressures.

These tables presented by Schneider et al. (2008) give a new perspective on the soil classification as it also gives information about the rigidity index (I_r on charts, I_G in this project) and consequently an idea about the soil's plasticity. As the the plastic failure zone around the penetrating cone increases the rigidity index increases, influencing the generation of excess pore pressure and the coefficient of consolidation (c_v) (Krage et al. (2004), Schneider et al. (2008)).

Robertson (2016) proposed an update for this chart, using Q_{tn} and new SBT boundaries in relation to dilative- or contractive behaviour, see figure 2.9. Positive values of U_2 tend to reflect large-strain contractive behaviour whereas negative values of U_2 reflect large-strain dilative behaviour. This chart is useful as a supplement to figure 2.7

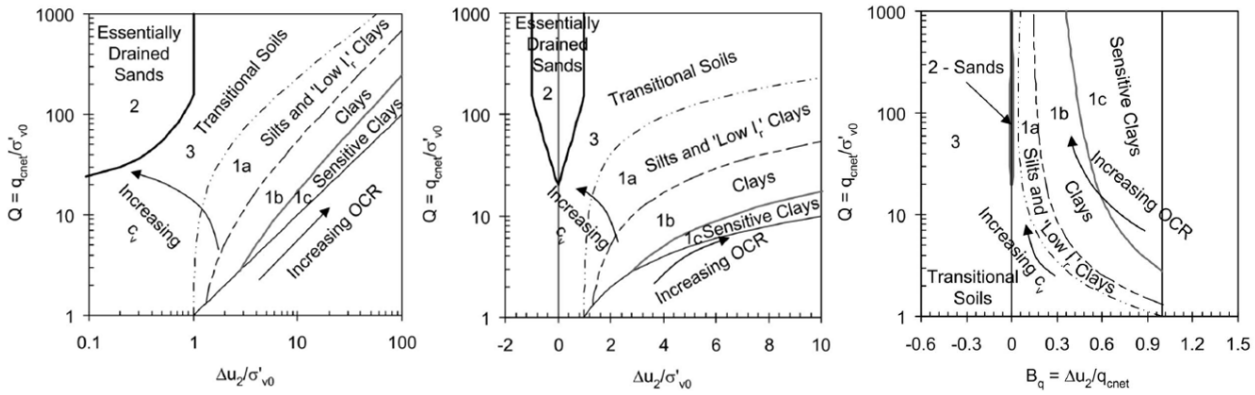

Figure 2.8: Soil classification charts based on drainage capability (Schneider et al. (2008)).

It must be noted that all the above mentioned charts are empirical and based on experience and results from different sites, mainly in the USA and Canada (Robertson (1986), Robertson (2016)). Because of this engineering judgment should be used when interpreting the data from the charts, and some adjustments/localization to correlate with sites under consideration might be necessary.

2.3 Soil identification by other methods

2.3.1 DMT

The results from the DMT investigation can also be used to classify the soil. The material index (I_D) works like the soil behaviour index and can be used to classify the soil numerically. The boundary between sand and silt lies at 1.8, soil with $I_D < 1.8$ is classified as sand, soil with I_D on the range of 0.6-1.8 classifies as silt and soil with $I_D < 0.1$ classifies as clay (Marchetti et al. (2001)). I_D, same as I_c is only a parameter reflecting the mechanical behaviour/rigidy of the soil and therefore it can misinterpret some soils types. Therefore should the results be taken with caution and only used for approximation.

2.3.2 USCS

To classify soil samples the Unified Soil Classification System (USCS) is the most common technique (Abrams et al. (2001)). The system, developed by the US Army, is based on textural and plastic behaviour of the soil and indicates how the material will behave as an construction material. The main properties used for the classification are listed as follows (Clayton et al. (1995)).

- Percentages of gravel, sand and fines (silt and clay), as well as fraction passing the No. 200 sieve (0.075 mm) in a grain distribution/sieving test.
- Shape of the grain size distribution curve from grain size distribution analysis

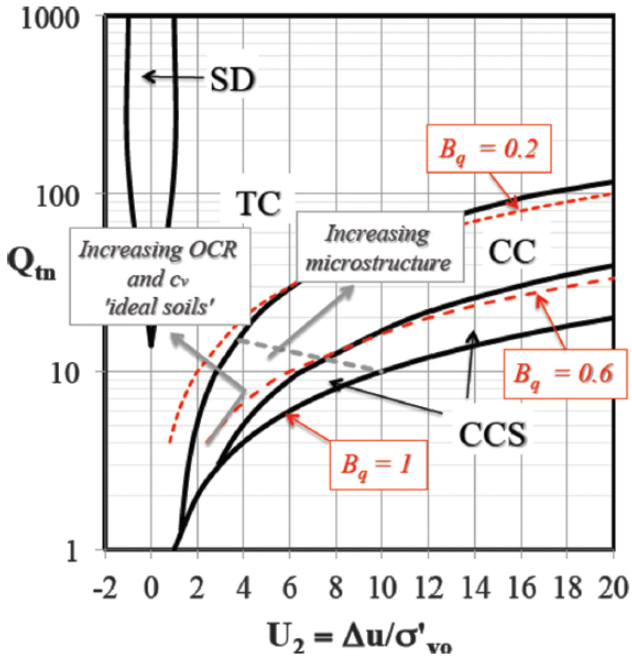

Figure 2.9: The updated Schneider et al. (2008) classification chart by Robertson (2016) based on Q_{tn} and U_2. New soil behaviour lines with additional information about B_q.

- Plasticity and compressibility characteristics of the soil, the Atterberg limits.

2.4 Parameters of sand

The results from the cone penetration test can be further interpreted to derive various parameters used in geotechnical practice. Table 2.2 shows the applicability and reliability of a certain parameters derived from CPTu data; 1 being highly reliable and 5 being not reliable at all (Robertson and Cabal (2014). Since cone penetration in granular soils is generally a drained penetration, no excess pore pressure should be generated due to the penetration. Due to this the information gained from CPTu in granular soils under drained penetration is different from the information CPTu provide for clayey soil which occurs under undrained penetration. (Lunne et al. (1997)). Most of the interpretation methods are obtained from penetration test done in a chamber in a laboratory and later correlated to field data.

Table 2.2: Applicability and reliability of derived parameters from CPTu data (Robertson and Cabal (2014)).

Soil type	Dr	Psi	K0	OCR	St	su	phi	E, G*	M	G0*	k	Ch
Coarse-grained (sand)	2-3	2-3	5	5			2-3	2-3	2-3	2-3	3-4	3-4
Fine grained (clay)			2	1	2	1-2	4	2-4	2-3	2-4	2-3	2-3

1 = high; 2 = high to moderate; 3 = moderate; 4 = moderate to low; 5 = low ; Blank = no applicability;
*improved with seismic data

The Relative density (D_r) has been for the longest time used as an intermediate soil parameter in cohesionless soil. The relative density, based on the ratio of actual decrease in volume of voids in a sandy soil (*in-situ* volume of voids to the maximum possible decrease in the volume of voids), takes a value between 0-1 and describes how much the sand can be compressed beyond its natural state Biryaltseva et al. (2016). Hence, it gives a valuable information about the compaction capability, and bearing capacity, of coarse grained soil. As well as it influences the resistance in the soil and the failure mechanism (Robertson and Cabal (2014)). Even though it is common knowledge that the stress and strength behaviour of the soil is to complicated to be explained with the relative density it is still popular in geotechnical practice, as it is too difficult and expensive to retrieve good samples in granular soil (Jamiolkowski et al. (2001)). The cone resistance is controlled by the density of sand, the *in-situ* vertical and horizontal effective stress and sand compressibility. Robertson and Campanella (1983) indicated that sands with high compressibility have a lower cone resistance than sands with the same relative density but lower compressibility capacity. The compressibility of sands tends to increase with increasing uniformity in grading, angularity of grains, mica or feldspar content, carbonate content and fines content.

However, recently it has become more common to explain the *in-situ* state of the soil in terms of a state parameter (Ψ), related to the critical-state line, due to the fact that the normal compression line is not unique for different condition. There is a strong relationship between the relative density of a soil and the state parameter, however the state parameter can acquire the current state over wider range of stress. Theoretically the state parameter is described as the difference between the *in-situ* void radio (e) and the critical state void ratio (e_{cs}) at the same mean effective stress, as explained in figure 2.10. The state parameter thereby joins the influence of the void ratio and stress level in reference to an ultimate, both critical and steady, state. The state parameter is highly dependent on the shear stiffness, shear strength, compressibility and plastic hardening, factors that must be tested in the laboratory for reliable results. Therefore it is recommended for high-risk projects to use combined results of laboratory and the CPTu for estimating the steady state parameter (Robertson and Cabal (2014)). The most valuable information that the state parameter gives is the information about dilative or contractive behaviour of the soil at large strains (Lunne et al. (1997)). That is, the behaviour of soils to change their volume under shearing, respectively expanding or contracting (Robertson (2016)). Positive values of Ψ represent states above the steady state line (contractive), whereas negative values represent states below the steady state line (dilative), as seen on figure 2.10. It has been suggested by Jefferies and Been (2006) that coarse grained ideal soils with a state parameter $\Psi < -0.05$ will tend to dilate at large strains when loaded in drained shear. Therefore it is to be expected that pore pressure drop and increase in effective stress at large strains in undrained shear will result in strain hardening. An important difference between the behaviour of "loose" or "dense" ideal soils of critical state. "Loose" soils generally contract under drained loading whereas "dense" soils tend to dilate at large shear strains (Robertson (2016)).

Robertson (2009a) updated the SBTn chart with contours describing the state parameter, see figure 2.11. These contours give approximate results and are only to be used to evaluate a value, for low-risk projects.

The shear strength of uncemented, coarse-grained soils is generally described with the peak secant friction angle (ϕ') and the attraction (a) over a stress range, $\Delta\sigma$', described by the Mohr-Coloumb failure criterion (τ_f =

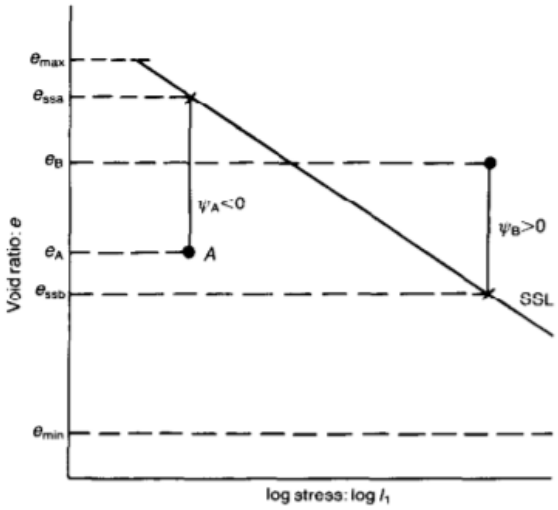

Figure 2.10: Definition of state parameter in sands. I_1 is the average principal effective stress (Konrad (1988)).

$(\Delta\sigma' + a) \cdot \tan(\phi)$ where τ_f is the shear strength) (Senneset et al. (1989)). The peak friction angle is dependant on both density of the soil and the stress path under loading, also the testing conditions (plane strain or triaxial testing) (Schanz and Vermeer (1996)). Typical value for the friction angle in sand varies between 29-42°, depending on the compaction of the sand. Friction angle of loose sand lies in between 29-33° whereas for dense sand the friction angle is between 35-42°, increase in fines content may also decrease the friction angle of the sand Senneset et al. (1989)).

In addition, Robertson (2009a) updated the SBTn chart to relate with the peak friction angle, see figure 2.11. As F_r increases, Q_{tn} decreases for a constant peak friction angle. This goes with observations of high values of ϕ' in compressible sands with relatively low values of cone resistance. The contours will also shift up at high values of F_r due to aging and cementation affects (Robertson and Cabal (2014)). It is worthy to mention that different relationships are used for fine grained soils since the penetration is undrained and the pore pressure and fines content influence the friction angle (Lunne et al. (1997), Robertson and Campanella (1983)).

The deformation properties of the soil are well described with the Young's modulus of the soil (Senneset et al. (1989)). And can thus well describe how much disturbance can be expected to happen around the cone during penetration. The relationship between the measured cone resistance and the Young's modulus is highly responsive to the stress and strain history of the soil as well as aging and the soils mineralogy (Robertson and Cabal (2014)). Generally will penetration into loose sand increase the density, and opposite for dense sands where penetration will produce a looser state. This does not describe the extent of the disturbed zone completely as it is a complicated function of initial state of stress, sand type and packing for normal consolidated sands (Konrad (1988). Typical values of the Young's modulus are 10-50 MPa for sandy soils and 70-170 MPa for gravelly soils (loose to compact)(Vegdirektoratet (1997b)).

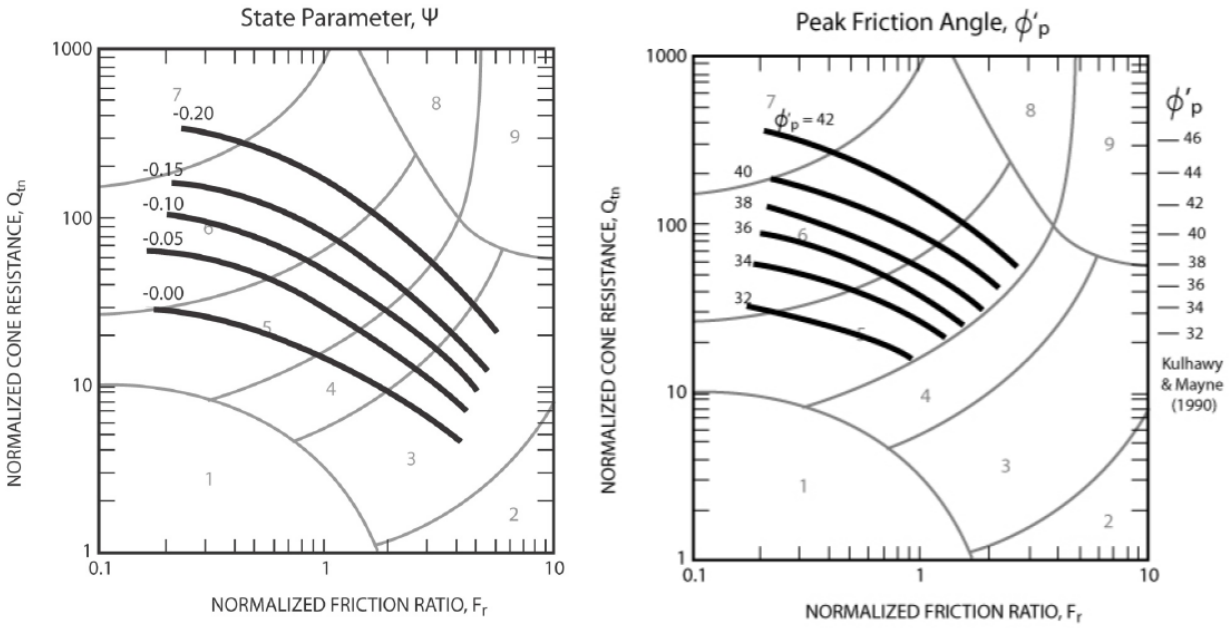

Figure 2.11: Updated Q_{tn}-F_s chart with contours of the Sate parameter (left) and the friction angle (right) (Robertson (2009a)). Explanations of zones can be found in table 2.1.

Chapter 3

Øysand research site

The sand site used in this project, called Øysand (Engilsh: sand island) is located in central Norway, approximately 15 km south of Trondheim in the Melhus municipality (see figure 3.1). The site mainly consists of fluvial- and deltaic material deposited at the mouth of the Gaula River which today runs to the east of the site with a discharge of ~100 m^3/s (Gundersen et al. (2018)). This can also be seen on a soil map for the area which is demonstrated in figure 3.2. On the edge of the "island" the map shows river deposits (yellow) overlying a thick layer of marine-deposits (blue). The depth to bedrock in the site is unknown, however, researches by the German army force, dating back to 1940 show at least 80 m thick deposits. The area used for geotechnical investigations at Øysand is approximately 35,000 m^2 and is today, only used for agricultural purposes (Quinteros et al. (2019)). The site is a part of a project called the Norwegian Geo-Tests Sites (NGTS) and is one of five sites under investigation in Norway (1. this sand-silty site at Øysand, 2. a silt site at Halden, 3. a soft clay site in Onsøy, 4. a quick clay site in Tiller close to Trondheim and 5. a permafrost site in Longyearbyen in Svalbard). The project is done in cooperation between the Norwegian Geotechnical Institute (NGI) and the Norwegian University of Science and Technology (NTNU), SINTEF Building and Infrastructure, the University centre in Svalbard and the Norwegian Public Roads Administrations (Gundersen et al. (2018)).

Since deglaciation started after the last Ice-Age, ~10,300 years ago, the site has been subjected to, and formed by glacial-isostatic rebound as well as fall of relative sea-level. The highest marine level being approximately 175 m.a.s.l.. In the period of 1,500-1,000 years ago the region emerged from sea which indicates that the deltaic sediments at Øysand are relatively young. The deposits, which are a product of glacially eroded bedrock and fluvially eroded marine- and glacial deposits, mainly consist of quartz, feldspar, illite and chlorite, which makes up the main proportion of clay. No special loading event is recognized in the area to imply overconsolidation in the soil. Today, the site is as good as flat and lies at an elevation of approximately 5 m.a.s.l., apart from a 7 m high cliff along the south part of the field. This 7 m high slope in the south of the area indicates a possible erosional process by the Gaula river that may have led to an overconsolidation in the soil deposits. If that is true, the OCR at the ground surface is estimated to 2.8 and decreases down to 1.5 at 6 m depth and 1.2 at 20 m depth below the ground surface. This means that the site classifies as normally consolidated (NC) to slightly overconsolidated (OC) (Quinteros et al.

Figure 3.1: Location of Øysand in relation to Trondheim, Norway (photos: www.maps.google.com (left) www.kart.finn.no (right))

(2019)).

A lot of geotechnical and geophysical testing has been done on site over the whole area for the top 20-30 m of the soil. These investigation are done in cooperation between NGI and NTNU as a part of a much larger project mentioned earlier in this chapter. These test include Total Soundings (TS), Cone Penetration Tests (CPTu), Seimsic Cone Penetration Tests (SCPTu) Seimsic Flat Dilatometer tests (SDMT), Piezometers, Permeability tests, Thermistors Strings (THS), Slug test (SLU) Multichannel Analysis of Surface waves (MASW), Symmetrical resistivity profiling (SRP), Multi-sensor Core Logging (MSCL), Electrical Resistivity Tomography (ETR), Ground Penetration Radar (GPR) and Self polarization. Sampling for laboratory testing was done with the Sonic Drill Sampler (SDS), the Geonor Push Piston Sampler (GPP), and open Push Piston Sampler (PPS) and the Japanese Gel Push Sampler (JGP). Quinteros et al. (2019) as well as Liu et al. (2019) have presented preliminary results of the data, both from field and laboratory investigations in the area. Figure 3.3 shows summary of the results.

The investigations show a general coarsening upward sequence in the sub-surface stratigraphy which can be divided into two groupings: The top 6-10 m that mainly consist of fine to coarse sand with presence of gravel (fluvial deposits) and the underlying 10 m consist of medium silty sand and sandy silt with traces of some organic material (deltaic soils). Meaning, as the depth increases the sand contains more silt and clay. The groundwater was found at approximately 1.9 m below ground. Since the river is affected by high- and low tide it results in more varying groundwater table closer to the river. In the laboratory grain size distribution curves showed that the soil Øysand ranges from silt to gravel, but the main soil type is silty sand. Classification from CPTu measurements

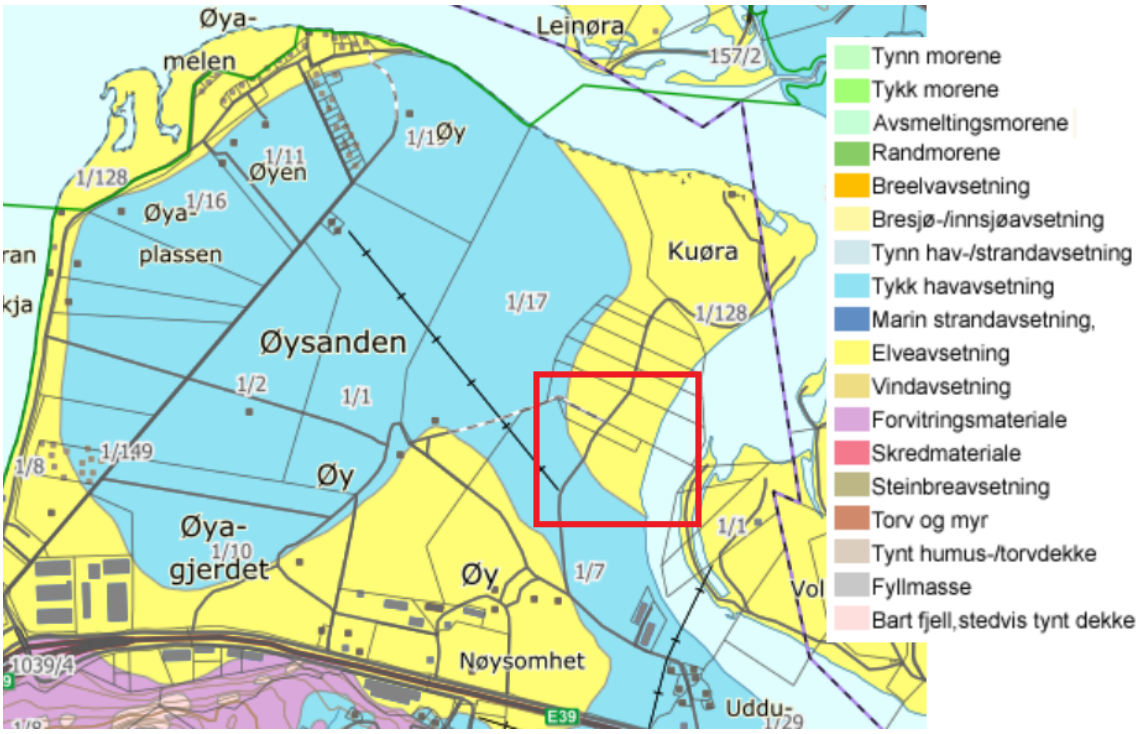

Figure 3.2: Soil map of Øysanden, showing river deposits (yellow) at the boarders and thick marine deposits (blue) in the middle (photo: www.geo.ngnu.no/kart/losmasse)

generally agree with laboratory results, as the data mainly falls into zones 4-6 on the SBTn chart (Robertson (1990)), described as silt mixtures to sand. Also, DMT measurements classify the soil as silty sand to sandy silt.

The geophysical survey consists of 6 recorded profiles in the area. Figure 3.4 shows the results from the ERT to about 30 m depth. The top 10 m layer of high resistivity corresponds to the first grouping of coarse and gravelly sand. Below the resistivity decreases significantly which represents the lower unit of silty and fine sand. On the figure it is also visible that the soil layers are not perfectly horizontal and the layer thickness varies between location in the field, where the coarsest layers are most evident to the north-east of the field. The inclination of the soil originates from the site being at the end of the stream channel, where the running river meets the "still" ocean. Due to the velocity decrease the fluvial sediments cannot be carried by the stream and deposit along the arcuate delta front. The dip of the sedimentary beds is in the direction of the current flow toward the deeper water (the ocean) (Easterbrook (1999)). The geophysical measurements show up to 25° inclination in the delta (Quinteros et al. (2019)). With continuous fall of the sea-level the river extends over the previous deltas and newer fluvial deposits settle above the deltaic material.

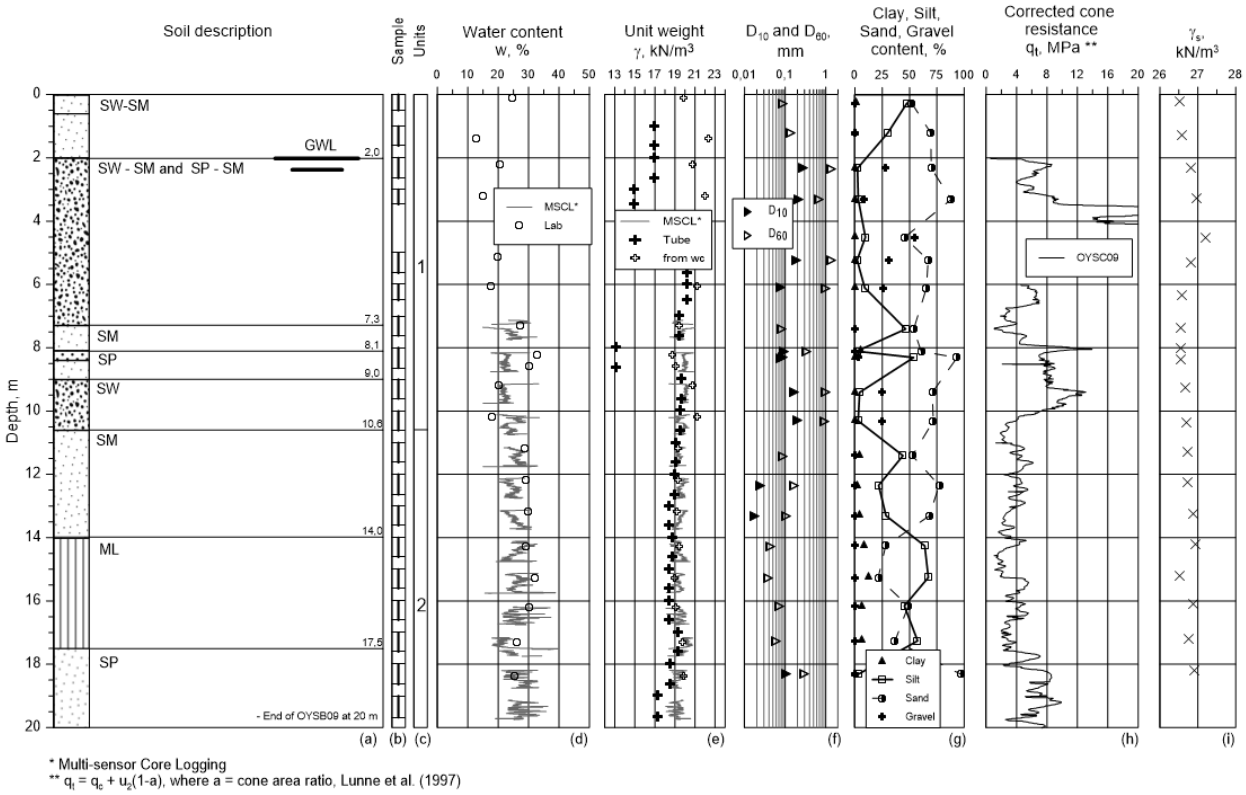

Figure 3.3: Borehole log from B09, sample hole located to the south-east of the site (Quinteros et al. (2019))

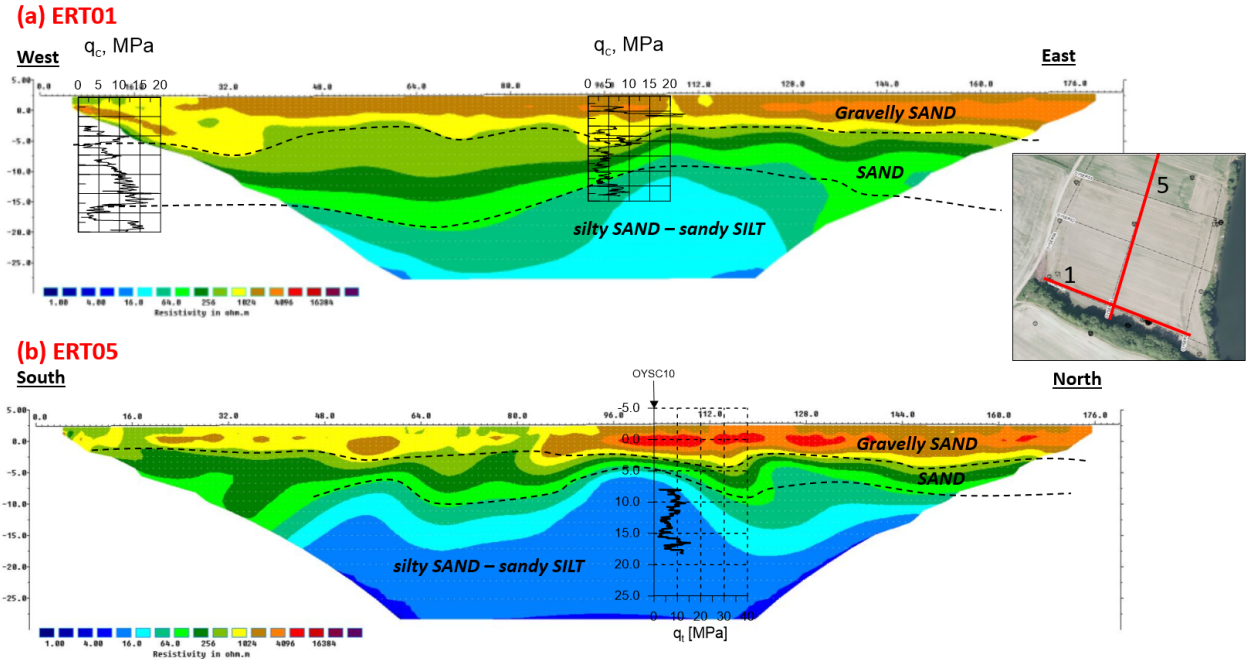

Figure 3.4: Results from Electrical Resistivity Tomography (ERT) test (Quinteros et al. (2019)).

Chapter 4

Methods and data

As mentioned in chapter 3 the soil of Øysand is generally in two groups. First, the coarser sandy soil down to ten meter depth and second the underlying layer of silty sand to sandy silt. The main focus point of this project is the coarse sand/gravelly layer detected between 3.5 and 5 m depth. For a better overview, data from the first grouping of 2-10 m depth is used. The aim of the project is to test the classification chart for the Øysand soil and to interpret and compare geotechnical parameters from empirical correlations based on results from both CPTu and DMT with theoretical values. This chapter is supposed to give a better understanding of the research strategy and the aim of the study. In appendix A a investigation map shows the location of the penetrations and sample holes used in this project. The investigations used in this project are mostly located in the southern part of the site. For comparison an additional sampling hole, DMT and CPTu in the middle of the field, ~ 150 m to the north west of the southern measurements is used.

4.1 Research strategy

To achieve the goal of the research 17 CPTu tests (C21, C22, C23, C24, C25, C26, C27, C28, C29, C30, C31, C32, C34, C35, C37, C39, C40), 2 SDMT measurements (D09 and D19) done by NTNU, and 2 piston samples (B09 and B19) done by NGI were used. The tests were chosen out of total of 36 CPTu tests and 3 DMT soundings due to their close vicinity to the sample holes and they also have more relativity to the project and therefore give more representable data. Figure 4.1 shows the available data of both samples and field investigations. For simplicity, the names of the boreholes have been shortened, the original test IDs can be found in Appendix B as well as the raw results from the penetration testings used in the project.

Based on the CPTu data, different soil types were identified and compared to the available borehole and SDMT data. In addition, correlations between the CPTu and DMT tests and related material properties for granular soils used in geotechnical practice were assessed to gain more information about the soil. In the laboratory grain size distributions as well as plasticity tests were performed to give more information about the soils stratigraphy and to check the reliability of the CPTu classifications charts.

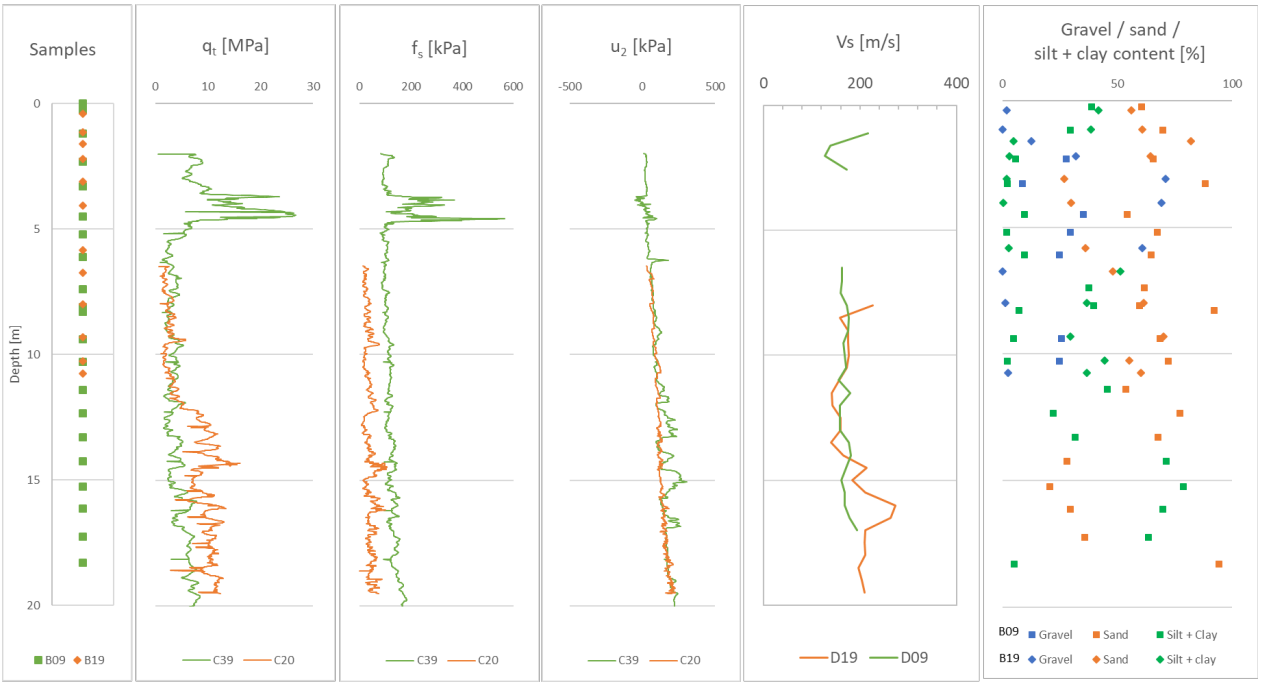

Figure 4.1: Location of samples with depth in B09 and B19, as well as results from representing CPTu and SDMT investigation and material content in each the samples. The results are presented with 1) The corrected cone resistance (q_t), 2) the sleeve friction (f_s), 3) pore pressure measurements (u_2), 4) shear wave velocity (V_s) and 5) material content. A map with locations of the boreholes can be seen in Appendix A.

For the presentation of the results points representing B09 will be marked with a square (■) and points representing B19 will be marked with a diamond (◇).

4.2 Processing of data

This section explains how the data accumulated from sampling, CPTu and DMT was processed for further interpretation.

4.2.1 CPTu

The cone penetration test with pore pressure measurement (CPTu) is an *in-situ* field test, carried on by penetrating a rod system (150 cm^2), with a conical cone (10 cm^2) mounted at the tip, into the ground at a constant rate of penetration (2 cm/sec). During the penetration, values of cone resistance (q_c), sleeve friction (f_s) and pore pressures (u) are recorded every 0.2-2 cm. The pore pressure was measured behind the tip of the cone (u_2) as it ensures the least damage and wear to the equipment. The location is also preferred as the pore pressure measurements are less influenced by compressibility due to the penetration and the measured pore pressures can be used directly to correct cone resistance (Campanella et al. (1982)). Before the cone penetration, or during, pre-drilling was necessary in some of the points due to coarse soils to avoid damaging the cone. Out of the total 44 CPTu tests achieved

on the site, logs that were pre-drilled through the coarsest layer between 3.5-5 m depth were neglected since they have lost their relation to the project. Data with high inclination from the initial vertical direction (> 2°) were also neglected as uncertainty in depth can skew the results (Lunne et al. (1997)).

Interpretation of the CPTu measurements were done using an Excel spreadsheet. At first, correction of the cone resistance to eliminate the effect of un-equal end affects was performed as well as correction on the depth due to inclination of the rod system during penetration ($z_c = z \cdot \cos(i)$). The corrected cone resistance is used even though not necessary, since the soil is coarse enough to neglect the unequal-end affect. As for the calculation of the *in-situ* pore pressure (u_0), no dissipation test results were available due to the coarseness of the soil, so pore pressure measurements from piezometers were used instead. This made it possible to calculate both the excess pore pressure (Δu) under penetration as well as the total overburden stress and the total effective overburden stress (σ_{v0} and σ'_{v0}).

Figure 4.2 shows the corrected cone resistance (q_t) for the selected CPTu. Spatial variability between the parameters is evident, which can also be seen on figure 4.2. Due to the inclination in the deltaic material the layer of the fluvial material is not perfectly horizontal and the thickness varies between locations. To correct for the depth difference C39 was chosen as a reference log (closest to B09) and other logs shifted up and down to match the layering. Figure 4.3 shows the cone resistance from 2-7 m depth after the logs have been "phased" depth-wise.

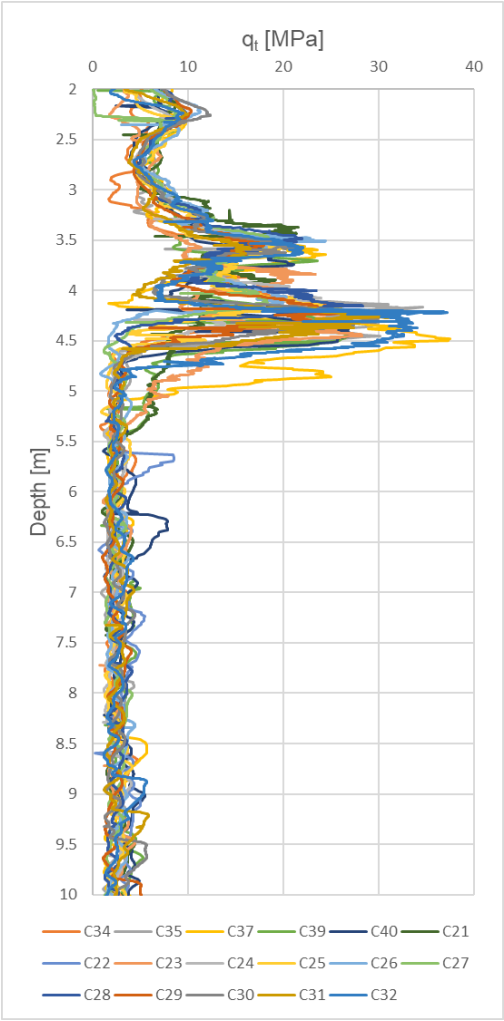

Figure 4.2: The corrected cone resistance from 2-10 m depth.

For use of the measured parameters (q_c, f_s and u_2) average values around the depth of samples were used, see figure 4.1. The samples at B09 were specified at specific depths, average over the sample depth ± 10 cm was taken. Sampling at B19 was taken over larger range and therefore is the measured CPTu data averaged over the whole range of sampling. An extra average was taken over the "peak" of the q_t, that point will be specified as *peak* and not by its depth. The peak varies from 20 to 75 cm thickness and represents the coarsest layer in the soil stratum. Because the data is phased so the layers match, the average might not be taken over the depth of the sample precisely, but where the layer actually lies within the CPTu log. The average of all CPTu's at each sample depth was then calculated to be used in for interpretation.

Further interpretation of the CPTu measurements mainly depends on additional parameters derived from the

measured parameters through theoretical and empirical relations. Those parameters, introduced in chapter 2, are:

- The friction ratio (R_f)
- Normalized friction ratio (F_r)
- Normalized cone resistance (Q_t)
- Pore pressure ratio (B_q)
- Normalized pore pressure ($\Delta U2$)
- Soil behaviour index (I_c) and the stress exponent (n)
- Updated normalized cone resistance (Q_{tn})
- Normalized clean sand cone resistance ($Q_{tn,cs}$)
- Sate parameter (Ψ)
- Relative density (D_r)
- Friction angle (ϕ')
- Young's modulus (E')
- Permeability (k)
- Small-strain rigidity index (I_G)
- Normalized Small-strain rigidity index (K_G^*)

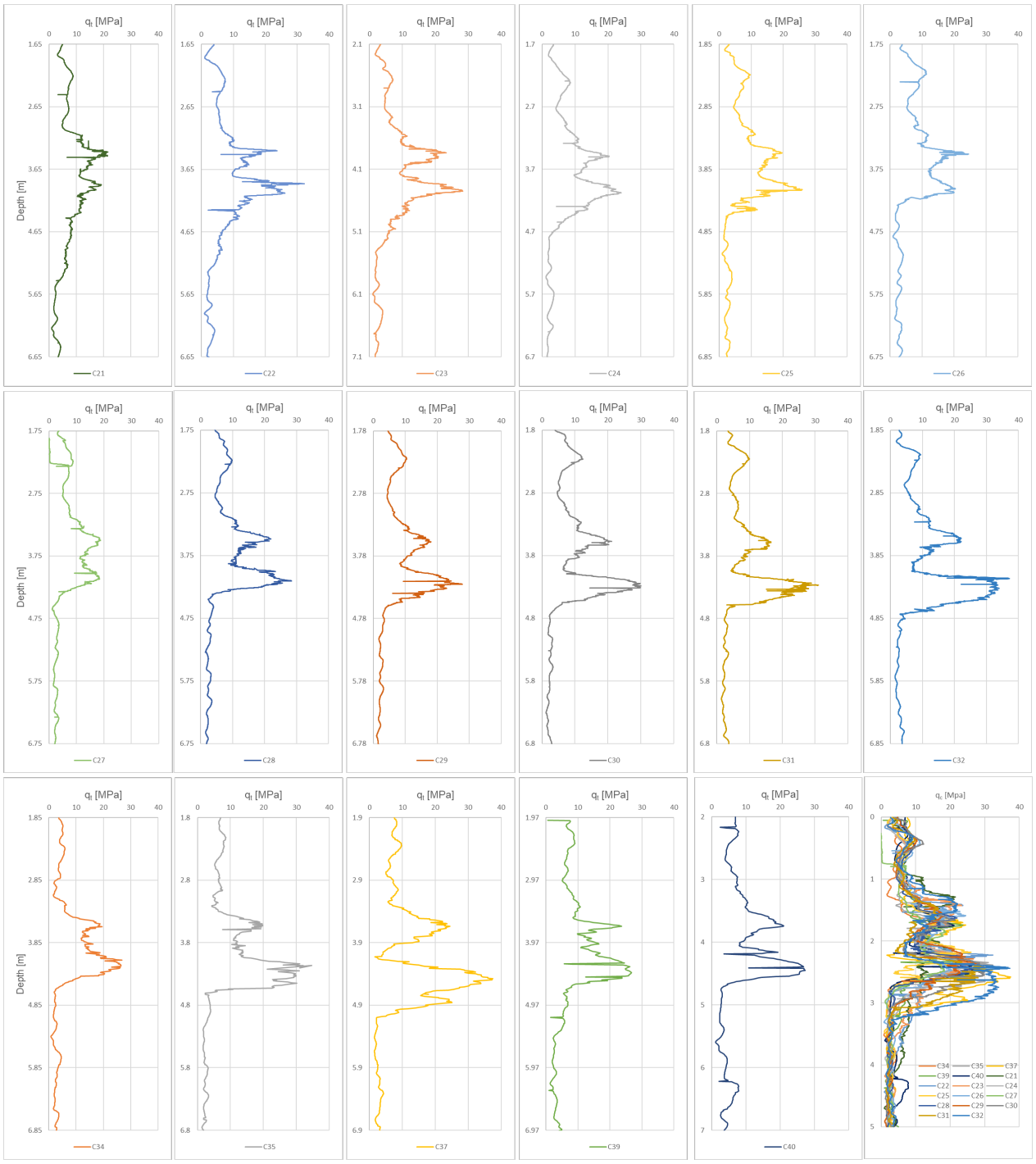

Figure 4.3: Corrected cone resistance after the CPTu's have been "phased" depth-wise.

4.2.2 SDMT

The flat dilatometer test (DMT) is an *in-situ* field test mainly used for stratigraphic profile determination. A stainless steel blade with an expandable steel membrane is penetrated into the ground at a constant rate of 2 cm/sec with the use of a drill rig and stopped every 20 cm to make a reading. The reading is done by inflating the membrane and consequently the pressure needed to begin movement of membrane off the sensing disc and cause a 1 mm expansion at the centre of the membrane is recorded. From these measurements pressures P_0, P_1 and the difference of the two, ΔP, are calculated and subsequently the intermediate parameters of the DMT (Marchetti (1980)). The additional seismic module measures the shear wave velocity every 50 cm during penetration.

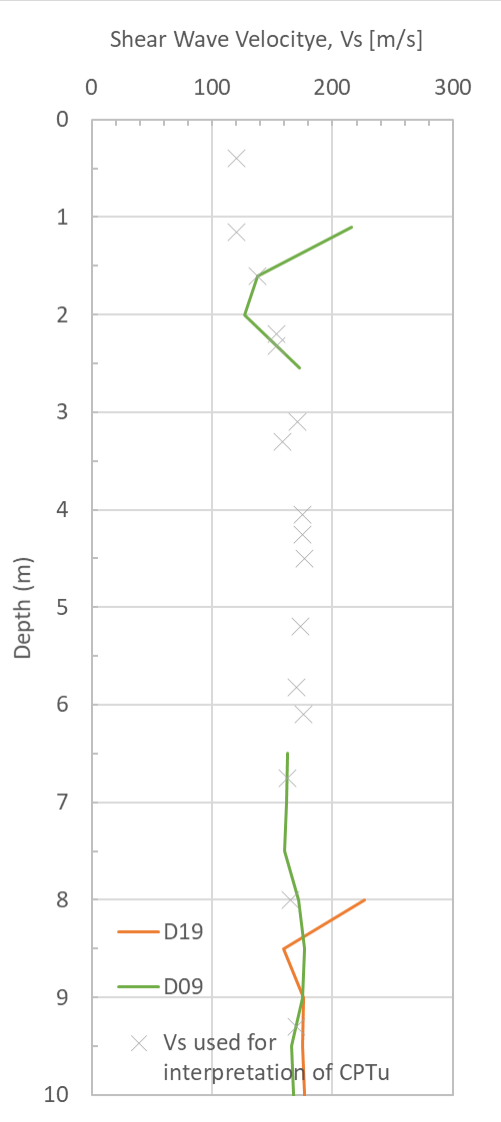

Figure 4.4: Shear-wave velocity measured by D09 and D19, as well as values used for interpretation (presented with small X).

Due to the coarseness of the soil pre-drilling was necessary in both D09 and D19. In D09 the testing was done in two parts, first between 1.10 and 2.55 m and secondly between 6.5 and 17 m. In D19 pre-drilling down to eight meter depth was required to prevent damaging the equipment. D19 consists of measurements from 8-20 m depth.

Interpretation of the SDMT measurements were done using an Excel spreadsheet which calculates the pressures and the intermediate parameters. In the interpretation process, these parameters were used continuously with depth and not only around the samples like with the CPTu results. For the calculation of the small-strain shear modulus (G_0), shear-wave velocity results from D09 were used until eight meter depth. For values deeper, average values of V_s from D09 and D19 were used (since D19 was pre-drilled to 8m). For the gap of measurements in D09 between 2.55 and 6.5 interpreted results from Quinteros et al. (2019) were used. Figure 4.4 shows the measured shear wave velocity at D09 and D10 as well as the values used for interpretation. To achieve values of the shear wave velocity at the same depth as the samples interpolation was used.

The intermediate parameters are then used to calculate additional geotechnical engineering parameters through theoretical and empirical relations. Those parameters are:

1. Friction angle (ϕ')
2. Constrained Modulus (M_{DMT})
3. At-rest earth coefficient (K_0)
4. Young's modulus (E')
5. Relative Density (D_r)
6. State parameter (Ψ)

4.3 Laboratory test procedures

The samples were retrieved by NGI using a ø54 mm GEONOR piston sampler to evaluate the mechanical properties of the soils. Continuous sampling was carried out down to 20 m depth. The accumulated samples are demonstrated in figure 4.5, for both B09 and B19. As seen on the figures the samples are disturbed and a lot of material is missing, specially the coarse layers. Due to the coarseness of the soil the chances of loosing grains, both fine and coarse, are high. Therefore are the samples not fully representable of the *in-situ* ground conditions.

At B09 samples down to 18.3 m depth are available and were tested by NGI. For the samples at B19, samples from 0-11 m depth were tested right away by the author at the laboratory at NTNU. The second half of the samples, down to 20 m depth, was taken by NGI for testing, those results were not available before the end of this project. Grain size distribution testing was of main interest for this project as it gives the best information about the soil type. Plasticity tests were also performed.

4.3.1 Grain size distribution

The grain size distribution is a method used to determine the fraction of soil grains across a specific range of grain sizes. The methods allows for identification of main soil type and amount of fines in the soil. The test was done in two steps. First dry sieving by sieving oven-dried material through sieves with square mesh openings. For this it was necessary to carefully brush the larger grains to remove attached fines off. The second step is for those samples that have more than 10% fines content (<0.075 mm). Then a hydrometer analysis, test based on sedimentation rate, was done on the fines content. The results were drawn up as grain size distribution curves in an associated grain size distribution chart. The curve is presented to show the percentages of particles finer than given particle size, plotted against the particle size on a logarithmic scale. The results are also used for classification according to the Unified Soil Classification System (USCS).

It is possible that elongated grains pass through the sieve along their longest axis, whereas plate shaped grains could drop along the diagonal in the mesh openings. It is not possible to account for these inaccuracies in the sieving analysis.

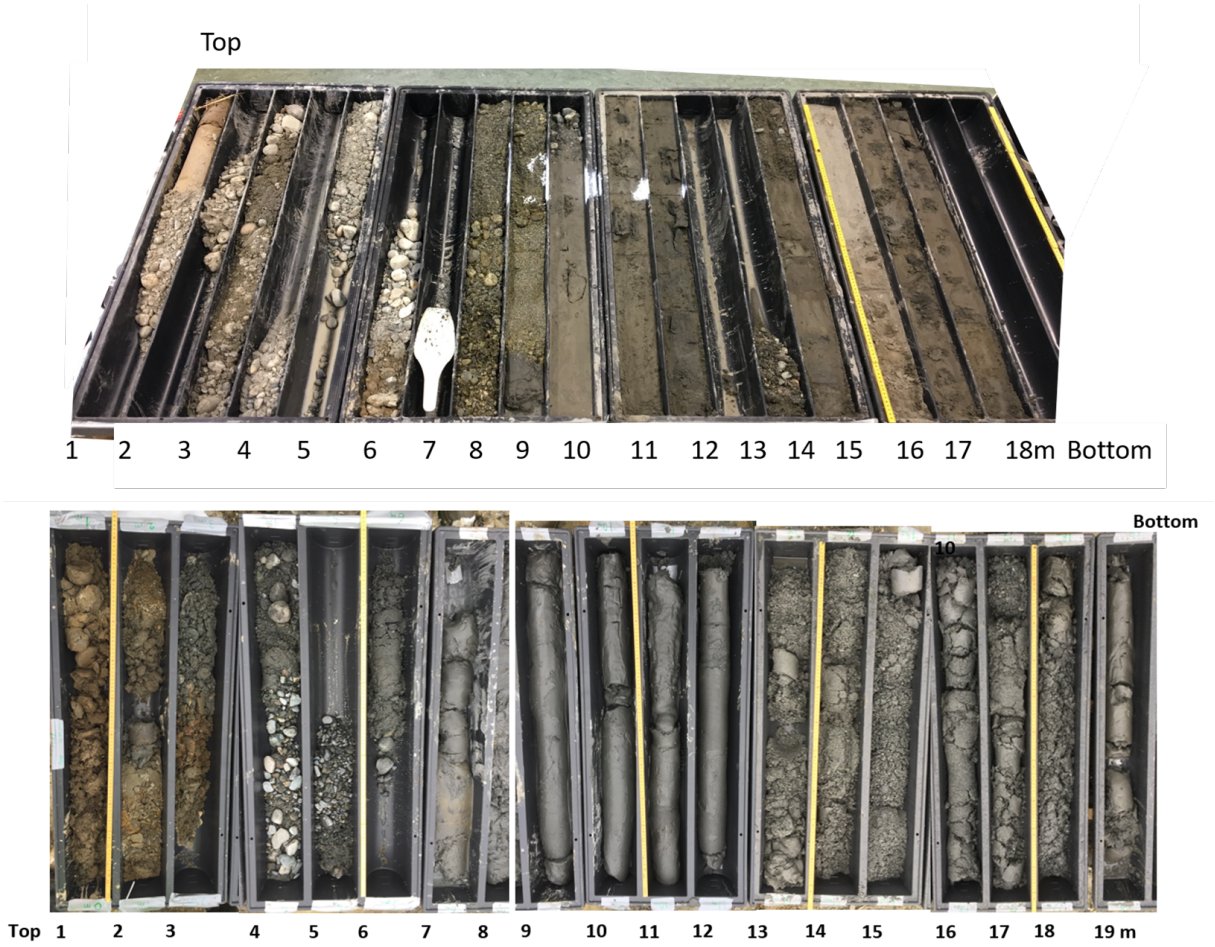

Figure 4.5: Soil samples from BH09 (top) and B19 (bottom).

4.3.2 Unified Classification System

According to the USCS, coarse grained soils are those that consist of more than 50% of the material being coarser than sieve No. 200 (0.075 mm). If more than 50% of the material goes through that sieve it is classified as fine grained soil. A rough table with step by step instructions for the USCS classification can be seen in figure 4.6.

Coarse grained soils are divided into gravel/gravelly soils (G) and sands/sandy soils (S), depending on how much % of the material passes through sieve No. 4 (4.75 mm). If more than 50% of the material passes through sieve No. 4 and retains on sieve No. 200, it is classified as sand or sandy. However if 50% or more retains on sieve No. 4, it is classified as gravel or gravelly. Further classification of gravels and sand is dependent on the amount of fine material within the sample. If less than 5% fines, the material is additionally classified as well-graded (W) or poorly-graded (P), depending on the coefficient of curvature (C_c) and the coefficient of uniformity (C_u) of the sample.

$$C_c = \frac{D_{30}^2}{D_{10} \cdot D_{60}} \tag{4.1}$$

$$C_u = \frac{D_{60}}{D_{10}} \tag{4.2}$$

Criteria for Assigning Group Symbols and Group Names Using Laboratory Tests[A]				Soil Classification	
				Group Symbol	Group Name[B]
COARSE-GRAINED SOILS	Gravels (More than 50 % of coarse fraction retained on No. 4 sieve)	Clean Gravels (Less than 5 % fines[C])	Cu ≥ 4.0 and 1 ≤ Cc ≤ 3.0[D]	GW	Well-graded gravel[E]
			Cu < 4.0 and/or [Cc < 1 or Cc > 3.0][D]	GP	Poorly graded gravel[E]
		Gravels with Fines (More than 12 % fines[C])	Fines classify as ML or MH	GM	Silty gravel[E,F,G]
			Fines classify as CL or CH	GC	Clayey gravel[E,F,G]
More than 50 % retained on No. 200 sieve	Sands (50 % or more of coarse fraction passes No. 4 sieve)	Clean Sands (Less than 5 % fines[H])	Cu ≥ 6.0 and 1.0 ≤ Cc ≤ 3.0[D]	SW	Well-graded sand[I]
			Cu < 6.0 and/or [Cc < 1.0 or Cc > 3.0][D]	SP	Poorly graded sand[I]
		Sands with Fines (More than 12 % fines[H])	Fines classify as ML or MH	SM	Silty sand[F,G,I]
			Fines classify as CL or CH	SC	Clayey sand[F,G,I]
FINE-GRAINED SOILS	Silts and Clays	Inorganic	PI > 7 and plots on or above "A" line[J]	CL	Lean clay[K,L,M]
	Liquid limit less than 50		PI < 4 or plots below "A" line[J]	ML	Silt[K,L,M]
		organic	$\frac{\text{Liquid limit – oven dried}}{\text{Liquid limit – not dried}} < 0.75$	OL	Organic clay[K,L,M,N] / Organic silt[K,L,M,O]
50 % or more passes the No. 200 sieve	Silts and Clays	Inorganic	PI plots on or above "A" line	CH	Fat clay[K,L,M]
	Liquid limit 50 or more		PI plots below "A" line	MH	Elastic silt[K,L,M]
		organic	$\frac{\text{Liquid limit – oven dried}}{\text{Liquid limit – not dried}} < 0.75$	OH	Organic clay[K,L,M,P] / Organic silt[K,L,M,Q]
HIGHLY ORGANIC SOILS	Primarily organic matter, dark in color, and organic odor			PT	Peat

[A] Based on the material passing the 3-in. (75-mm) sieve.
[B] If field sample contained cobbles or boulders, or both, add "with cobbles or boulders, or both" to group name.
[C] Gravels with 5 to 12 % fines require dual symbols:
GW-GM well-graded gravel with silt
GW-GC well-graded gravel with clay
GP-GM poorly graded gravel with silt
GP-GC poorly graded gravel with clay
[D] $Cu = D_{60}/D_{10}$ $Cc = \frac{(D_{30})^2}{D_{10} \times D_{60}}$
[E] If soil contains ≥15 % sand, add "with sand" to group name.
[F] If fines classify as CL-ML, use dual symbol GC-GM, or SC-SM.
[G] If fines are organic, add "with organic fines" to group name.
[H] Sands with 5 to 12 % fines require dual symbols:
SW-SM well-graded sand with silt
SW-SC well-graded sand with clay
SP-SM poorly graded sand with silt
SP-SC poorly graded sand with clay
[I] If soil contains ≥15 % gravel, add "with gravel" to group name.
[J] If Atterberg limits plot in hatched area, soil is a CL-ML, silty clay.
[K] If soil contains 15 to <30 % plus No. 200, add "with sand" or "with gravel," whichever is predominant.
[L] If soil contains ≥30 % plus No. 200, predominantly sand, add "sand" to group name.
[M] If soil contains ≥30 % plus No. 200, predominantly gravel, add "gravelly" to group name.
[N] PI ≥ 4 and plots on or above "A" line.
[O] PI < 4 or plots below "A" line.
[P] PI plots on or above "A" line.
[Q] PI plots below "A" line.

Figure 4.6: Rough demonstration of the unified soil classification system (ASTM International (2018)).

Where D_{10}, D_{30} and D_{60} are the particle sizes corresponding to 10%, 30% and 60% passing on the cumulative particle-size distribution curve, respectively. If the material consists of more than 12% fines the classification also becomes dependent on the plasticity of the soil (Atterberg limits). Therefore gets an additional classification of silty sand/gravel (SM/GM) if little or no plasticity, or as clayey sand/gravel (SC/GC) if the plasticity is significant. If the fines content is between 5-12% a dual symbol is required; i.e. well-graded gravel/sand with silt (GW-GM/SW-SM)

or poorly graded gravel/sand with clay (GP-GC/SP-SC), depending on plasticity. Also if gravelly soil contains ≥15% sand the group name "with sand" is added to the end. Same for the sandy soil that contains ≥15% gravel, then "with gravel" is added.

Fine grained soils are classified into clay (C) and/or silt (M) depending on their plasticity presented by the Atterberg tests: liquid limit (LL) and plasticity Index (PI). Additionally to the classification of fine material the soil is classified "with gravel" or "with sand" if 15-30% material retains on the No. 200 sieve, depending on the predominant one. If the material contains ≥30% of predominantly sand or gravel, "sandy" or "gravelly", respectively, is added to the group name.

The third classification category which includes highly organic soils is identified by visual examination (organic matter, dark in color and has an organic odor) and is classified as peat (P).

4.4 Detailed interpretation of measured data

Once the measured data as been corrected and necessary parameters calculated it is easier to interpret the data and attain useful geotechnical engineering parameters commonly used in practice.

4.4.1 Soil identification

As specified in in the literature review the best way to identify soils is by using available classification charts presented by various authors. To get the most precise results one should start by looking at the micro-structure of the soil as the classification charts and other empirical correlations work best with "ideal"-soil or soil with no or little micro-structure. Classification charts based CPTu parameters proposed by Robertson (1990), Robertson (2009a), Robertson (2016) and Schneider et al. (2008) were chosen for soil identification in this project as no micro-structure was present. These charts should give a reasonable prediction of the soil type, however, since these charts are global in nature there might be some overlapping of data.

For comparison with the charts the soil behaviour index (I_c) obtained from CPTu data as well, the material index (I_D) obtained from DMT data and the Unified Soil Classification System were used.

4.4.2 Geotechnical engineering parameters

From the *in-situ* investigations there are many empirical and theoretical correlations to derive geotechnical engineering parameters used in practice.

Table 2.2 shows the applicability and reliability of a certain parameters derived from CPTu data; 1 being highly reliable and 5 being not reliable at all. It is evident that CPTu results in sand can give different information than CPTu results in clay. In this project it will be focused on those parameters derived from CPTu applicable in sand, with the minimum moderate reliability (3). For comparison the same parameters will be derived from DMT results. Equations used are summarized in table 4.1.

4.4.2.1 Relative density

For comparison of the calculated relative density based on results of the CPTu with equations presented in table 4.1. The relative density can also be estimated from DMT data. Figure 4.7 shows the recommended correlation between the relative density (D_r) and the horizontal stress index (K_D). This correlation was originally presented by Campanella and Robertson (1986) and has been updated few times to its present state. This is ideal for normal-consolidated (NC), uncemented sands. If the sands are over-consolidated and/or cemented the correlation will overestimate the relative density (Marchetti et al. (2001)).

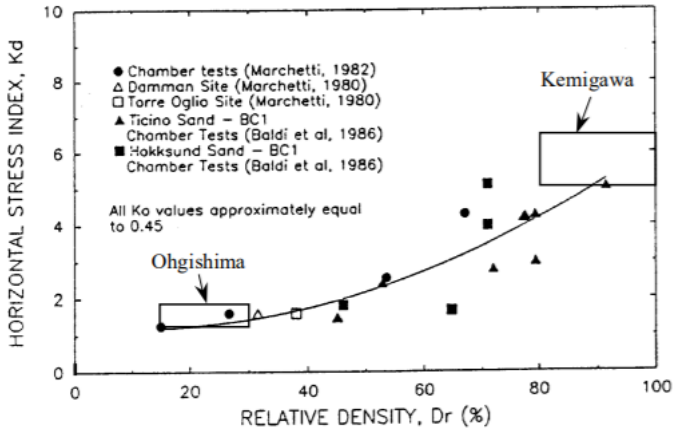

Figure 4.7: Correlation K_D-D_r for NC-uncemented sands (Marchetti et al. (2001)).

4.4.2.2 State parameter

Based on previous methods (Plewes et al. (1992), Jefferies and Davies (1991), Jefferies and Been (2006)), Robertson (2009a) developed contours of the state parameter on the updated Q_{tn}-F_s SBTn chart for uncemented, Holocenic age soil (formed after the last Ice-Age), see figure 2.11. These contours give approximate results and are only to be used to evaluate a value for low-risk projects. Robertson (2010) presented a numerical relationship between the CPTu data and the state parameter contours from the SBTn chart. This empirical relationship is based on the clean sand equivalent normalized cone resistance ($Q_{tn,cs}$) which describes the *in-situ* state of sandy soils (Robertson and Cabal (2014)).

The state parameter can also be estimated from DMT results through P_1 (the pressure needed to cause a 1 mm expansion of the membrane) and the average stress state ($I_1 = \frac{\sigma_1+\sigma_2+\sigma_3}{3}$, where $\sigma_2 = \sigma_3 = \sigma_1 \cdot K_0$). The at-rest earth coefficient (K_0) is calculated from the horizontal stress index (K_D), as seen on table 4.1. The available relationship between the state parameter and the DMT results, obtained by Konrad (1988), is shown in figure 4.8. The behaviour is controlled by the normalized steady state parameter (Ψ/Ψ_1). When $\Psi < 0$ the behaviour is dilative and Ψ_1 can be approximated as e_{min} - e_{max}, as for when $\Psi > 0$, Ψ_1 is contractive and dependent on the compressibility of the sand in its loosest state and on the slope of the steady state line.

The values of e_{min} and e_{max} are generally estimated from laboratory results and can vary from 0.1-0.8 depend-

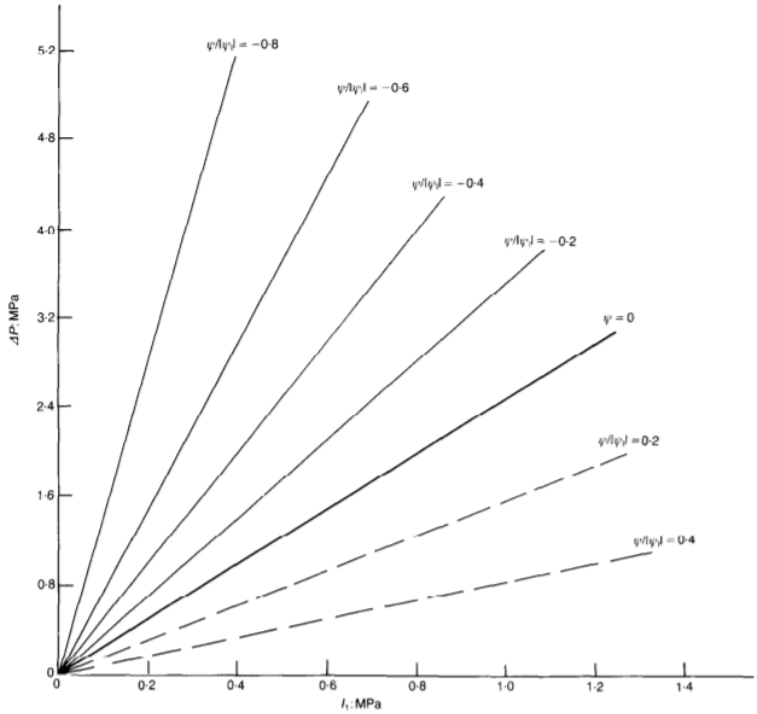

Figure 4.8: Correlation between P_1 and the normalized state parameter (Ψ/Ψ_1) (Konrad (1988))

ing on the *in-situ* state. Those values were derived from the minimum and maximum dry density presented by Quinteros et al. (2019) for the Øysand site and take values on the range of 0.35-0.47.

4.4.2.3 Friction angle

More than one relationship has been presented between CPTu data and the friction angle, all shown in table 4.1. The relationships based on the state parameter, the critical state friction angle and the clean sand equivalent normalized cone resistance have an advantage over the older correlations since they include the importance of grain characteristics and mineralogy as well as the soil type through (Robertson and Cabal (2014)).

Using the Dilatometer test to estimate the friction angle is not the most reliable correlation, however, it can give a good prediction of the shape of the friction angle (ϕ') with depth. A commonly used correlation based on the horizontal stress index (K_D) is presented in table 4.1 and generally is a lower boundary value, with an underestimation of about 2-4° (Marchetti et al. (2001)).

4.4.2.4 Young's modulus

This correlation of the Young's modulus to the CPTu data through the SBTn index and the corrected cone resistance are presented in table 4.1.

Calculating the Young's modulus from DMT data is a difficult task as there is no obvious relationship between the modulus (M_{DMT}) and the dilatometer modulus (E_D). However, by using the material index (I_D) and the hor-

izontal stress index (K_D), in addition to the modulus, a correction factor can be derived (R_M) which connects all intermediate parameters of the DMT together and makes it possible to calculate the Young's modulus. The relationships are presented in table 4.1.

4.4.2.5 Hydraulic conductivity

The hydraulic conductivity (k) describes how easily fluid can travel through the soil through pore spaces and fractions. Theoretical values of permeability are available in relation to Robertson (1990) classification chart (see figure 2.1). These values, based on the soil classification index (I_c), can also be calculated with equations presented in table 4.1. Unfortunately no relationship was found between DMT measurements and the permeability. However, a relationship between D_{10} and the hydraulic conductivity can be found. Hazen (1930) proposed a simple empirical relationship which is still used today, applicable for both fine- and coarse grained soils.

$$k = C \cdot D_{10}^2 \tag{4.3}$$

Where D_{10} is the 10% passing grain size (cm) and C is a constant varying from 0.5-1.5. An average value of C = 1 was chosen for the calculation.

Table 4.1: Summary of equations used for calculations of geotechnical engineering parameters, based on data from CPTu and DMT.

Parameter	Symbol	CPTu		SDMT	
Relative density	D_r	$D_r = \frac{1}{C_2} \cdot \ln \frac{Q_{tn}}{C_0}$	Robertson and Cabal (2014)	Correlation with horizontal stress index, K_D Figure	Marchetti et al. (2001)
		$D_r = \frac{1}{C_2} \cdot \ln \frac{q_c}{C_0 \cdot (\sigma'_{v0})^{C_2}}$	Baldi *et. al.* 1986 in Lunne et al. (1997)		
		*$C_0 = 15.7/157$, $C_1 = 0.55$, $C_2 = 2.41$			
State parameter	Ψ	$\Psi = 0.56 - 0.33 \cdot \log(Q_{tn,cs})$	Robertson and Cabal (2014)	Correlation with ΔP and average stress state Figure	Konrad (1988)
		*$Q_{tn,cs} = K_c \cdot Q_{tn}$, if $I_C > 1.64$, else $Q_{tn,cs} = Q_{tn}$			
		*$K_c = 5.581 \cdot I_c^3 - 0.403 \cdot I_c^4 - 21.63 \cdot I_c^2 + 33.75 \cdot I_c - 17.88$			
Friction angle	ϕ'	$\phi' = 17.6 + 11 \cdot \log(Q_{tn})$	Kuhlawy & Mayne 1990 (in Robertson and Cabal (2014))	$\phi' = 28 + 14.6 \cdot \log(K_D) - 2.1 \cdot \log(K_D)^2$	Marchetti et al. (2001)
		$\phi' = \arctan\left[\left(\frac{1}{2.68} \cdot \left(\log \frac{q_c}{\sigma'_{v0}}\right) + 0.29\right)\right]$	Robertson and Campanella (1983)		
		$\phi' = \phi_{cv} - 48 \cdot \Psi$	Robertson (2010)		
		$\phi' = \phi_{cv} + 15.84 \cdot \log(Q_{tn,cs}) - 26.88$	Robertson and Cabal (2014)		
		*ϕ_{cv} = 33-40°			
Stiffness Modulus	E'	$E' = \{0.015 \cdot 10^{0.55 \cdot I_c + 1.68}) \cdot (q_t - \sigma_{v0})\}$	Robertson (2009a)	$E' = \frac{(1+\nu)(1+\nu)}{(1-\nu)} \cdot M_{DMT}$	Marchetti (1980)
				*$M_{DMT} = R_M \cdot E_D$	
				$I_D < 3.0$, $R_M = 0.14 + 2.36 \cdot \log(K_D)$ If $I_D > 3.0$, $R_M = 0.5 + 2 \cdot \log(K_D)$ If $0.6 < I_D < 3.0$, $R_M = R_{M,0} + (2.5 - R_{M,0}) \cdot log(K_D)$ $R_{M,0} = 0.14 + 0.15 \cdot (I_D - 0.6)$ If $K_D > 10$, $R_M = 0.32 + 2.18 \cdot \log(K_D)$	
Permeability	k	$10^{0.952 - 3.04 \cdot I_c}$, for $1 < I_c < 3.27$	Robertson and Cabal (2014)	-	-
		$10^{-4.52 - 1.37 \cdot I_c}$, for $3.27 < I_c < 4$			
At-rest earth coefficient	K_0	-	-	$K_0 = 0.376 + 0.095 K_D - 0.0017 \frac{q_c}{\sigma'_{v0}}$	Marchetti et al. (2001)
				$K_0 = 0.376 + 0.095 K_D - 0.0046 \frac{q_c}{\sigma'_{v0}}$	
				*artificial sand (top) / natural Po river sand (bottom)	

Chapter 5

Results and interpretation of data

This section presents the results of the soil classification, based on results from both *in-situ*- and laboratory testing, following the procedures introduced in chapter 4.

5.1 Soil behaviour type

5.1.1 CPTu

According to procedures recommended by Robertson (2016) the first thing to do is to check if any micro-structure is presented in the soil. As seen on figure 5.1 no micro-structure should be expected in the soil as it classifies as "ideal". The fact that the soils classify as "ideal increases the reliability of which increases the reliability of all theoretical and empirical relation used for detail interpretation of CPTu data.

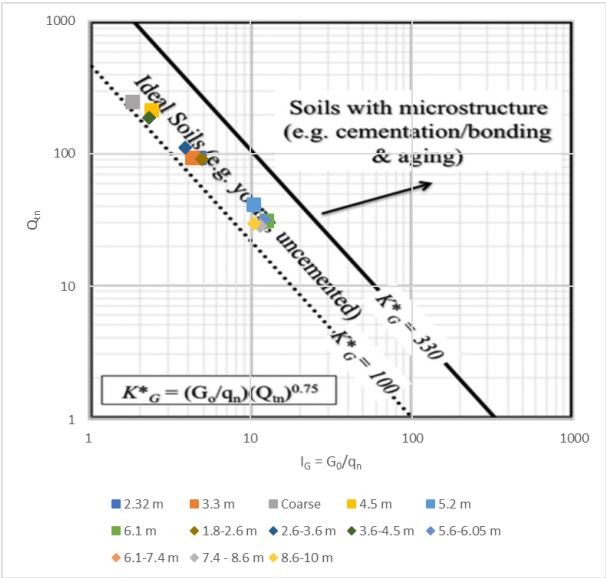

Figure 5.1: Chart presented by Robertson (2016), no micro-structure is to be expected in the soil.

According to the Q_{tn}-F_r classification chart presented by Robertson (2016) the data from the top ten meters of the soil classifies as dilative sands, see figure 5.3. Further, the data can be classified as soil type according to the SBTn chart. It is evident that the soil falls into three groups by depth. The first layer (I) of clean sands from 1.8-3.5 m depth, the second layer (II) which lies close to the boarder of gravelly sands and clean sands from 3.5-5 m depth and the third layer (III) of clean sands to sand mixtures, silty sand to sandy silt, from 5 - 10 m depth. The second chart presented by Robertson (1990), Q_t-B_q, presents the same groupings, however, the classification is coarser. Groups (I) and (II) classify as gravelly sand and group (III) classifies as clean sands.

The soil behaviour index presented with the SBTn chart as well as the distribution of the calculated soil behaviour index versus the standard classifications are shown on figure 5.3. The calculated I_c, calculated with equation 2.9, gave values on the range of 1.66-1.78 for group (I), of 1.45-1.62 for group (II) and of 2.19-2.49 for group (III). When compared to the theoretical values presented by Robertson (2009a) both groups (I) and (II) fall within zone (6) of clean sands to silty sand.

The pore pressure ratio ranges between -0.1 and 0.1 for the ten meter soil column.

Classification charts presented by Schneider et al. (2008), see figure 5.2, show the same groups by depth. groups (I) and (II) classify as essentially drained sands, group (I) being coarser than group (II). group (III) lies on the boarder of essentially drained sands and translational soils, emphasizing the classification by the Robertson charts of sand mixtures. The updated chart by Robertson (2016) shows the material as dilative sand.

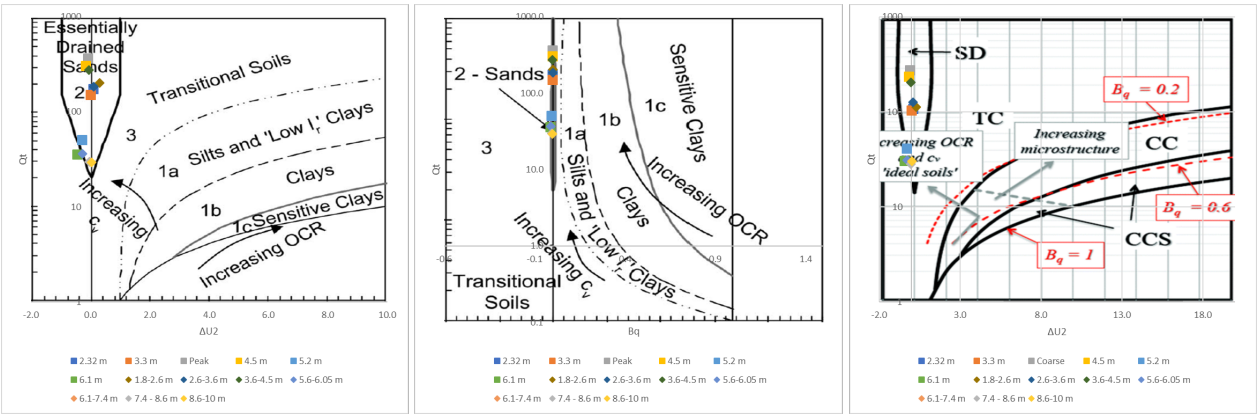

Figure 5.2: Results of soil classification based on charts presented by Schneider et al. (2008) (left and middle), and the updated chart by Robertson (2016) (right).

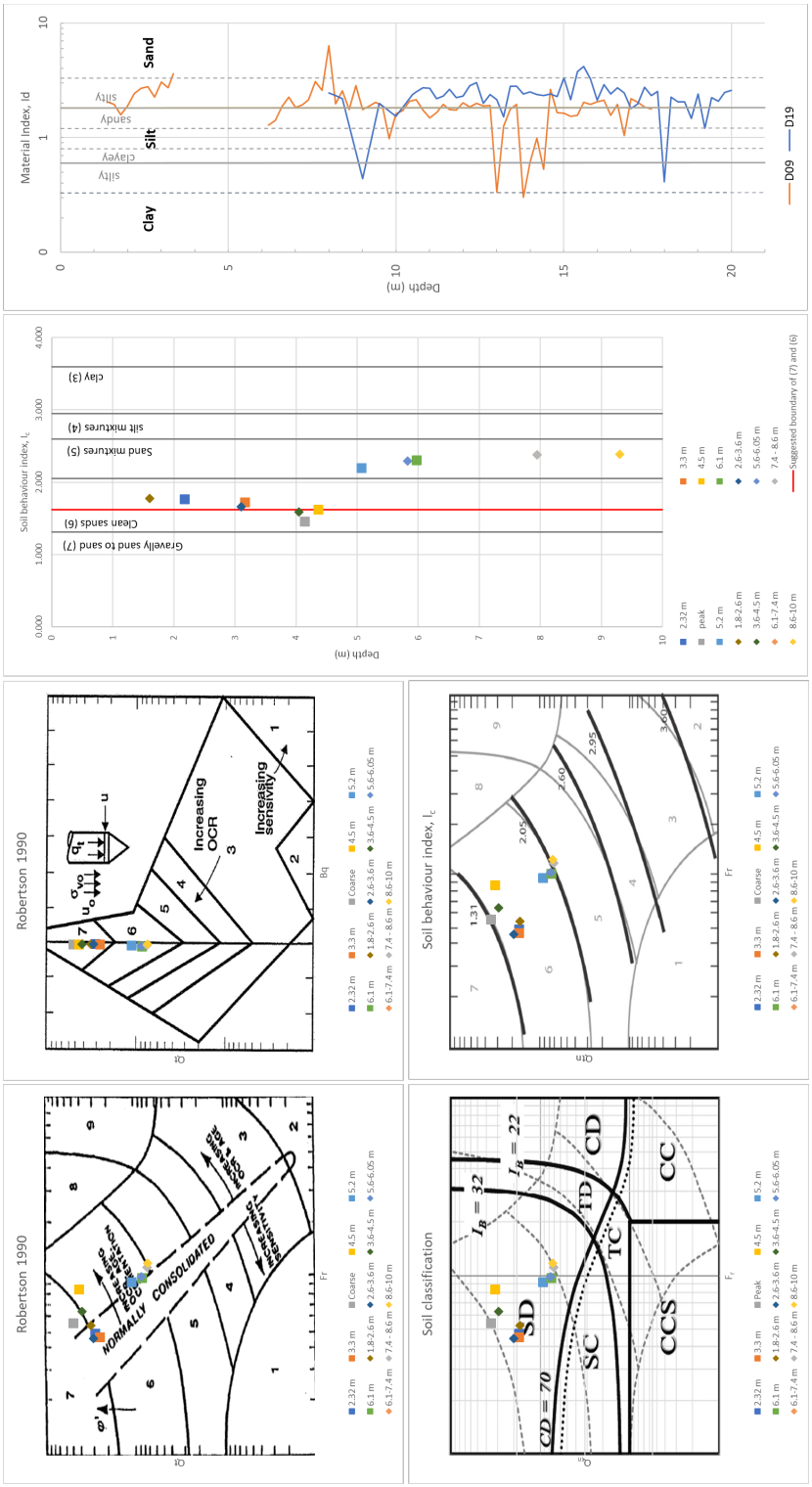

Figure 5.3: Results of SBTn charts: (Top) Soil classification according to Robertson (1990), (bottom left) Soil classification according to Robertson (2016) (bottom right) SBTn with contours of the SBTn Index (I_c) (Robertson (1990)) (To the right) the calculated SBTn index with depth (To the far right) The material index (I_D) from the DMT test with depth.

5.1.2 DMT

The material index I_D calculated from the measured parameters of the dilatometer gives an indication of the penetrated soil type. Figure 5.7 shows the index with depth for both D09 and D19. In D09 the soil mainly classifies as silty sand and sandy silt, with a coarse sand around 8.5 m depth. Unfortunately it was necessary to pre-drill trough the coarsest layer between 3.5-5 m depth in both testings, which does emphasize the coarseness of the layer. In total, it is evident that the soil column at D09 is finer than the soil at D19. Below ten meter depth the soil is sandy at D19 while it classifies more as sandy silt at D09 with a clayey silt / silty clay layer just below 15 m depth.

5.1.3 Shear wave velocity

Measurements of the shear wave velocity in D09 and D19 are presented in figure 4.4. Pre-drilling was necessary from 2.5-6 m depth at D09 and all the way down to eight meter depth at D19 due to coarse soil.

At D09, below six meter depth the velocity can be estimated as 170 m/s. However, at D19 the velocity can be divided in two. The first, between 8-14 m depth where the velocity can be estimated 160 m/s. The second layer below 14 m depth with the average velocity of 217 m/s and a peak of 274 m/s. Again indicating that the soil is coarser in D19.

The classification chart published by Robertson 1995 (Lunne et al. (1997)) which is based on the small-strain shear modulus (G_0) classifies the soil in the same groups as the Robertson 2016/Robertson 1990 chart, however the classifications are coarser. Group (I) from 2-3.6 m depth classifies as sand, group (II) as gravelly sand from 3.6-5 m depth and group (III) from 5-11 m depth as sand mixtures. The data was also plotted up using the normalized cone resistance depending on the calculated stress exponent, n (Q_{tn}). It shows the same classifications, however, the Q_{tn} is generally lower than Q_t as expected in coarse soils.

5.1.4 Grain size distribution

The samples from both sample holes (B09 and B19) are presented in figure 4.5. In B09 the samples show sandy soil with some gravel in the top eight meters of the soil column. A lot of material is also missing from theses depths. Below seven meter depth the soil becomes finer and looks more compact, indicating the increasing fines content. Another coarse layer is found between 13-15 m depth where material is missing. The conditions are similar in B19. The soil looks finer in the top three meters, however, between 3-5 m depth the soil seems to consist of sand/gravel with larger grain sizes than in B09. At seven meter depth the fines content increases and until 13 m depth the soil looks silty and compact. The second layer in B19 also seems to be thicker as the sample indicate sandy soil down to 19 m depth.

The grain size distributions curves (GSDC) for B09 and B19 are shown on figure 5.5. Results from B19 were only available down to 11 m depth. It is evident that the data groups in two: group (a) of sand with varying content of silt and gravel, reaches from 2-10 m depth in BH09 and from 1.5-6 m depth in B19. According to the USCS the group (a) classifies mainly as sand with gravel and/or silt in BH09. However, the material in B19 is coarser and classifies

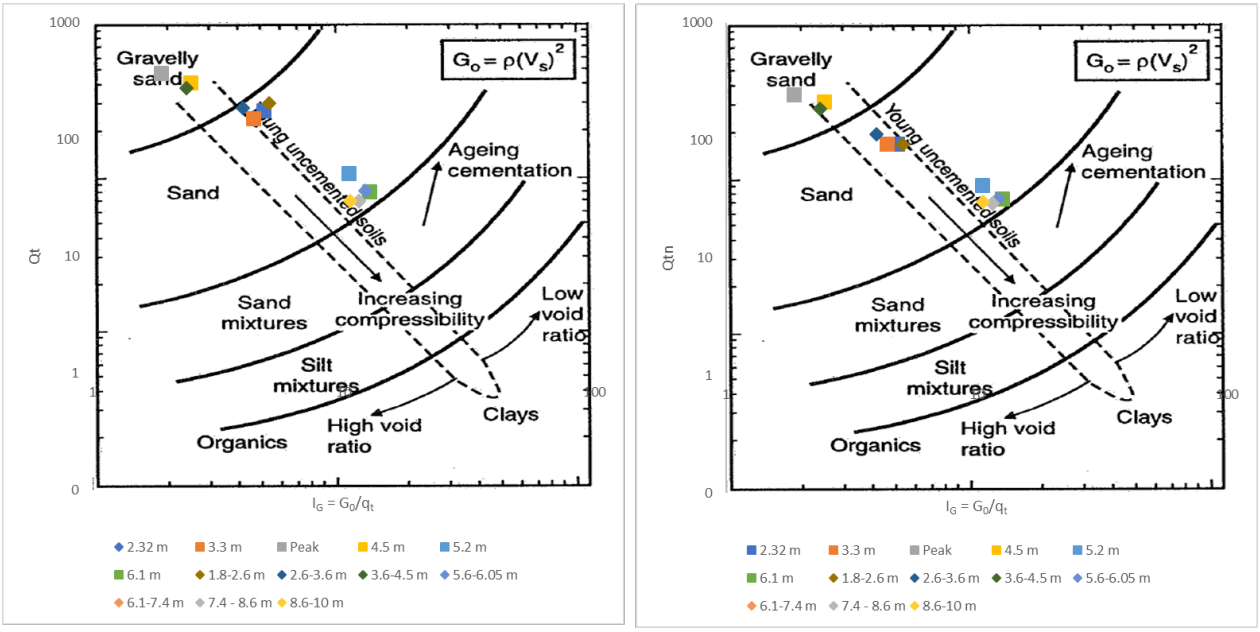

Figure 5.4: Classification chart based on the small-strain shear Modulus (G_0) and Q_t (left) and also with the Q_{tn} based on the stress exponent, n (right).

as gravel with sand. The second group (b), under- and overlying group (a), classifies as sand mixture as the layers vary between silty sand to sandy silt.

It is evident that the portion of sand is in majority at Øysand and generally lies between 40-80% of the total sample. In the top 6 m the gravel content exceeds the content of silt and clay with about 20-40% of the total sample in B09. In B19 the gravel content ranges between 15-70% of the total sample, hence the gravel classification. Below 6 m depth the silt and clay content increases to 20-80% of the total sample and dominates the gravel content, which decreases with depth. With an exception at ca. ten meter depth in B09 where the gravel content increases to >20% of the total sample.

Comparison of results from the SBTn charts and the USCS with depth are presented in table 5.2.

5.1.5 Plasticity

Plasticity test according to the Atterberg methods were done on samples from B19. No plasticity was measured in the soil.

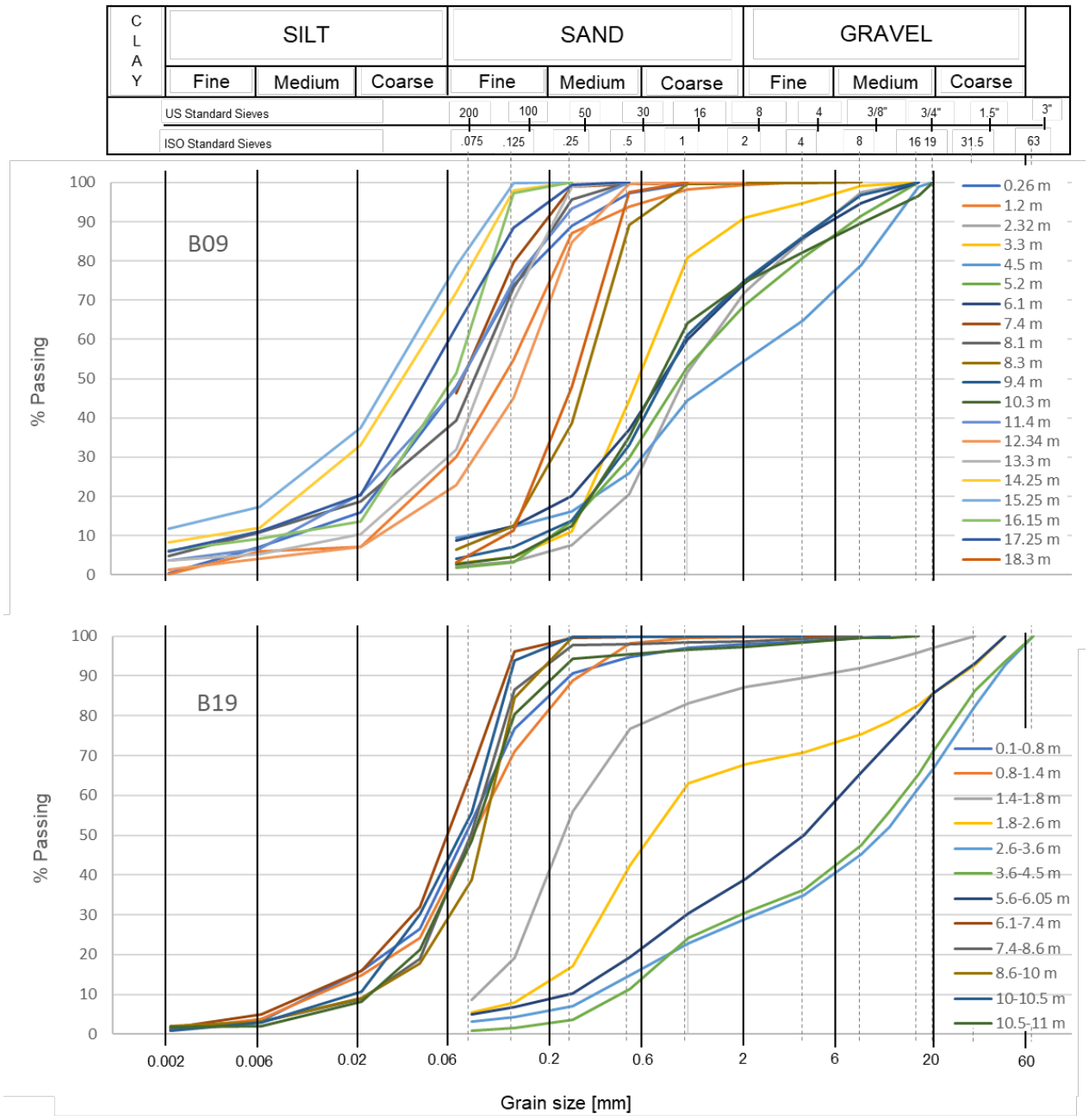

Figure 5.5: Representative GSDC for B09 (top) and B19 (bottom).

5.2 Engineering parameters

This section presents the results of the calculated geotechnical engineering parameters used in practice, based on data from CPTu and DMT. The results will be presented in terms of the three classification groups (I, II and III) mentioned earlier. The results are plotted up in figure 5.7. Design values for each group were also chosen,

presented in table 5.1 and shown on figure 5.7.

Table 5.1: Chosen design values for the classified groups.

	Depth	Relative density	Sate parameter	Friction angle	Young's modulus	Permeability
	[m]			[°]	[Mpa]	[m/s]
Group (I)	1.8-3.5	0.7	-0.15	38.5	38	4.E-05
Group (II)	3.5-5	1	-25	44	82	5.E-04
Group (III)	5-10	0.22	-0.08	34	35	2.E-06

5.2.1 Relative Density

The relative density was calculated using interpreted CPTu data with equations presented in table 4.1. The equations give similar results, with 97% correlation, as seen on figure 5.7. Equation presented by Robertson and Cabal (2014) seems to give a slightly higher values than equation presented by Baldi *et. al.* 1986 (in Lunne et al. (1997)), specially for the sand mixtures as values for the clean sand seem to fit very well. Values of the relative density correlated from the DMT results do not differ a lot from the calculated values for group (I), however for group (II) and (III) they seem to underestimate and overestimate the relative density, respectively.

For group (I) the calculated relative density lies between 0.7 and 0.8, between 1 and 1.12 for group (II) and between 0.1-0.4 for group (III). The chosen design values are presented in table 5.1.

5.2.2 State parameter

The state parameter was calculated using equation presented in table 4.1 and as well to empirical correlations presented by Robertson (2009a).

The calculated values range between -0.14 and -0.1 for group (I), between -0.22 and -0.19 for group (II) and between -0.04 and -0.03 for group (III), see figure 5.7. As seen on figure 5.6, the value of the state parameters decreases with the groups. group (II) has values < -0.2, group (I) lies between -0.15 and -0.2 and group (III) lies on and slightly below the -0.15 line. The theoretical values seem to be somewhat lower than the calculated values of the state parameter. The state parameter calculated by the DMT shows much lower values. Due to lack of information about the exact minimum and maximum void ratios it was necessary to assume the value from the dry density. These assumptions have a huge impact on the resulting state parameter.

A chosen design value for each group can be seen in table 5.1

5.2.3 Friction angle

From the CPTu data the friction angle can be estimated from four different relationships, equations presented in table 4.1, as well as from a classification chart from Robertson (2009a). Friction angle estimated from the DMT is

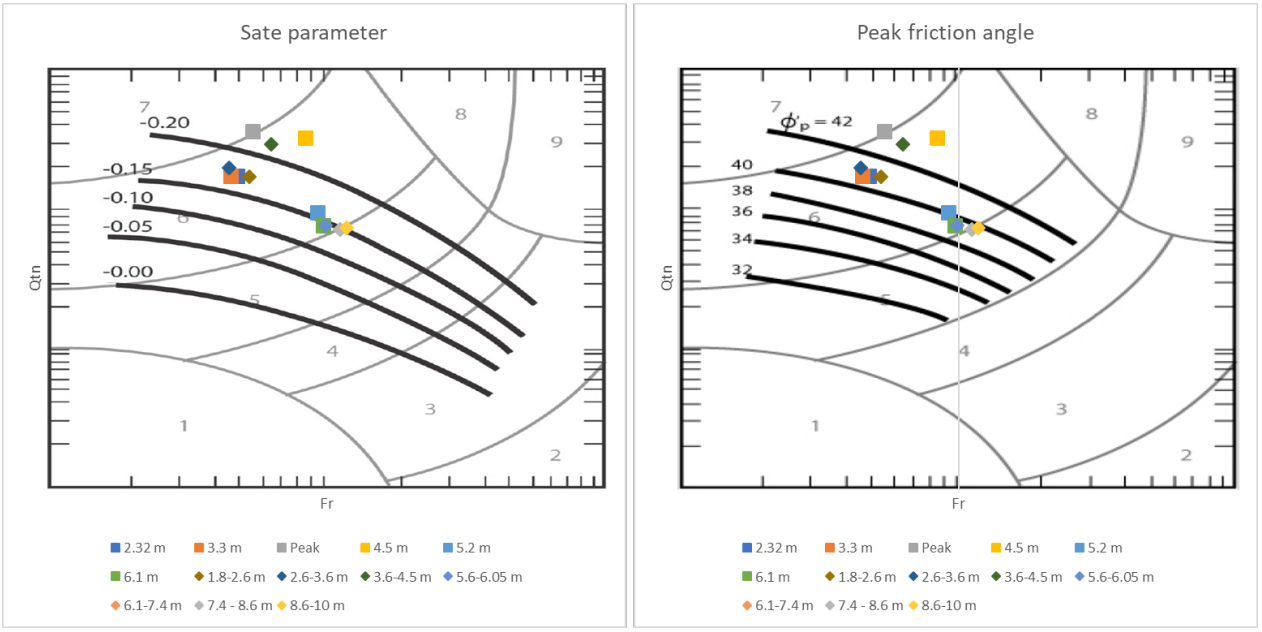

Figure 5.6: (Left) SBTn with contours of the state parameter (Ψ) and (right) SBTn with contours of the peak friction angle (ϕ') (Robertson (1990)).

dependent on the horizontal stress index (K_D) and calculated from equation also presented in table 4.1. Friction angles with depth can be seen on figure 5.7. Below 5 m depth it is the friction angle depending on the clean sand normalization that seems to over-estimate the friction angle. However, below 5 m depth the friction angle based on the state parameter gives the highest values. For group (I) the friction angle lies around 38-39°, for group (II) the friction angle is approximately 42-45° and for group (III) it starts around 34° and decreases down to 32-33°. According to the classification chart presented by Robertson (2009a), see figure 5.6, the friction angle for group (II) is higher than 42°, approximately 41° for group (I) and approximately 39-40° for group (III). A chosen design value for each group can be seen in table 5.1.

The friction angles derived from the DMT results give continuous information about the friction angle. On average they seem to fit quite well together, however since the DMT is continuous with depth it is more sensitive to the silty/clayey layers that have a lower friction angle.

5.2.4 Young's modulus

The young's modulus can be calculated both depending on CPTu data and with the intermediate DMT data, as seen in table 4.1. As seen on figure 5.7 the correlation between the Young's modulus calculated from CPTu and from DMT vary a lot, where the Young's modulus calculated from CPTu has higher results.

According to the results of the CPTu, E', takes a value between 40 and 50 MPa for group (I), 80-92 MPa for group (II) and 33-45 MPa for group (III). As for the DMT the value of E' varies with depth, below 5 m depth the value in D09 is on average approximately 20 MPa and only around 10 MPa in D19. A chosen design value for each group

can be seen in table 5.1

5.2.5 Permeability

The permeability was calculated from the CPTu results with equation presented in table 4.1. According to theoretical values presented by Robertson (2009a) in table 2.1 the permeability of the soil should range between $1{\cdot}10^{-7}$-1 m/s. The calculated values mainly fall within zone (6) and (5) of the SBTn chart as clean sand to sand mixtures. group (I) takes values between $5{\cdot}10^{-5}$ and $1{\cdot}10^{-4}$ m/s (zone 6), group (II) takes values between $1.6{\cdot}10^{-4}$ and $5.1{\cdot}10^{-4}$ m/s (zone 6) and group (III) takes values between $1.8{\cdot}10^{-6}$ and $7.5{\cdot}10^{-6}$ m/s (zone 5).

The results from the Hazan formula give comparable results to he CPTu, as seen on figure 5.7.

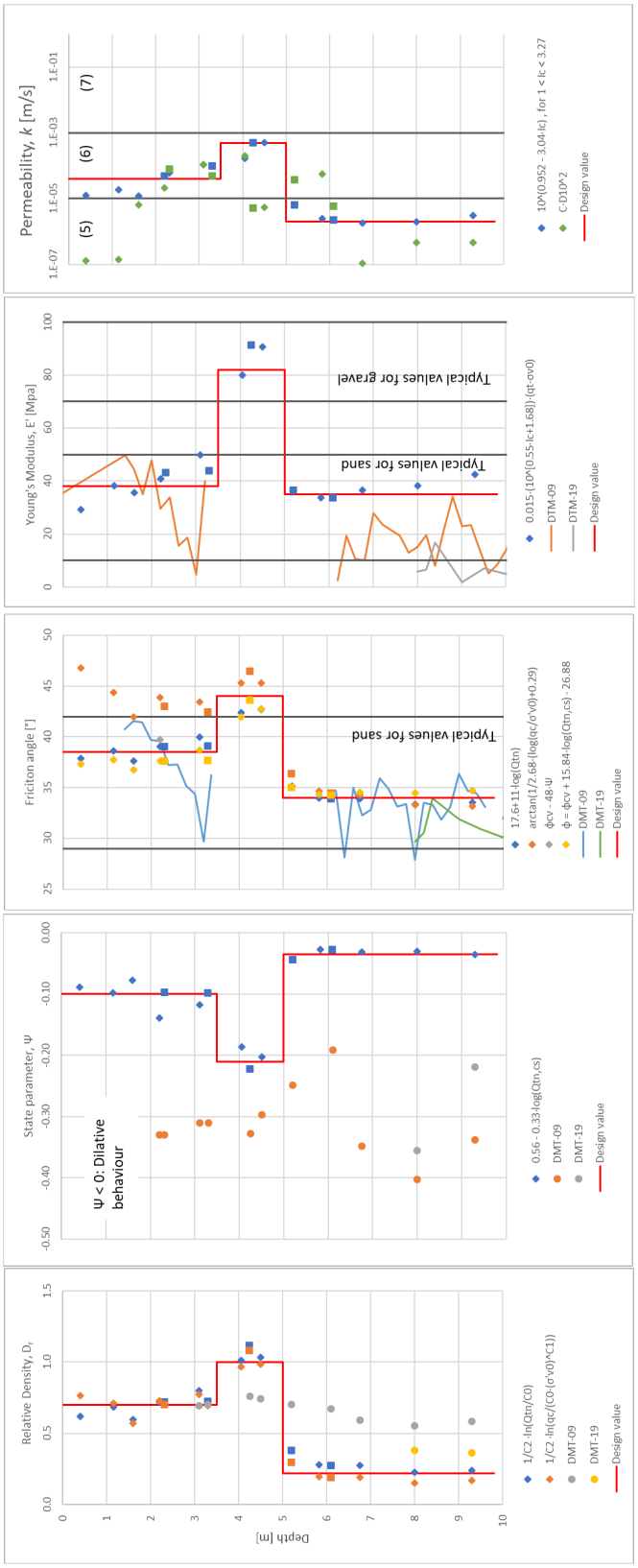

Figure 5.7: Result from parameter interpretation from CPTu and DMT. Results for the relative density, state parameter, friction angle and the Young's Modulus respectively.

Table 5.2: Summary of soil classification at Øysand, results from SBTn charts and the USCS.

Depth [m]	**BH09**	**Robertson 1990 Q_{tn}-F_r**	**Robertson 1995 Q_t-G_0/q_t**	**BH19**	**Depth [m]**
2.32	Poorly graded sand with gravel	(6) Sands: clean to silty	(6) Sands: clean to silty	Poorly graded sand with silt & gravel	1.8-2.6
3.30	Poorly graded sand	(6) Sands: clean to silty	(6) Sands: clean to silty	Well graded gravel with sand	2.6-3.6
4.50	Well graded sand with silt and gravel	(6/7) Sands: clean to silty / gravelly sand	(7) Gravelly sand	Poorly graded gravel with sand	3.6-4.5
5.22	Well graded sand with gravel	(6) Sands: clean to silty	(6) Sands: clean to silty		
		(6) Sands: clean to silty	(6) Sands: clean to silty	Poorly graded gravel with silt and sand	5.6-6.05
6.10	Well graded sand with silt and gravel	(6) Sands: clean to silty	(6) Sands: clean to silty	Sandy silt	6.1-7.4
7.40	Sandy silt	(5) Sand mixtures: silty sand to sandy silt	(6) Sands: clean to silty	Sandy silt / Silty sand	7.4-8.6
8.10	Well graded silty sand / clayey sand	(5) Sand mixtures: silty sand to sandy silt	(6) Sands: clean to silty		
8.30	Poorly graded silty sand / clayey sand	(5) Sand mixtures: silty sand to sandy silt	(6) Sands: clean to silty		
9.40	Poorly graded sand with gravel	(5) Sand mixtures: silty sand to sandy silt	(6) Sands: clean to silty	Silty sand	8.6-10

Chapter 6

Discussion

6.1 Penetration in sand

The results highlight how the fines content in the soil control the behaviour of the soil under penetration. Even though the soil classifies as coarse (more than 50% > 0.075 mm) the fines control the behaviour and the response of the soils. With more fines in the soil the grain-to-grain contact increases and subsequently the permeability decreases and the penetration becomes more smooth. This is presented in figure 6.1 which schematically shows the penetration sands with dominating gravel content versus penetration in sands with some gravel. The thrust of the cone is not large enough to penetrate through the gravelly sands and in that case test must be stopped. However in finer sands there might be some uncertainty in the measured cone resistance as the cone might just be pushing, further compressing, the particles as it penetrates. Therefor does the ratio between coarse and fine particles highly affect the outcome of the measured cone resistance. This can also be seen when a CPTu profile is compared to the material content, presented in figure 4.1. At 5 m depth the cone resistance decreases significantly indicating more silty soil, at the same time the fines content increases on the cost of the sand portion of the sample. Even though the gravel content is still relatively high the CPTu profile is more affected by the increase in fines content. Figure 6.2 shows the failure mechanism in sandy soil due to rod penetration. It is evident how the penetration disturbs the soils in near vicinity of the point of shearing.

According to Robertson and Campanella (1983) a sand layer with a thickness of 10-20 times the cone diameter is necessary to obtain presentable values of the layer. This also is affected of the compaction of the sand, if it is at loose or dense state. The denser the sand, the more stiffness it has to resist the penetration of the cone. Even though the grain-to-grain contact increases with increased fines in the soil the stiffness decreases, which results in an easier penetration of the cone. The largest uncertainty in this matter is the boundary of how large percentage of fines versus granular material is needed so the penetration is dominated by the effects of the fines rather than the granular soil. Since the fines of the soil seem to have more weight in controlling the soil behaviour during penetration of the CPTu some misinterpretation can be expected with corresponding soil classification. The

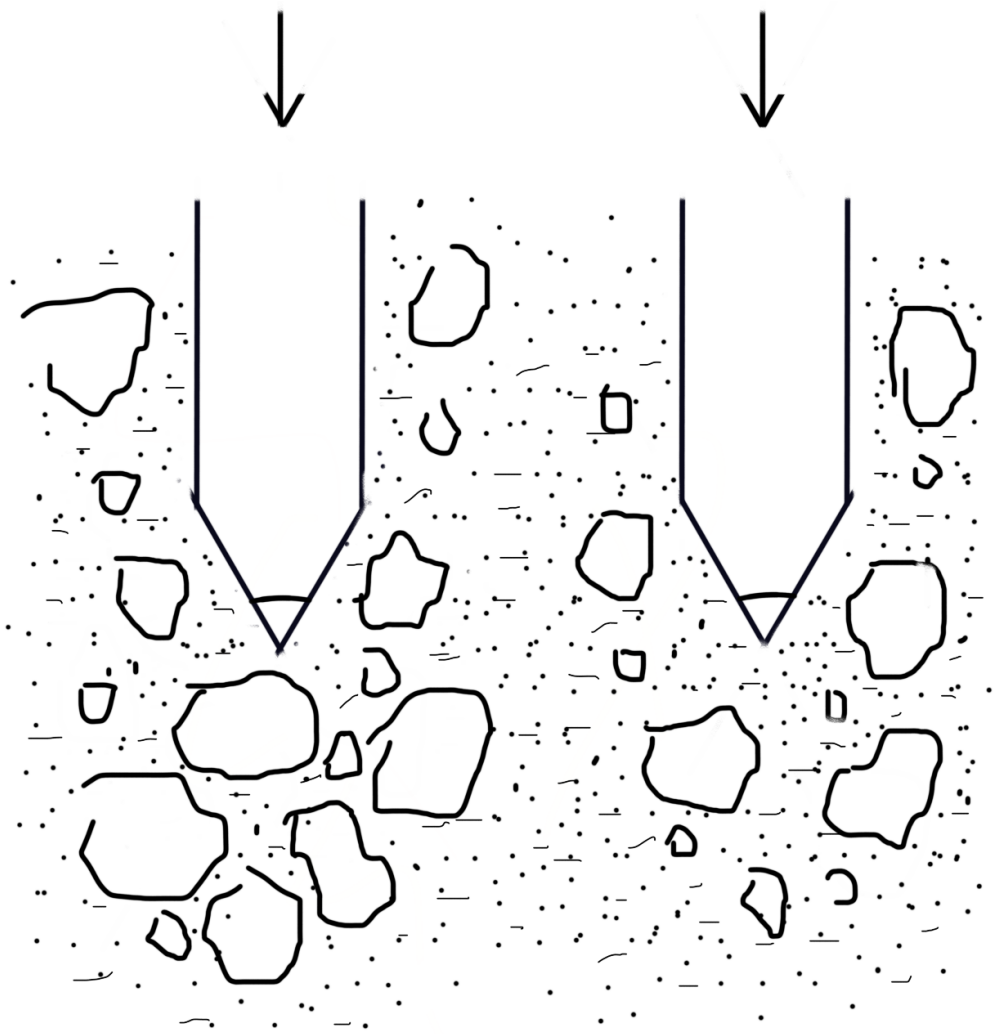

Figure 6.1: Schematic of penetration in gravelly sands (left) versus finer (right).

diameter of the cone also has an important influence on the penetration. As the diameter increases the cone takes more load and the cone resistance increases. This can also be visualized in figure 6.1, if the diameter of the cone would increase there would be more resistance to the cone. The results may also vary more with increased diameter due to larger skin friction on the cone (Raman et al. (2017)). Other things that can affect the measurements of the CPTu parameters are axial loading in the area, change in temperature with depth, inclination of the probe, lack of calibration and wear of equipment (Lunne et al. (1997)).

Generally it is detected that the results of the DMT are good and fit well with the CPTu and theoretical values. Which proves the DMT to be a good *in-situ* testing method in sandy soils. However, it is the authors opinion that the CPTu has more input over the DMT penetration, even though both tests provide real-time data, the CPTu provides the investigator with readily interpretable information and the interpretation process is overall easier. The

penetration ability of the two penetrations is similar, neither of them is fully equipped to penetrate too coarse soils.

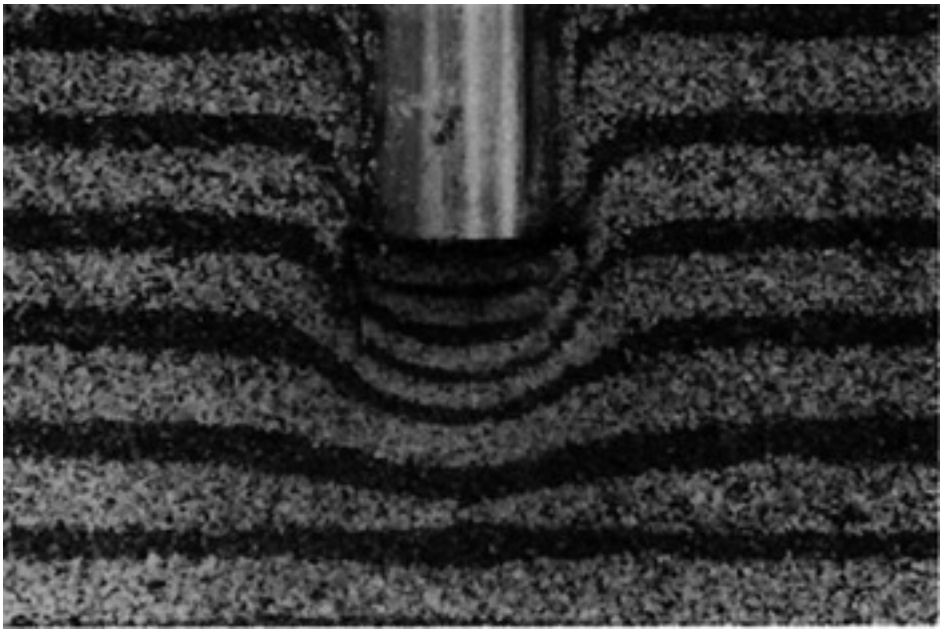

Figure 6.2: Observed failure behavior of sand under pile tip (Wang et al. (2013)).

6.2 Soil identification

The soil in Øysand was classified using the SBTn charts based on measured CPTu parameters, presented by Robertson (2016), Robertson (1990) and Schneider et al. (2008), which all use CPTu parameters normalized with respect to vertical stress and the stress exponent (n). To support the classification from the CPTu data soil classifications based on DMT measurements and results of laboratory testings on samples were used for comparison. The soil behaviour index (I_c) was also used for comparison.

All methods give fairly similar results of the top ten meters of the soil stratum, with obvious three groups. Group (I) from 2-3.5 m depth, classified as clean sand: sand to silty sand with the calculated I_c on the range of 1.65-1.8. Group (II) from 3.5-5 m depth which classifies on the boarder of gravelly sand to clean sand where I_c ranges from 1.45-1.62. And the last group (III) from 5-10 m depth classified on the boarder of clean sands and sand mixtures: silty sand to sand silty, with a I_c between 2.2 and 2.5. According to the theoretical values of I_c group (III) should classify purely as sand mixtures (see figure 5.3). The soil classification based on the shear wave velocity/small strain shear stiffness also shows the same three groups. However, group (II) classifies as gravelly sand and group (III) as clean sand. That resembles more the classification based on the USCS, where group (I) classifies as sand/silty sand, group (II) classifies as gravel with sand (B19) or gravelly sand (B09) and group (III) classifies as silty sand or sandy silt.

The newer classifications charts (Robertson (2009a), Robertson (2016)) are based on the normalized cone resistance with the calculated stress exponent (Q_{tn}). The procedure of calculating the stress exponent depends on

the calculated soil behaviour index which is dependent on the normalized cone resistance. Therefore it is possible to see the effects of the changing soil behaviour index and normalized cone resistance as the stress exponent decreases from one, which is the starting value, to the calculated value. According to literature n=1 is supposed to overestimate the normalized cone resistance for coarse soils, thus, the calculated stress exponent. With decreasing stress exponent the normalized cone resistance decreases and is supposed to represent the *in-situ* state of the soil better. However, as the cone resistance decreases it indicates finer soils as seen on the classification charts. According to the SBTn chart the coarse group (II) goes from classifying as gravelly sand to clean sand as the stress exponent decreases. Hence, it does not recognize the coarse soils, seen in samples, properly. The classification chart based on the shear wave velocity (V_s) is originally related to the normalized cone resistance (Q_t) with the stress exponent n=1, as well as the Robertson 1990 Q_t-B_q chart. Both of these charts classify the coarse layers between 3.5-5 m depth, in accordance to the USCS. Therefore is the use of those classification charts recommended for interpretation of the soil at Øysand, given that measurements of the shear wave velocity are available in near distance of the CPTu for the first mentioned chart. The charts also show reliable results if the normalized cone resistance based on the calculated stress exponent is used. Robertson and Cabal (2014) stated that the soil behaviour index is more precise then the SBTn chart, as it has 80% reliability compared to samples. And, by shifting the boundary of the soil behaviour index between gravelly sands and clean sands to 1.61 instead of 1.31 the gravelly soil at Øysand should be recognized fully.

A similar site can be found near the city of Vila do Conde in Portugal. Like the Øysand site, the site lies at the mouth of the river Ave and therefore suffers from tidal influence and demonstrates the effect of sedimentary deposition. The project, presented by GómezSara et al. (2016), looks at the top five meters of the soil from three CPTu's in close vicinity. According to the SBTn chart the soil mainly consists of clean sand to silty sand (zone (6)) with thin layers of sand- and silt mixtures. They layering varies highly between each CPTu and it is also noted that the SBTn charts seem to not represent the granular material shown in samples. The continuity of the layers was phased with a statistical multivariate method to get an average soil stratum of the site.

6.3 Geotechnical parameters of the Øysand sand

Comparison between the calculated geotechnical parameters from CPTu and DMT can be seen on figure 5.7. From these results design values were chosen to represent the properties of the Øysand sand site, as presented in table 5.1. A unique value was chosen for each group of soil classification. The different methods used for calculation (summarized in table 4.1) are mostly derived from laboratory, small scale, penetration in ideal conditions with different types of sand and therefore are some differences to be expected.

The results from CPTu and DMT seem to give fairly similar result and as presented in figure 5.7 the values of all parameters fit quite well with the theoretical values. The largest difference between the two tests can be noticed between the state parameter and the Young's Modulus. The results of the state parameter correlated from DMT results and the average stress is dependent on the normalized state parameter which is the difference between the

minimum and maximum void ratio. According to Geotechdata.info (2013) the difference between minimum and maximum void ratio of silty gravels or sandy and silty gravels is approximately 0.1. However, for poorly/well graded sands or gravelly sands with little fines a value of 0.45 can be expected and the difference in silty sand can be as much as 0.6. An average value of 0.4 was attained from dry density results from Quinteros et al. (2019). A value as low as 0.12 seems to be better fitting to match the results of the calculated state parameter from CPTu results. Another fault of estimating the state parameter from DMT results is that the correlation does not allow for a precise higher ratio between the state parameter and the normalized state parameter lower than -0.8 which does not give correct results. However, both calculated and empirical results of the state parameter show dilative behaviour in the soil. This agrees with triaxial results done on samples from Øysand, presented by Quinteros et al. (2019), which also show dilative behaviour.

The values of the Young's modulus from DMT and CPTu differ greatly, specially below 5 m depth where the DMT seems to underestimate the parameter with a difference of up to 30 MPa between the two methods. The expected values for sand lie between 10-50 MPa which the data fits between. Gravelly soils usually take values between 70-170 MPa, the coarsest layer between 3.6-5 m depth takes a value around 80-90 MPa.

The calculated relative density gives values > 1.0 for group (II). This is theoretically impossible. The values between the relationships presented by (1) Robertson and Cabal (2014) and (2) Baldi *et. al.* 1986 (in Lunne et al. (1997)) compare very well, where the values from (1) give slightly higher results. The values from (2) do not exceed 1, though they go close, and therefore is that method recommended for coarse soils.

The calculated friction angle fits within the boundary of typical values of sand. There is some scatter in the results in the sandy top five meters and the method presented by Robertson and Campanella (1983) seems to overestimate the friction angle by up to 5°. In the bottom five meters all methods agree on friction angle approximately 34°. The fact that the different correlations agree better in the finer soils increases the reliability of the results in that soil type, and decreases the reliability of the correlations in granular soil.

The calculated results of the permeability, based on CPTu results as well as on the Hazan formula, agree well with one another, with a difference of about four orders magnitude in the top ten meters. The permeability takes values fitting within zones (6) and (5) for the top and bottom five meters of the soil, respectively. Quinteros et al. (2019) presented results of permeability from different methods from 6-18 m depth, including results from a flow cone laboratory test and a slug test done in field. The flow cone results seem to fit well with the calculated permeability in this project. However, compared to the results of the slug test which show, the calculated permeability in this project seems to underestimate the permeability and represents finer soil in the bottom five meters. The slug test results of the bottom five meters do compare to the results of the top five meters of the calculated permeability in this project.

Chapter 7

Summary

Øysand, a natural sand site located in central Norway, is part of a project called the Norwegian GeoTest site. Øysand is one of five sites used in this project that aims to gain more information of different types of soils in Norway. The area used for geotechnical investigations at Øysand spans approximately 35,000 m^2. The site mainly consists of fluvial material, underlain by deltaic material deposited at the mouth of the Gaula River which today runs to the east of the site. The deposits, are a product of glacially eroded bedrock and fluvially eroded marine- and glacial deposits. A lot of geotechnical and geophysical testing has been done on site over the whole area for the top 20-30 m of the soil, as well as sampling for testing in laboratory. Due to the problem of obtaining representative, undisturbed samples in granular soil more focus is put on obtaining quality data from *in-situ* tests such as the CPTu and DMT tests. This project is based on 17 Cone Penetration Tests, 2 seismic Dilatometer tests as well as 2 logs of continuous sampling.

The main objective of this project was to test the classification charts presented in literature based on CPTu parameters. To comparison, results of DMT and sampling were used. The second goal of the project was to provide representative geotechnical parameters for the Øysand site. It includes the determination of the relative density (D_r), the state parameter (Ψ), the peak friction angle (ϕ'), the Young's Modulus (E') and the hydraulic conductivity (k). The project focuses on the top ten meters of the soil stratum and specially the coarsest layer between 3.6-5 m depth.

Results from the Robertson classification charts based on CPTu data showed the ten meter soil column in three groups. The first layer (I) of clean sands from 1.8-3.5 m depth, the second layer (II) which lies on the boarder of gravelly sands and clean sands from 3.5-5 m depth and the third layer (III) of clean sands to sand mixtures, silty sand to sandy silt, from 5 - 10 m depth. With corresponding values of the soil behaviour index I_c of 1.66-1.78 for grouping (I), 1.45-1.62 for grouping (II) and 2.2-2.5 for grouping (III).

- It was evident from the results that the Robertson charts based on the normalized cone resistance with the calculated stress exponent do not classify the coarsest layer in Øysand (III) properly. Though gravel is evident in the samples the CPTu still classifies the sand as clean to silty.

- For the Øysand site it is recommended to use the classification chart presented by Robertson (1995) based on shear wave velocity, as it recognizes the gravelly sand layer. This chart is originally based on the normalized cone resistance with a stress exponent = 1. The chart also shows reliable results when using the normalized cone resistance with the calculated stress exponent and therefore it is recommended to use it together with the rigidity index.
- If shear wave velocity data is not available it is recommended to use the soil behaviour index for soil classification at Øysand. It is also suggested to shift the boundary between the gravelly sand and clean sand (zones (7) and (6) according to the SBTn chart) from 1.31 to 1.61.

Comparison of geotechnical parameters derived from CPTu and DMT data showed fairly good correlation between the two test methods. The values are as expected from theoretical values for sand and gravelly sand. From results of both the methods design values were chosen to represent the soil in the top ten meters at Øysand.

7.1 Recommendations for further work

A challenging task for the Øysand site would to accumulate good samples of the soil. In May 2019 a project to freeze the ground was started. This should hopefully provide representable samples of the *in-situ* layering. By testing these samples in the laboratory better and more reliable geotechnical parameters would be provided as well as precise classification of the soil.

Another challenge would be to look into the role of coarse and fine soils under penetration, and their behavioural relationship, in more detail. This would be done to get better general understanding of CPTu penetrations. Also to look better into the stress exponent (n) and the effect it has on the classification of the soil according to the empirical charts compared to samples.

Generally more research on granular soils under penetration is needed.

Bibliography

Abrams, J., Smith, L., and Ryan, M. (2001). *FM 5-472, Materials Testing - Field manual*. Department of the Army.

ASTM International (2018). *Standard Practice for Classification of Soils for Engineering Purposes (Unified Soil Classification System) - Active Standard ASTM D2487*. U.S. Department of Defense.

Baligh, M. and Levadouz, J. (1980). Pore pressure dissipation after cone penetration. *Massachusetts Institute of Technology, Department of Civil Engineering, Construction Facilities Division*.

Begemann, H. (1965). The friction jacket cone as an aid in determining the soil profile. *Proceedings 6th International Conference on Soil Mechanics and Foundation Engineering*, 1:17–20.

Biryaltseva, T., Mörz, T., Brandt, S., Kreiter, S., Gerdes, U., and Ossig, B. (2016). Relative densities and void ratios derived from CPT data using in-situ field calibration. *5th International Conference on Geotechnical and Geophysical Site Characterisation, ISC*, 1:383–388.

Campanella, R., Gillespie, D., and Robertson, P. (1982). Pore pressures during cone penetration testing. *Proceedings of the 2nd European symposium on penetration testing*, ESOPT2:507–512.

Campanella, R., Gillespie, D., Robertson, P., and Greig, J. (1986). Use of piezometer cone data. *ASCE Speciality Conferance In-situ 86 Use of In-situ Testing in Geotechnical Engineering, Geotechnical Special Publication GSP*, pages 1263–1280.

Campanella, R. and Robertson, P. (1986). Estimating liquefaction potential of sands using the flat plate dilatometer. *Geotechnical Testing Journal*, 9(1):38–40.

Clayton, C., Matthews, M., and Simons, N. (1995). *Site Investigation - Ch. 7 Undisturbed sampling techniques*. Department of Civil Engineering, University of Surrey, 2 edition.

Douglas, B. and Olsen, R. (1981). Soil classification using electric cone penetrometer. *Symposium on Cone Penetration Testing and Experience, Geotechnical Engineering Division, ASCE*, pages 209–227.

Easterbrook, D. (1999). *Surface Processes and Landforms*. Pearson.

Geotechdata.info (2013). Soil void ratio. http://www.geotechdata.info/parameter/soil-void-ratio.html. Accessed: 14.05.2018.

Gundersen, A., Quinteros, S., L'Heureux, J., and Lunne, T. (2018). Soil classifications of NGTS sand site (Øysand, Norway) based on CPTu, DMT and laboratory results. *Cone penetration Testing*, pages 324–328.

GómezSara, F., Rios, S., and Fonseca, A. (2016). Statistical interpretation of soil classification from CPTu tests in fluvial sediments. *Conference: 16° Congresso Nacional de Geotecnia*.

Hazen, A. (1930). *Water supply, in American Civil Engineering Handbook*. Wiley.

Huang, A. and Huang, Y. (2007). Undisturbed sampling and laboratory shearing tests on a sand with various fines content. *Soils and foundations*, 47(4):771–781.

Jamiolkowski, M., Presti, D., and Manassero, M. (2001). Evaluation of relative density and shear strength of sands from cone penetration test (CPT) and flat dilatometer test (DMT). *ASCE Geotechnical Special Publication*, 119:201–238.

Jefferies, M. and Been, K. (2006). *Soil Liquefaction – A critical state approach*. Taylor & Francis, 2 edition.

Jefferies, M. and Davies, M. (1991). Soil classification by the cone penetration test: discussion. *Canadian Geotechnical Journal*, 28(1):173–176.

Jefferies, M. and Davies, M. (1993). Use of CPTu to estimate equivalent SPT n_{60}. *Geotechnical Testing Journal*, 16(4):458–468.

Jones, G. and Rust, E. (1982). Piezometer penetration testing CPTu. *Proceedings of the 2nd European Symposium on Penetration Testing, ESOPT II*, 2:607–613.

Kokusho, T. and Yoshide, Y. (1997). SPT N-value and S-wave velocity for gravelly soils with different grain size distribution. *Soils and Foundations*, 37(4):105–113.

Konrad, J. (1988). Interpretation of flat plate dilatometer tests in sands in terms of the state parameter. *Géotechnique*, 38(2):263–277.

Krage, C., Broussard, N., and Dejong, J. (2004). Estimating rigidity index (I_r) based on CPT measurements. *3rd International Symposium on Cone Penetration Testing*, pages 727–735.

Liu, Z., Amdal, A., L'Heureux, J., Lacasse, S., Nadim, F., and Xie, X. (2019). Spatial variability of medium dense sand deposit. *AIMS Geosciences*. to be published.

Lunne, T., Robertson, P., and Powell, J. (1997). *Cone Penetration Testing in Geotechnical Practice*. Spoon Press, Taylor & Francis Group.

Marchetti, S. (1980). In-situ test by flat dilatometer. *Journal of the Geotechnical Engineering Division*, 106(ASCE 15290):299–321.

Marchetti, S., Monaco, P., Totani, G., and Calabrese, M. (2001). The flat dilatometer test (DMT) in soil investigations. *Report of the ISSMGE Technica1 Committee 16 on Ground Property Characterisation from In-situ Testing*.

Marchetti, S., Monaco, P., Totani, G., and Marchetti, D. (2008). In situ tests by seismic dilatometer (SDMT). *From Research to Practice in Geotechnical Engineering*, GSP 180:192–311.

NGF (2010). *Veiledning for utførelse av trykksondering*. Norsk geoteknisk forening/Norwegian geotechnical society, 3 edition. NGF publication No. 5.

Plewes, H., Davies, M., and M.G., J. (1992). CPT based screening procedure for evaluating liquefaction susceptibility. *45th Canadian Geotechnical Conference*, pages 383–388.

Quinteros, S., Gundersen, A., L'Heureux, J., Carraro, A., and Jardine, R. (2019). Øysand research site: Geotechnical charaterization of deltaic sandy-silty soils. *AIMS Geosciences*. to be published.

Raman, K., Dayakar, P., and Raju, K. (2017). An experimental study on effect of cone diameters in penetration test on sandy soil. *International Journal of Civil Engineering and Technology (IJCIET)*, 8(8):1581–1588.

Robertson, P. (1986). In-situ testing and its application to foundation engineering. *Canadian Geotechnical Journal*, 23(4):573–594.

Robertson, P. (1990). Soil classification using the cone penetration test. *Canadian Geotechnical Journal*, 27(1):151–158.

Robertson, P. (2009a). Interpretation of cone penetration test - a unified approach. *Canadian Geotechnical Journal*, 46(11):1337–1355.

Robertson, P. (2009b). CPT-DMT correlations. *Journal of Geotechnical and Geoenvironmental Engineering*, 135(11):1762–1771.

Robertson, P. (2010). Estimating in-situ state parameter and friction angle in sandy soils from CPT. *2nd International Symposium on Cone Penetration Testing*.

Robertson, P. (2016). Cone penetration test (CPT)-based soil behaviour type (SBT) classification system - an update. *Canadian Geotechnical Journal*, 53(12):1910=1927.

Robertson, P. and Ahmadi, M. (205). Thin-layer effects on the CPT q_c measurement. *Canadian Geotechnical Journal*, 42:1302–1317.

Robertson, P. and Cabal, K. (2014). *Guide to Cone Penetration Testing for Geotechnical Engineering*. Gregg Drilling & Testing Inc., 6 edition.

Robertson, P. and Campanella, R. (1983). Interpretation of cone penetraiton tests - part I (sand). *Canadian Geotechnical Journal*, 20(4):718–733.

Robertson, P. and Wride, C. (1998). Evaluating cyclic liquefaction potential using the cone penetration test. *Canadian Geotechnical Journal*, 35(3):441–459.

Sadrekarimi, A. (2016). Evaluation of CPT-based characterization methods for loose to medium-dense sands. *Soils and Foundations*, 56(3):460–472.

Sanglerat, G. (1972). *The Penetrometer and Soil Exploration*. Elsevier Publishing Company.

Sanglerat, G., T.V., N., Sejourne, M., and Andina, R. (1974). Direct soil classification by static penetrometers with special friction sleeve. *Proceedings Europian Symposium on Penetration Testing*, 2:337–344.

Schanz, T. and Vermeer, P. (1996). Angles of friction and dilatancy of sand. *Géotechnique*, 46(1):145–151.

Schmertmann, J. (1978). *Guidlines for Cone Penetration Test, Performance and Design*. U.S. Department of Transportation, Federal Highway Administration Report, fhwa-ts-78-209 edition.

Schneider, J., Mcgillivray, A. V., and Mayne, P. W. (2004). Evaluation of scptu intra-correlations at sand sites in the lower mississippi river valley, usa. *Proceedings of the 2nd International Conference on Site Characterisation*, 1:1003–1010.

Schneider, J., Randolph, M., Mayne, P., and Ramsey, N. (2008). Analysis of factors influencing soil classification using normalized piezocone tip resistance and pore pressure paramters. *Journal of Geotechnical and Geoenvironmental Engineering - ASCE*, 134(11):1569–1586.

Senneset, K., Janbu, N., and Svanø, G. (1982). Strength and deformation parameters from cone penetrations tests. *Proceedings of the European Symposium on Penetration Testing, ESOPT II*, pages 863–870.

Senneset, K., Sandven, R., and Janbu, N. (1989). Evaluation of soil parameters from piezocone tests. *Transportation research record 1235*, pages 24–37.

Vegdirektoratet (1997a). *Feltundersøkelser - Håndbok R211*. Statens Vegvesen.

Vegdirektoratet (1997b). *Laboratorieundersøkelser - Håndbok R210*. Statens Vegvesen.

Wang, J., Xu, Y., MA, L., and Shen, S. (2013). An approach to evaluate hydraulic conductivity of soil based on CPTu test. *Marine Georesources & Geotechnology*, 31:242–253.

Appendix A

Field investigation map

- Top: Overview of the Øysand test site (1:1000)
- Bottom: Zoom in to the testing cluster in the sout-east corner of the site (1:75)

Maps from www.norgeskart.no.

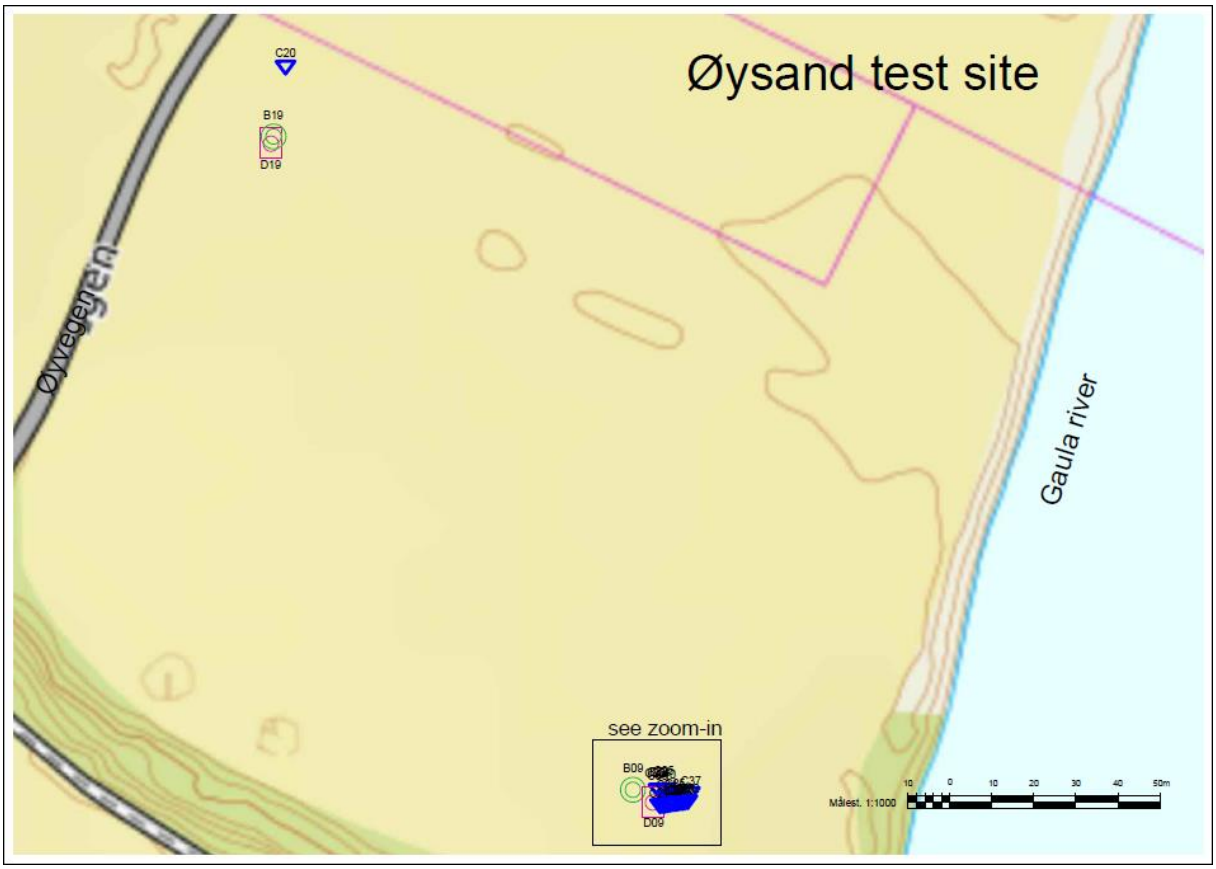

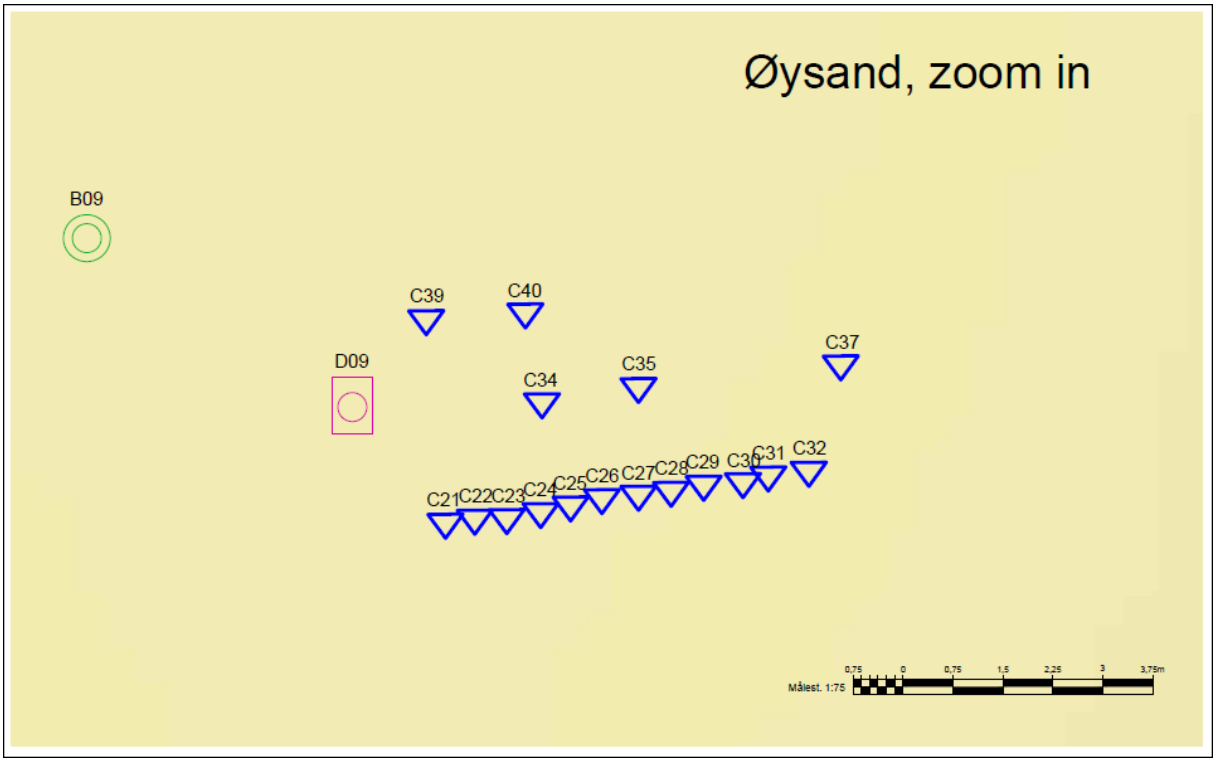

TEGNFORKLARING

CPTU (C) Sample (B) Dilatometer (D)

Appendix B

Results of CPTu

Table B.1: Overview of testing at Øysand used in this project.

Test ID	Project ID	Test
OYSB09	B09	ø54 mm sample
OYSB19	B19	ø54 mm sample
OYSC20	C20	CPTu
OYSC21	C21	CPTu
OYSC22	C22	CPTu
OYSC23	C23	CPTu
OYSC24	C24	CPTu
OYSC25	C25	CPTu
OYSC26	C26	CPTu
OYSC27	C27	CPTu
OYSC28	C28	CPTu
OYSC29	C29	CPTu
OYSC30	C30	CPTu
OYSC31	C31	CPTu
OYSC32	C32	CPTu
OYSC34	C34	CPTu
OYSC35	C35	CPTu
OYSC37	C37	CPTu
OYSC39	C39	CPTu
OYSC40	C40	CPTu
OYSD09	D09	DMT
OYSD19	D19	DMT

Graphic results from the CPTu and DMT measurements used in this project.

The results from the CPTu consist of the

- Corrected cone resistance (q_t)
- Sleeve friction (f_s)
- Measured pore pressure (u_2), calculated *in-situ* pore pressure (u_0) and excess pore pressure (Δu)
- Inclination (i) during penetration

The results from the DMT consist of the

- Material index (I_D)
- Horizontal stress index (K_D)
- Constrained modulus (M_{DMT})

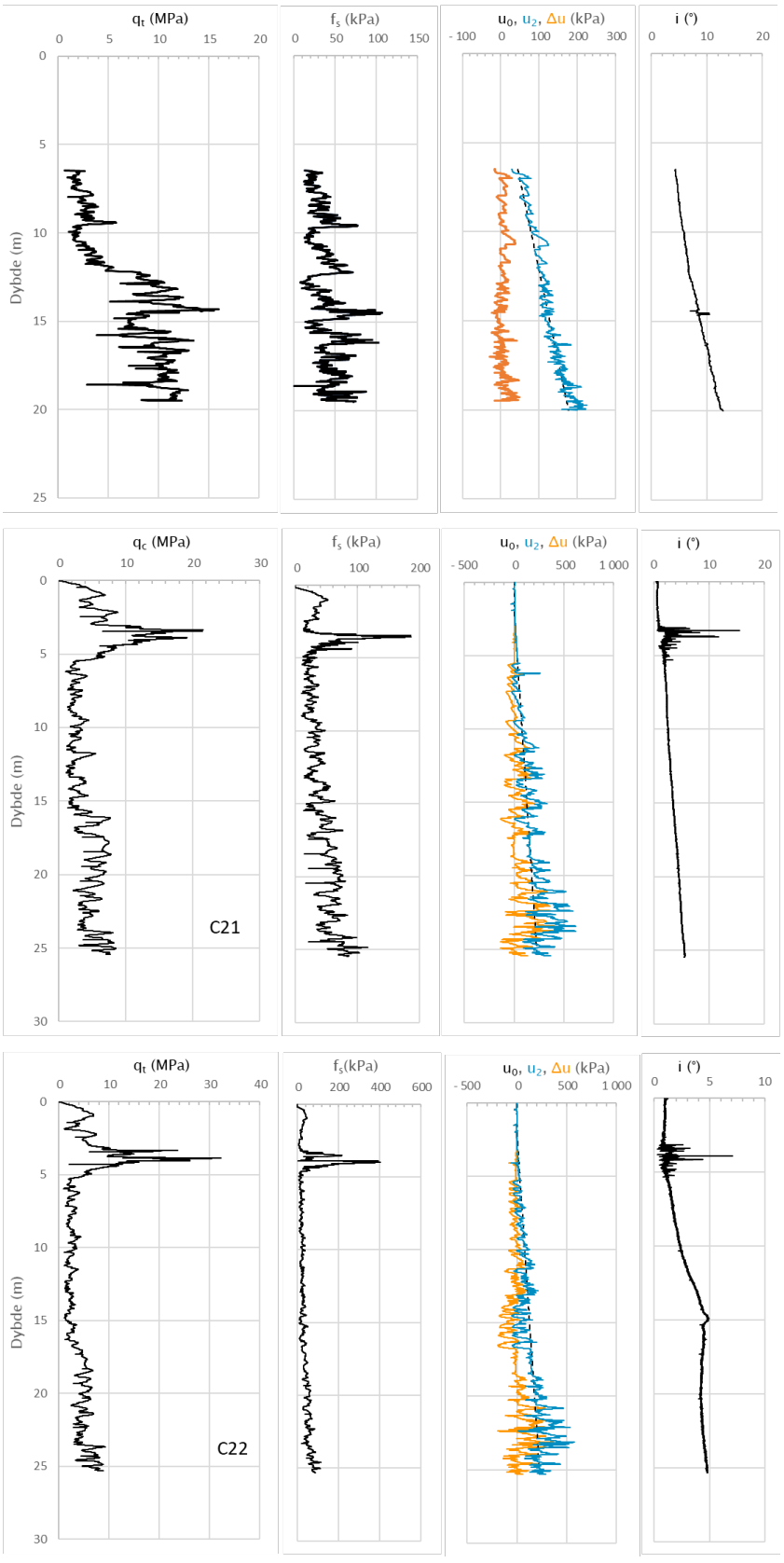

Figure B.1: Results from CPTu tests C20-C22

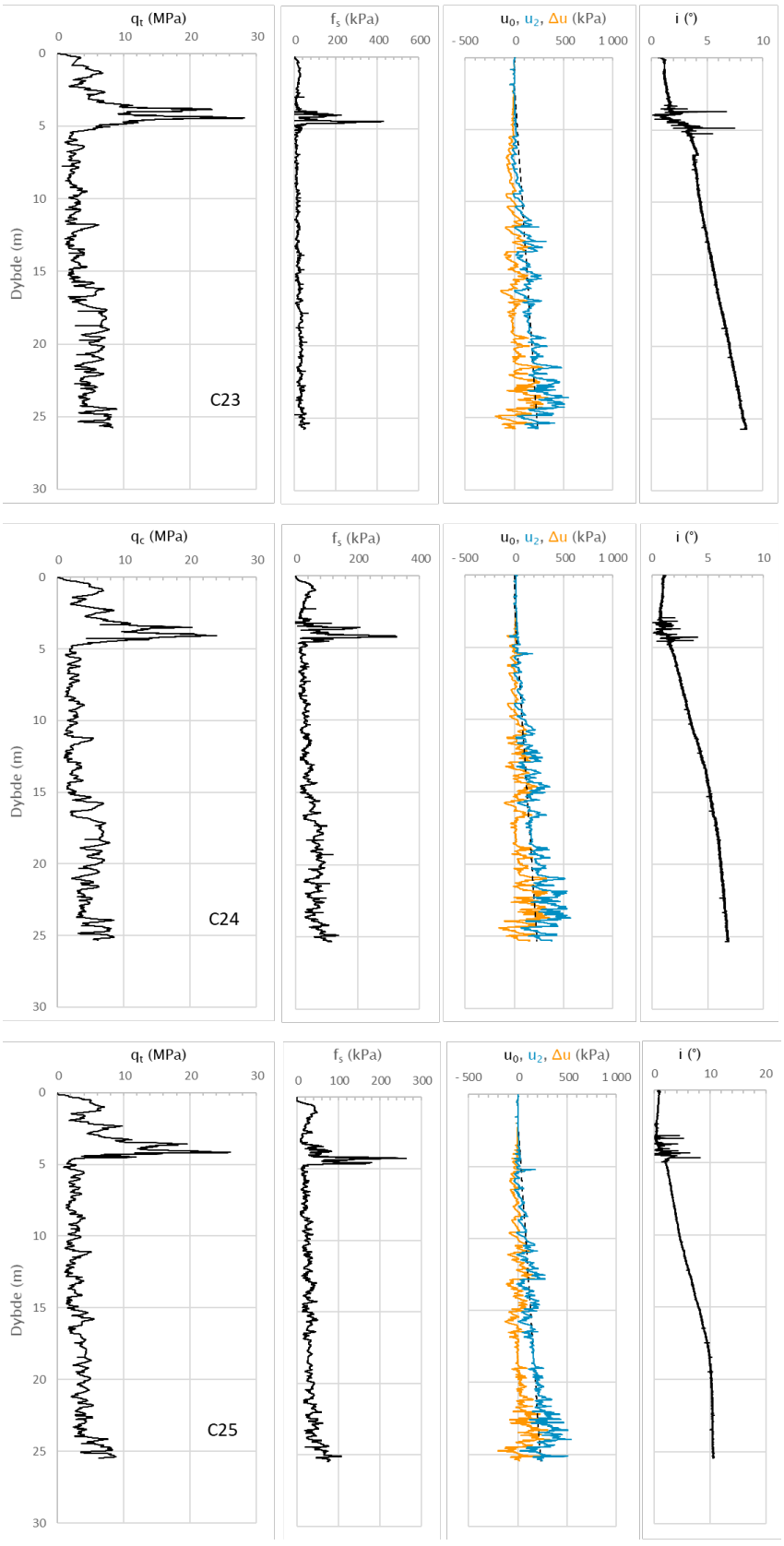

Figure B.2: Results from CPTu tests C23-C25

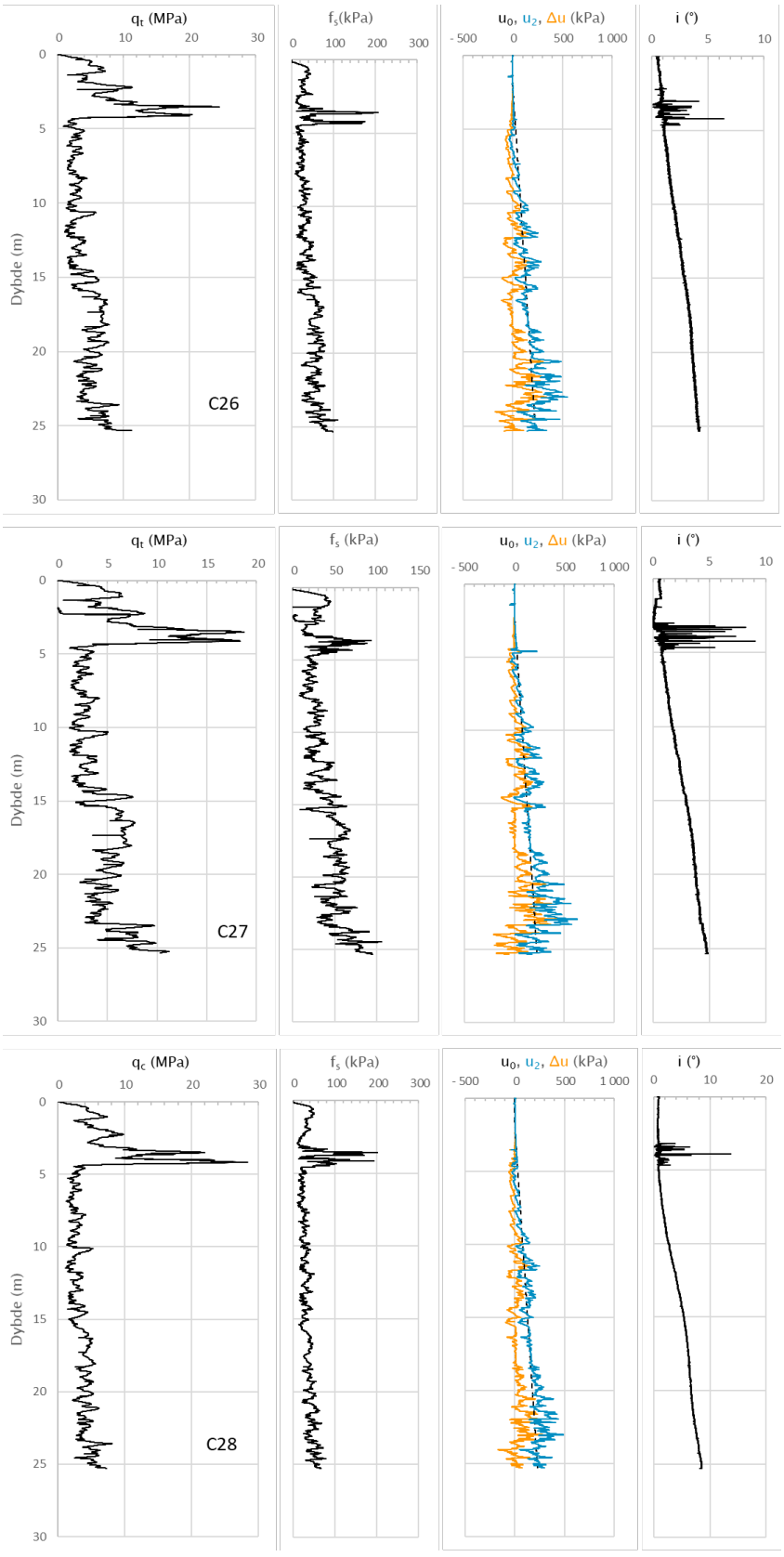

Figure B.3: Results from CPTu tests C26-C28

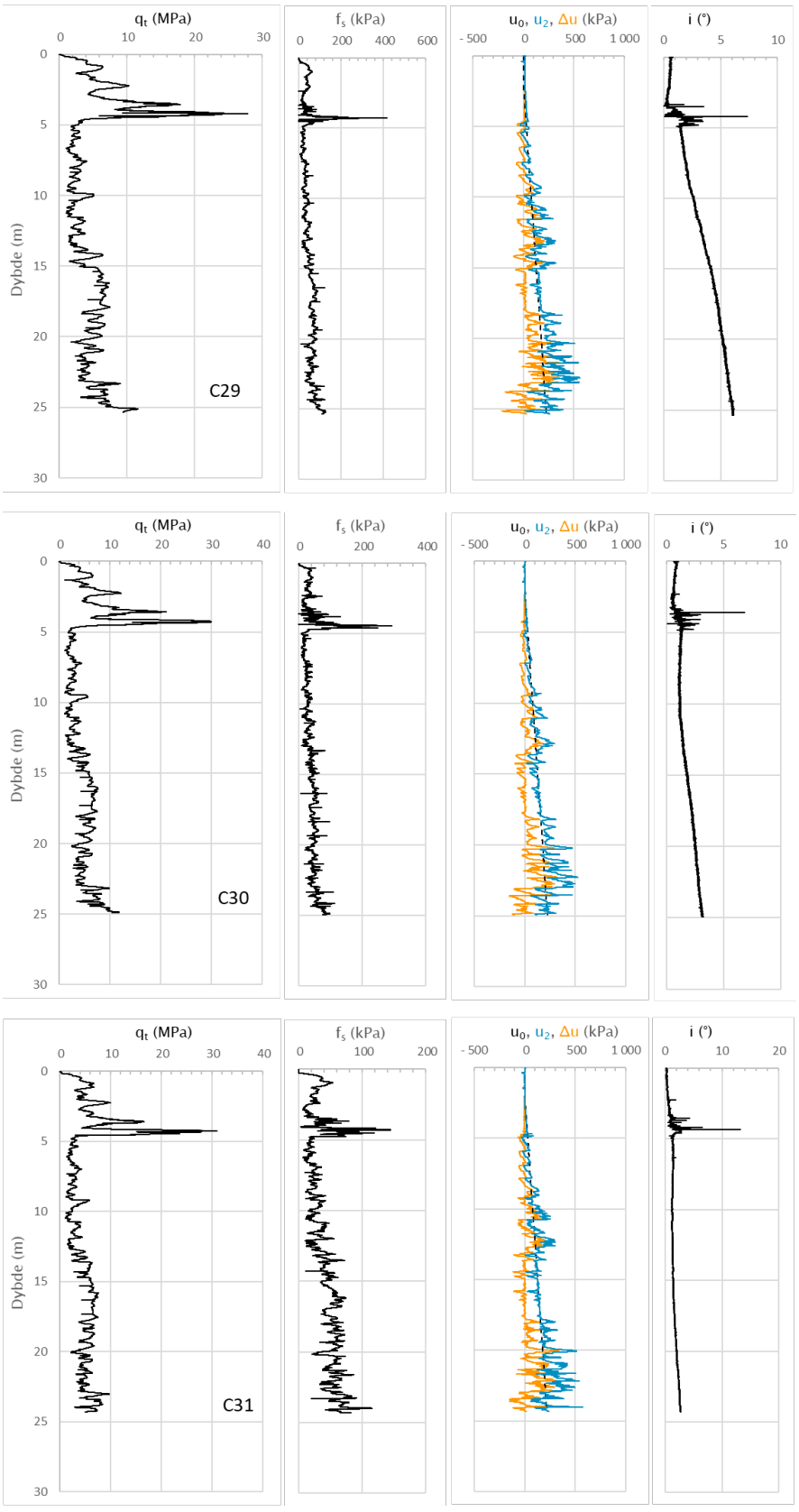

Figure B.4: Results from CPTu tests C29-C31

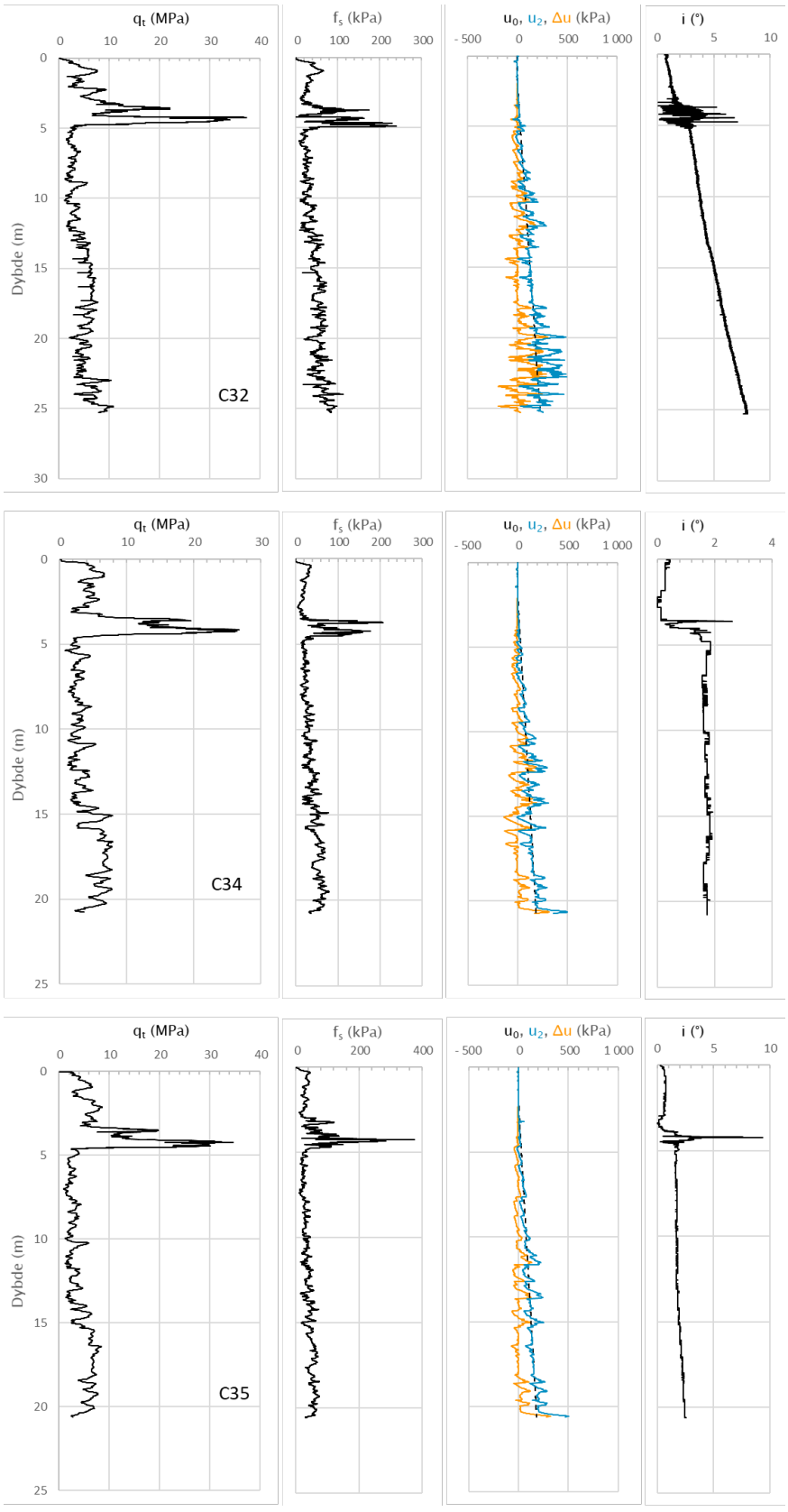

Figure B.5: Results from CPTu tests C32-C35

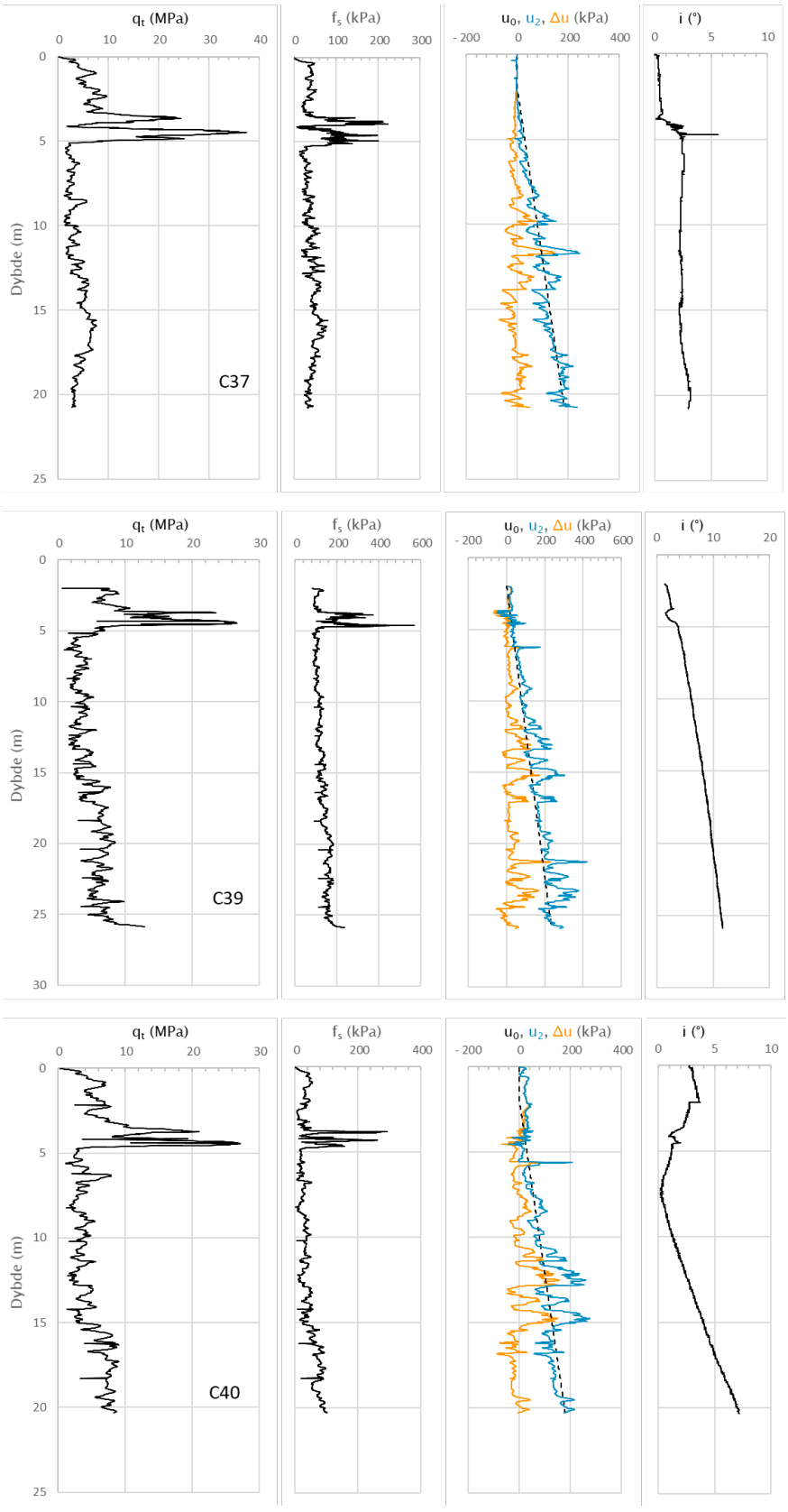

Figure B.6: Results from CPTu tests C37-C40

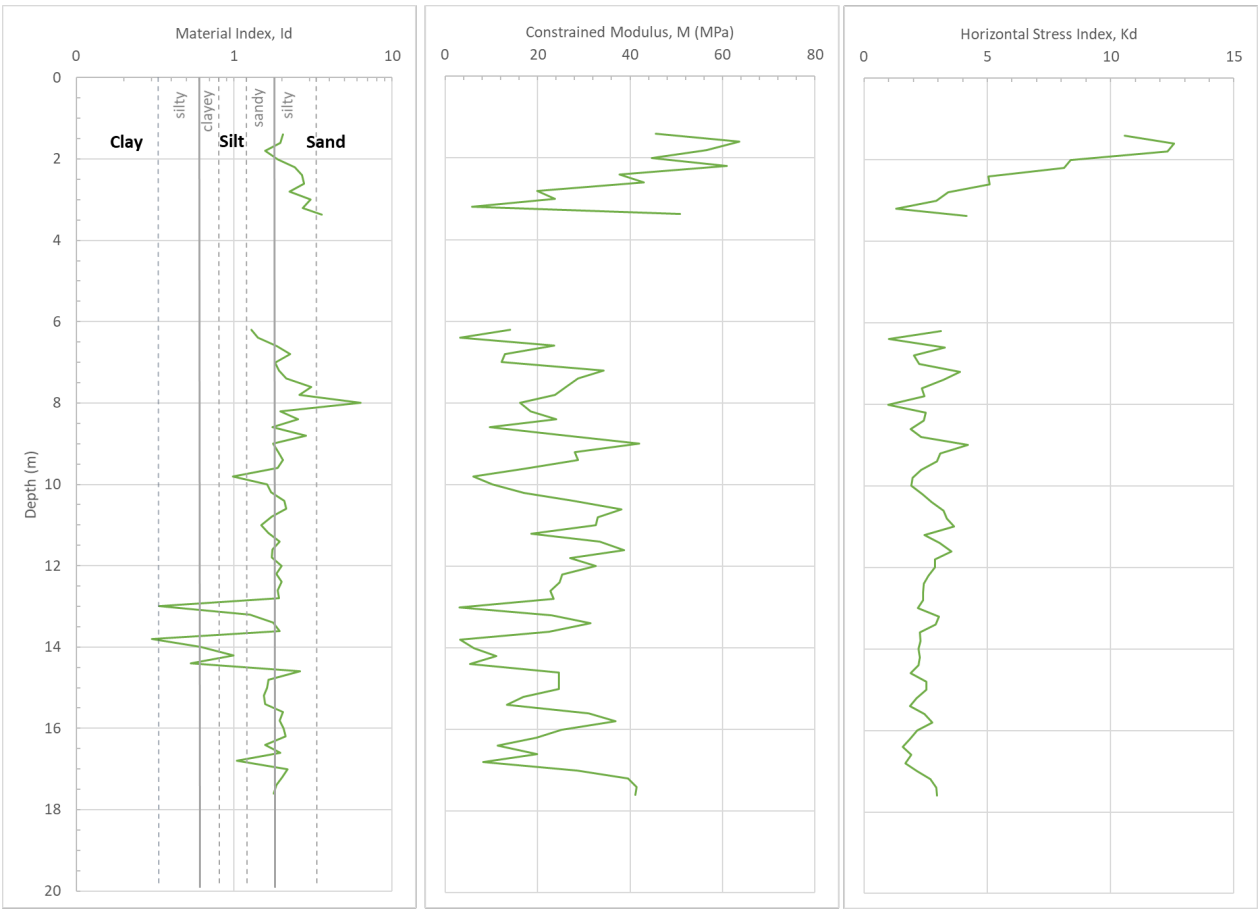

Figure B.7: Results from DMT D09

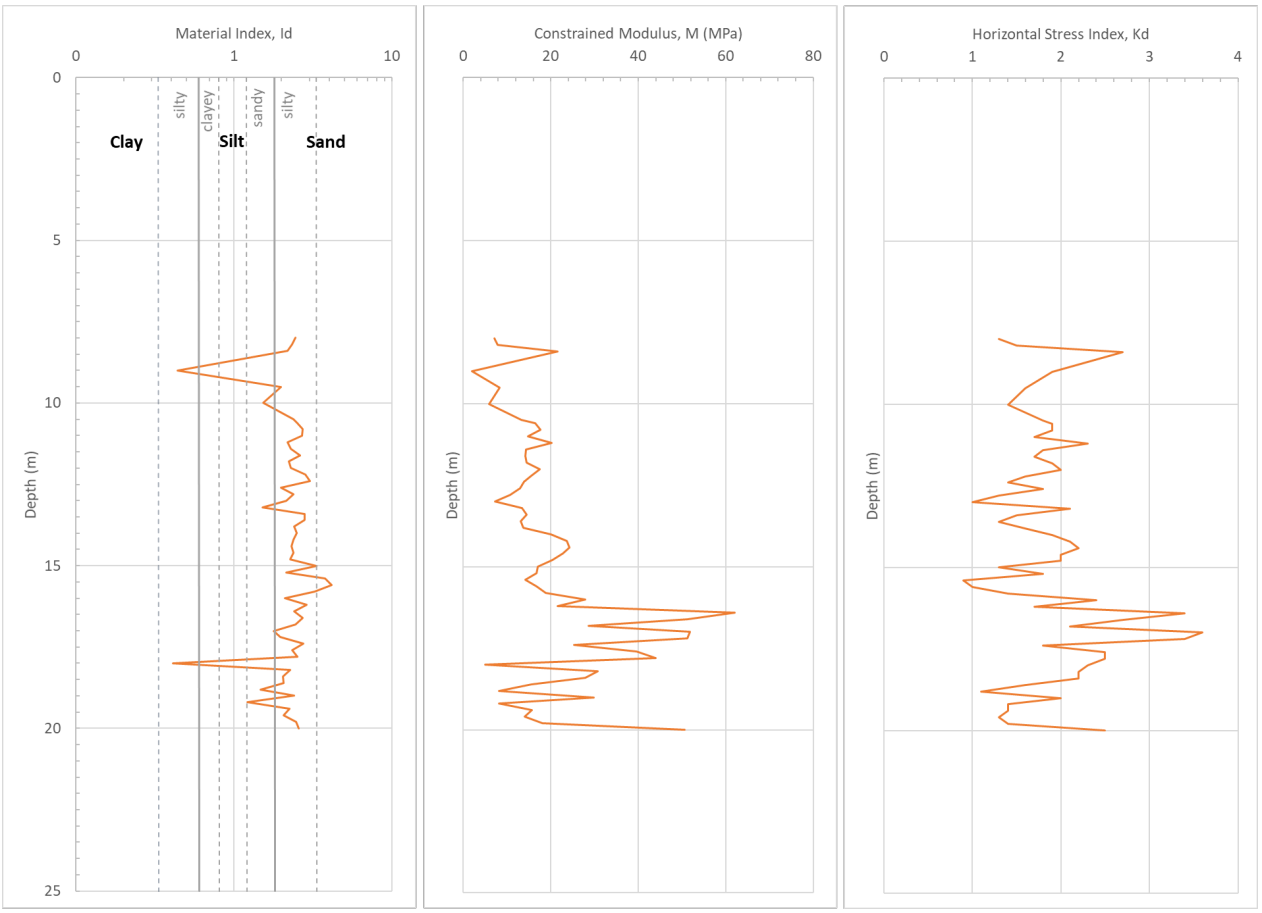

Figure B.8: Results from DMT D09